Russian Chemical Reviews **84** (2) 159 – 193 (2015) © 2015 Russian Academy of Sciences and Turpion Ltd

DOI 10.1070/RCR4438

Electrosynthesis of nanostructures and nanomaterials

O A Petrii

Department of Chemistry, M V Lomonosov Moscow State University
Leninskie Gory 1, str. 3, 119992 Moscow, Russian Federation

The possibilities of electrochemical synthesis of nanostructures and nanomaterials are considered. The problems and prospects of the development of research in this field are discussed. Electrosynthetic methods are classified, their specific features and advantages are demonstrated in comparison with other physical and chemical methods. Examples of electrosynthesis of nanomaterials and their use in various devices are offered.
The bibliography includes 613 references.

Contents

I. Introduction 159
II. Synthesis of nanomaterials by electrodeposition 160
III. Template, quasitemplate and epitaxial electrodeposition 166
IV. Methods of electroless deposition and galvanic displacement. Synthesis of core – shell nanostructures 169
V. Selective dissolution of alloys 174
VI. Electrochemical modification of nanoparticles 178
VII. Electrochemical nanodispersion 179
VIII. Electrosynthesis of nanostructures in melts 181
IX. Electrosynthesis of nanoparticles on the liquid/liquid interface 182
X. Electrosynthesis of nanomaterials in the probe microscope configuration 184
XI. Conclusion 185

I. Introduction

The development of methods for synthesizing nanostructured materials with desired properties and thorough characterization and practical applications of these materials form a promising and actively developing area of modern science and technology. The building blocks of nanomaterials have the size from 1 to 100 nm in at least one dimension. Nanomaterials are characterized by a clear dependence of their properties on the size and shape of structural units.

The interest in nanomaterials is caused by their unique chemical, catalytic, electrochemical, electronic, optical, magnetic, transport, photochemical, adsorption and mechanical properties, which account for wide application of nanomaterials in catalysis/electrocatalysis, quantum electronics, non-linear optics, photonics, sensors, devices for data display and storage and also in biology, medicine and other fields. For many electrochemical applications of nanoparticles, of primary importance are their high surface-to-volume ratio and the size dependence of their electronic properties.

To date, various methods have been proposed for synthesizing nanoobjects (*e.g.*, see Refs 1 – 20). The most important synthetic strategies are based on liquid-phase chemical and photochemical methods. As a rule, nanoparticles are thermodynamically unstable and prone to agglomeration (aggregation); hence, their practical use requires the development of stabilization methods. The publications cited above also analyzed the methods used to study the properties of nanoparticles, particularly, the methods of determination of their size and size distribution.

Particular electrochemical methods for synthesizing nanomaterials were discussed to one or another extent in several reviews.[1, 2, 5, 6, 9 – 20] In the general case, the electrochemical methods can be considered as a special kind of liquid-phase chemical methods with participation of electrons supplied by the external circuit. The electrochemical synthesis can be carried out in both the top-down mode, where bulk materials or powders are converted into colloids or clusters, and the bottom-up mode in which chemical compounds serve as the precursors. Furthermore, the electrochemical methods were successfully used for modifying nanoparticles synthesized by other methods. The electrosynthesis of nanostructures is a part of nanoelectrochemistry and nanotechnology.[20 – 22]

The classification of nanostructured materials is being upgraded as the new classes of nanoparticles appear.[19, 23] A

O A Petrii Doctor of Chemistry, Professor, Leading Researcher of the Chair of Electrochemistry at the Department of Chemistry, MSU. Telephone: (7-495) 939 55 01, e-mail: petrii@elch.chem.msu.ru
Current research interests: interface structure, electrocatalysis, new electrode materials.

Received 15 December 2013
Uspekhi Khimii **84** (2) 159 – 193 (2015); translated by T Ya Safonova

sufficiently universal classification of nanomaterials can be constructed in terms of dimensionality:[19]

— zero-dimensional 0D (for instance, quantum dots, adatoms, heterogeneous arrays of nanoparticles, core–shell structures, spherical nanowells, *etc.*);

— one-dimensional 1D (nanowires, nanorods, nanotubes, nanostrips, nanoribbons, *etc.*);

— two-dimensional 2D (continuous islets, branched planar structures, self-assembled monolayers, nanoplates, nanosheets, nanowalls, nanodisks, *etc.*);

— three-dimensional 3D (dendrite structures, nanohelixes, nanocones, nanocolumns, nanoflowers, *etc.*).

The images of certain typical nanostructures of various classes can also be found in the aforementioned review.[19]

The electrochemical methods are successfully used to produce all types of nanostructures and nanomaterials. Moreover, the major target of electrochemists is further improvement of electrolytic coatings and electrochemical devices, namely, chemical power sources, fuel cells, supercapacitors, electrolyzers, electrodialyzers, sensors, electrochromic devices and photoelectrochemical solar energy converters.†

At present, the specialists engaged in the synthesis of nanostructures, particularly, in the electrosynthesis, tend to direct their efforts toward the preparation of particles of the desired size, shape and topology and also of hybrid materials.[7,27–33]

The purpose of the present review is to demonstrate the wide diversity and potentialities of the electrochemical methods for nanomaterial synthesis. The review was by no means aimed to cite all the existing literature because exhaustive citing even for a relatively short time period (~10 years) is impossible in the framework of a standard review. In each case, the author restricted himself to citing the examples of electrochemical syntheses most typical from his point of view.

II. Synthesis of nanomaterials by electrodeposition

The development of methods for synthesizing and studying nanostructures and nanomaterials had started much earlier than the prefix 'nano' became so conventional and widely known. Whereas in the colloid chemistry the onset of this line of research is associated with the synthesis of gold sols by Faraday in 1857, in electrochemistry the first nanostructured materials were synthesized as early as the beginning of the 19th century by the method of electrodeposition (or electroplating). The electrodeposition of platinum for which the formation of nanostructured deposits is typical, was carried out in 1805 by Brugnatelli, Professor of University of Pavia (Italy) by using a voltaic pile.[34,35] Electrodes of platinized platinum (platinum plates, wire nets or wires coated by platinum electroplates) came to use at the end of the 19th century.[36]

Electrodeposition pertains to the most thoroughly elaborated sections of electrochemistry (see, *e.g.*, monographs[37–42] and reviews[43–46]). At present, the electrodeposition process is widely and successfully used to synthesize nanomaterials of metals, alloys, oxides, hydroxides, semiconductors, conducting polymers, solid complex compounds, salt phases. Electroplating can be carried out in two-, three-, or four-electrode cells in various modes: potentiostatic mode, galvanostatic mode, pulse mode with programmed potential or current pulses of different length and shape, alternating-current mode, *etc.* The wide possibilities as regards controlled electrodeposition of nanostructures are offered by linear sweep voltammetry.

The main feature of electrochemical methods is that the process of electrosynthesis can be controlled by varying either the electrode potential or the current density. Moreover, the coulometric control over the deposition process becomes possible. Electrodeposition allows nanoparticles to be grown directly on the substrate surface, which affords the electrode materials to be used in practice. However, while using electrodeposition on a substrate, it is difficult to grow monodisperse nanoparticles.

In nanochemistry, methods have been developed for preparing suspensions of nanoparticles with a high degree of monodispersion (the deviation from the average size does not exceed 10%).[47] A strategy of synthesizing colloid particles with a narrow size distribution was proposed by LaMer[48] and Reiss[49] based on combining the stages of instantaneous nucleation‡ and the subsequent growth of nuclei under diffusion control. Even for the instantaneous nucleation and the diffusion-controlled growth of particles, the metal electrodeposition on the electrode surface usually produces particles with a fairly wide size distribution, the relative standard deviation of the particle diameter being 20%–50% (*e.g.*, see Refs 50–68). As the particles grow, not only the diameter distribution but also the height distribution is broadened.[67,68] However, certain exclusions are known. Thus, the electrosynthesis of silver nanoparticles with the diameter of ~100 nm and a high degree of monodispersion was described[69] as well as the electrodeposition of monodisperse nickel nanoparticles.[70]

For the development of approaches to electrodeposition of monodisperse nanoparticles and various nanomaterials (*e.g.*, nanowires, ultrathin films, arrays of nanoclusters), it is highly important to elucidate in detail the nature of nucleation and growth phenomena in the early deposition stages. Such research usually theoretically relies on the model of Scharifker–Hills,[71,72] which assumes the formation (instantaneous or progressive) of randomly arranged spherical or hemispherical nuclei on the uniform surface and their further growth under the diffusion, mixed or kinetic control. The growth proceeds as a result of direct reduction of metal ions on the surface, provided the Gibbs free energy decreases upon the addition of atoms to a cluster (the Volmer–Weber mechanism). The further consideration takes into account that zones depleted of the reagent appear in the vicinity of nuclei, resulting in a decrease in the deposition rate; the zones become wider, overlap and the nuclei coalesce. For spherical diffusion, the progressive nucleation is described by the following dependence of the total electrochemical current (I) on time (t):

$$I(t) = \beta z \mathrm{F} c \left(\frac{D}{\pi t}\right)^{1/2} \left\{1 - \exp\left[-\frac{1}{2} k_\mathrm{n} N_0 \pi \gamma (8\pi c V_\mathrm{m})^{1/2} D t^2\right]\right\} \quad (1)$$

† Nanomaterials synthesized by non-electrochemical methods were often used in designing efficient devices for energy conversion and storage (*e.g.*, see Refs 6, 13, 14, 19, 24–26). And the other way round, the electrosynthetic methods proposed by electrochemists can be demanded in the other field of nanoscience and nanotechnology.

‡ The term 'instantaneous nucleation' refers to the situation where the formation of a new nucleus proceeds faster than its growth begins.

For instantaneous nucleation, the dependence is

$$I(t) = zFc\left(\frac{D}{\pi t}\right)^{1/2}\left\{1 - \exp[-N_0\pi(8\pi cV_m)^{1/2}Dt]\right\} \quad (2)$$

In these equations, $\beta = 1$ (see Refs 71, 72) or 4/3 (see Refs 73, 74); F is the Faraday constant; z, D and c are the oxidation state of the discharging ions, the diffusivity and concentration of metal ions; k_n is the rate constant for nucleation; N_0 is the total number of nucleation sites; $\gamma = 4/3$ (see Refs 41, 71, 75); V_m is the molar volume of the deposited metal.

The Scharifker – Hills model was analyzed and advanced in a large number of studies with the use of analytical approaches, more accurate numerical calculations and statistical methods (*e.g.*, see Refs 70 – 87). The views on metal electrodeposition with diffusion-controlled growth of nuclei, which were developed ~10 years ago, were systematized in a review by Hyde and Compton,[46] in which the data for several systems analyzed in the framework of the developed theoretical models of nucleation – growth were tabulated.

The experimental studies of the electrochemical nucleation involve measuring the current *vs.* time dependences (transients) at a constant deposition potential and comparing them with the dependences calculated using Eqns (1) and (2). The quantities k_n, N_0 and D can be found from experimental transients by fitting procedures (in particular, see Ref. 88). Thus, in Fig. 1, the current transients shown in dimensionless coordinates for the electrodeposition of gold nanoparticles on glassy carbon at two different potentials are compared with the curves calculated for progressive and instantaneous nucleation.[66] Evidently, the experimental transients adequately agree with those predicted by the theory. Similar conclusions were drawn in some other studies where analogous measurements and calculations were performed. Knowing the coordinate of the transient maximum and the equation of the theoretical model for instantaneous nucleation [71]

$$(I_{max}t_{max})^2 = 0.065(zF)^2\left(c^3/8\pi V_m N_0^2\right)^{1/2} \quad (3)$$

one can calculate the quantity N_0 and then the rate constant for nucleation k_n. In the above equation, I_{max} is the current in the transient maximum, t_{max} is the time in which the maximum current is reached.

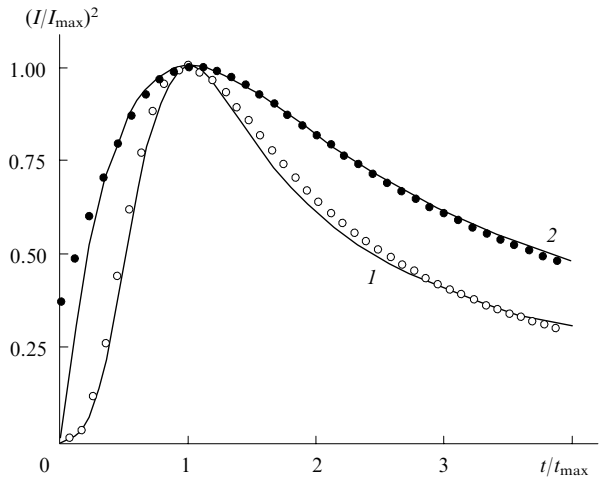


Figure 1. Experimental current transients in the dimensionless coordinates measured during the gold electrocrystallization at the potential of 0.84 (*1*) and 0.64 V (*2*) *vs.* the normal (standard) hydrogen electrode on glassy carbon (points) and calculated transients (curves) for progressive (*1*) and instantaneous (*2*) nucleation.[66]

Direct information on the shape, size and density of nuclei can be acquired by using scanning (SEM) or transmission (TEM) electron microscopic methods and also by probe methods (atomic force/scanning tunnelling microscopy). For the gold deposition at 0.64 V *vs.* the normal hydrogen electrode, the SEM method has demonstrated that the value of N_0 is two orders of magnitude higher than that calculated from Eqn (3).[66] Hence, the model used fails to describe the interaction between the growing particles in this particular case. Such a deviation between calculated and experimental values of N_0 was also mentioned for other cases of electrodeposition,[89 – 97] although there are some examples of agreement between the theory and the experiment.[98, 99] It was noted that not only the density of nuclei but also their size in a given time interval often differ from those expected theoretically.[88] It was noted [100] that the course of transients in the initial moments involving electric double layer charging, adsorption, stepwise electrode process, *etc.* is not entirely clear (these segments are not seen in Fig. 1); furthermore, the nature of nucleation sites, the kinetics of growth of nanoscale nuclei, the size of shielding zones, *i.e.*, regions around the nuclei in which new nuclei cannot be formed, are also insufficiently clear. Thus, the attempts to advance the theory of formation and growth of nanoparticles are still topical.

In addition to this, the experimental methods for studying the nucleation of nanoparticles and the initial stages of their growth are being advanced. First of all, this concerns the methods of adequate visualization of these processes *in situ*, *i.e.*, in the course of electrodeposition.[46, 57, 66, 88, 94 – 96, 101 – 108] Considerable body of information was obtained by the probe techniques although the early stages of nucleation and growth are difficult to characterize on the atomic level by these methods. The electron microscopic observations with real-time video recording open up the challenging prospects. For this purpose, special electrochemical cells to be used inside the electron microscope chamber have been designed.[88, 96, 107, 108] Probably, the TEM gold grid with sputtered carbon holds the highest prospects as the electrode for such electrochemical cells.[88, 108]

Among the unexpected results obtained recently with the use of this method, mention should be made of the bimodal size distribution of silver nanoparticles (on a carbon substrate) observed in the early stages of electrodeposition.[88, 108] As the coarser clusters ($d > 6$ nm) increase in their number and volume, the smaller clusters ($d \approx 1 – 2$ nm) located near the coarse particles do no grow and decrease in number due to their attachment to other clusters. This is an argument in favour of aggregative electrochemical growth mechanism through the surface diffusion and coalescence of nanoclusters. Moreover, it was found that a part of coarse particles ($d > 15$ nm) represent single crystals (even if defective), whereas almost

the same fraction of middle-size clusters ($d = 6-15$ nm) are polycrystalline (with crystal domains of 1–3 nm). This cannot be explained in terms of the classical models of nucleation–growth. The bimodal size distribution of nanoparticles and the aggregation mechanism of their growth were discussed recently by certain research groups in the field of colloid synthesis of nanocrystals.[109,110]

The random nature of nucleation and the difficulties with the quantitative analysis of the electric signal that arises at a large number of growing crystals makes it reasonable to study the electrodeposition on a nanoelectrode that is so small that only one nucleus can form on its surface.[100,104] It should be stressed that measuring the current transients provides information on the nucleation and growth of nanoparticles in time intervals inaccessible for other experimental methods.

To correctly compare the scopes of electrochemical and chemical methods of synthesis of nanoparticles, one should first of all reduce the effect of the substrate nature on the nucleation process, which is quite substantial in the former methods and is absent in the latter case. The substrate effect cannot be totally eliminated but can be mitigated by using substrates with a low surface energy, for instance, the freshly formed (by cleavage) basal face of highly oriented pyrolytic graphite (HOPG), glassy carbon, some other carbon substrates and also silicon.

Penner *et al.* studied the electrodeposition of platinum,[50,57] silver,[52] copper,[54] cadmium[55,111] and zinc[56] on HOPG by the non-contact atomic force microscopy. They have shown that although all of the conditions for instantaneous nucleation and diffusion-controlled growth were fulfilled, the high degree of monodispersion of deposit particles could not be reached and the deviation from the average size increased in the course of deposition (Fig. 2). The following two factors were mentioned as the possible reasons. First, the distribution of nuclei was not totally random due to the presence on the surface of step edges in which the nucleation proceeds easier than on terraces. Second, the diffusion zones of neighbouring nanoparticles on the electrode surface were observed to interact with one another. The latter effect cannot be eliminated by solution stirring (*e.g.*, by using a rotating electrode); however, it can be weakened and the degree of monodispersion can be increased by decreasing the electrode potential (overvoltage) after the initial nuclei have been generated at a high overvoltage, *i.e.*, by using two-step electrodeposition (Fig. 3).[50,112]

The method of two-pulse potentiostatic electrodeposition was pioneered by Sheludko and Todorova[113] and modified many times later (*e.g.*, see Ref. 79). However, it was Penner (see p. 3343 in Ref. 50) who was the first to draw attention to the conditions that would allow for transferring the main ideas of nucleation and growth for metal electrodeposition to the controlled electrosynthesis of nanostructures. He has shown that the growth of monodisperse nanoparticles on HOPG occurs if the nucleation pulse is short and during the second pulse, only the growth of the already formed nuclei can occur, *i.e.*, he stressed the importance of the careful choice of pulse parameters.

This method was successfully used by Plieth *et al.*[69,114] for electrodeposition of silver and gold nanoparticles on indium–tin oxide (ITO). They have also illustrated[115] the choice of pulse parameters for the controlled growth of monodisperse nanoparticles on this substrate. As a result,

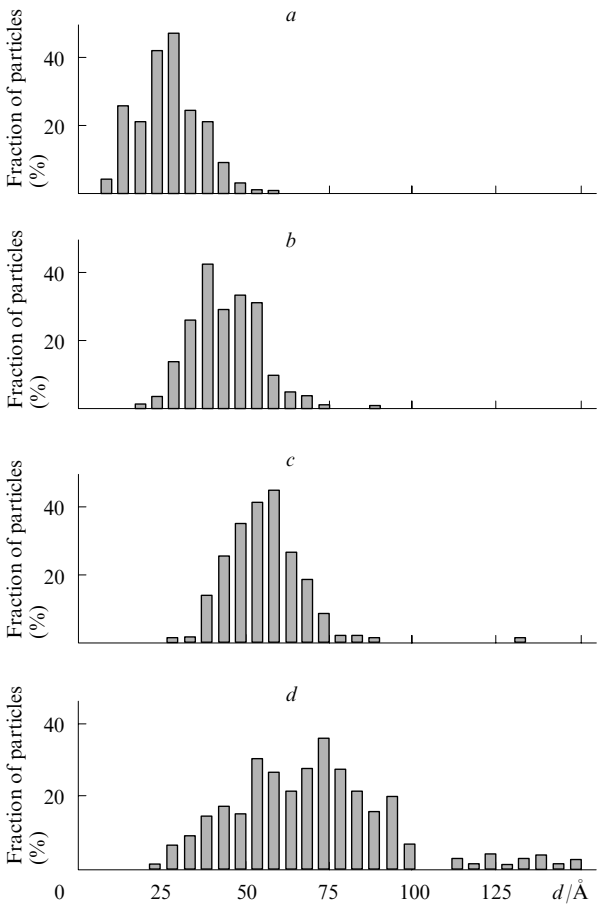


Figure 2. Column diagrams of the size distribution of platinum nanoparticles plotted using the data of non-contact atomic force microscopy at different time intervals after the beginning of deposition.[57]

Fig.	*a*	*b*	*c*	*d*
t/ms	10	50	70	100
d/Å	26	43	54	72
Δd/Å	9	10	11	32

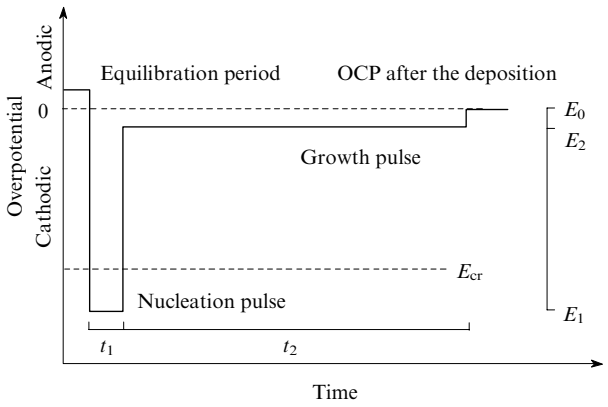


Figure 3. Schematic of potential pulses used to increase the degree of monodispersion of electroplates.
OCP is the open-circuit potential, E_{cr} is the critical nucleation potential, E_0 is the potential after the completion of deposition, E_1 is the nucleus formation potential, E_2 is the nucleus growth potential.

they obtained a material suitable for observing the surface-enhanced Raman signals (SERS). This material was studied by combining the methods of scanning confocal microscopy, Raman spectroscopy and local scanning electron microscopy.[116]

Schiffrin and co-workers[68] synthesized platinum nanoparticles differing in both their diameter and height by using a pulse method and HOPG as the substrate. According to their results, the multipulse method makes it possible to control not only the nucleation and growth but also the substrate properties. Thus, they have demonstrated that the potential-induced hybridization of graphene layers in HOPG affects the kinetics of nucleation.

The courses of nucleation and particle growth depend on the solution composition. This was demonstrated by analyzing the current transients for the platinum deposition on HOPG in the presence of chloride, sulfate and perchlorate anions.[117]

When carbon supports are used, they should be specially pretreated; moreover, attention should be paid to the presence of active redox groups on their surface. These groups can selectively react with precursors and other solution components. Thus, the spontaneous deposition of platinum on HOPG from solutions (both aqueous and non-aqueous) containing $PtCl_6^{2-}$ to afford heterogeneous, randomly arranged nanoparticles,[57, 60, 67, 68, 118] which have a strong effect on further nucleation and growth of nuclei, was described. The nature of spontaneous deposition is still unclear. The preliminary oxidation of HOPG by so-called protective pulse[68] was shown to eliminate the spontaneous deposition of platinum. It is also important to take into account the possible contamination of resulting nanoparticles with carbon particles. This long known phenomenon has attracted again the attention of scientists.[119] Indeed, for electrochemists, HOPG is a very interesting material to be used as the substrate.[120] In particular, this is associated with the presence of the sp^2-carbon structural motif, which is the same for HOPG, carbon nanotubes and graphene. Glassy carbon is also often used as the substrate. Being amorphous, the latter does not induce the formation of a preferential structure of the deposits.

Besides HOPG and glassy carbon, other carbon materials were also used as the substrates in the electrodeposition of nanoparticles, for instance, spectroscopically pure graphite,[121] diamond,[122] Sibunit,[123] and also carbon filaments, nanotubes, and graphene (see Section III).

Indium–tin oxide has high optical transparency (favourable for visualization of nanoparticles and investigation of their optical properties), high electric conductivity, the stability of electrochemical and physical properties and wide electrochemical window; this is why ITO was used as the substrate in many studies mentioned above[69, 114–116] and also in some other works (*e.g.*, see publications[124–131]). For the same reason, attention of scientists was drawn to fluorine-doped tin oxide (FTO).[106] Platinum nanoflowers (Fig. 4) were grown in one-step electrodeposition on ITO.[131] These nanoobjects exhibit enhanced electrocatalytic activity and higher resistance to poisoning in the reaction of methanol electrooxidation as compared with common nanostructured platinum catalysts. Gold nanoparticles synthesized by ITO potential cycling in the gold-plating electrolyte displayed enhanced activity with respect to glucose electrooxidation.[130] It was noted that as the potential corresponding to the cathodic cycling limit decreased at the fixed anodic limit, the average size of nanoparticles increased.

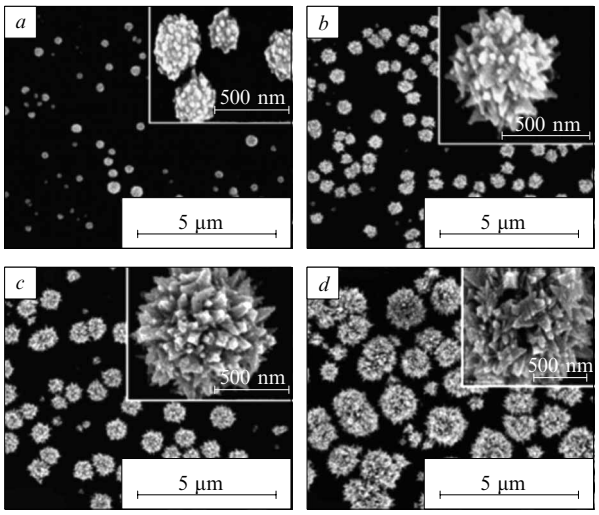


Figure 4. SEM images of Pt nanostructures deposited on ITO at −0.2 V *vs.* the normal calomel electrode from a solution of 3 mM H_2PtCl_6 + 0.5 M H_2SO_4 during various time intervals.[131]
t /s: (*a*) 25, (*b*) 400, (*c*) 1000, (*d*) 40 000.

The wide use of metal/semiconductor junctions in modern electronic devices and the fact that their synthesis involves electrochemical methods have stimulated the detailed studies of the nucleation and growth of metal nanoparticles on typical semiconductors. Most often, semiconducting substrates interact weakly with metal atoms. This makes them similar to the aforementioned carbon substrates. Thus, the deposition of silver on the n-Si(111) and glassy carbon surfaces was compared by analyzing the current transients in combination with atomic force microscopic (AFM) and SEM data.[62] For n-Si, in contrast to glassy carbon, a clear change of the deposition mechanism was observed following increase in the cathodic potential, namely, the progressive mechanism switched to the instantaneous one. The rate of silver deposition was lower on glassy carbon than on silicon. For both substrates, strong dependence of the nucleation-site density on the potential was observed but the calculated number of sites turned out to be one order of magnitude lower on silicon.

The general concepts of metal electrodeposition on the semiconductor surface were considered in a publication[132] where the role of the substrate band structure and the dependence of the electrodeposition mechanism on the metal adatom–semiconductor binding energy and the ratio of interatomic distances in the bulk metal and semiconductor were discussed. The deposition of a series of metals (Au, Cu, Pt) on the surface of n-Si(100)[133] and also on the TaN barrier layer[134] was studied.

Romankiw and co-workers[135] analyzed the nucleation and the growth of gold nuclei on the surface of n-Si(100) in the presence of thallium ions, which were used as the regulating additive in gold electrodeposition. Attention was focused on the density of nucleation sites and the size uniformity of the nuclei. The addition of thallium for galvanosatic electrodeposition led to the formation of dendrite deposits. The highest density of nuclei was observed at high current densities and Tl^+ concentrations.

Additional complications arise when metal substrates with the surface energy higher as compared with substrates considered above are used. As a rule, metal substrates have the high concentration of nucleation sites. The possible deposition at potentials more positive than the equilibrium potential of the metal–metal ions system, so-called underpotential deposition (UPD), should be taken into account (see, *e.g.*, a review [136]). Various surface defects can affect the nucleation of nanoparticles. The crystal lattice of the substrate can also affect the structure of nanoparticles and induce the epitaxial growth of the deposit (Fig. 5). In certain systems, the formation of surface alloys is possible. Additional difficulties arise due to reconstruction of the substrate surface and its lifting. As regards fundamental research, the electrodeposition on well-characterized surfaces, *e.g.*, individual faces of single crystals, is especially fruitful (*e.g.*, see Refs 136–146).

On the substrate, nanoparticles are subjected to ageing, which involves coalescence and decrease in the true surface area. These processes affect the electrocatalytic activity and other properties of the material. Two mechanisms of ageing were discussed. They are called the 'Ostwald ripening' and the 'Smoluchowski ripening'.[88, 147–150] The Ostwald ripening is associated with the growth of coarse particles due to the addition of smaller ones, whereas the Smoluchowski ripening is associated with the diffusion and coalescence of clusters irrespective of their size (aggregation mechanism).

The electrodeposits of platinum metals on various substrates pertain to the most thoroughly studied nanostructured materials described in a vast number of publications and several reviews (one of the latest reviews on the chemical and electrochemical deposition of platinum metals was published by Rao and Trivedi [151]). Most attention is devoted to nanostructured deposits of platinum,[152–158] platinum–ruthenium alloy [159, 160] (due to its high electrocatalytic activity in methanol oxidation) and palladium [123, 161] (as the model hydrogen-sorbing material). One of the most important research topics is elucidation of how the potential affects the deposit properties. Another aspect related to the previous one concerns determination of the deposit structure and defects. The characteristic features of electrodeposits were mentioned such as the decrease in the crystallographic parameter a, high microstrains (especially at higher deposition potentials) and the considerable concentration of dislocations and grain boundaries. The complex nature of electrodeposits calls for further investigations.

Savinova and co-workers [123] have developed a method for selective electrodeposition of palladium (from fractions of monolayer to several monolayers) on carbon-supported gold nanoparticles. The sorption of hydrogen by these materials and their electrocatalytic activity in dihydrogen oxidation were studied. The specific features of the behaviour of palladium monolayers were discussed with attention drawn to the presence of microstrains and defects that can give rise to changes in the density of states in the d-band of the palladium band structure (the geometric factor). The important role is given to electronic interactions with a gold nanoparticle (the ligand effect in terms of the Norskov model [162]). Finally, the surface reactivity of the Pd/Au system depends on the assembly effect, *i.e.*, the formation of various Pd_xAu_y assemblies, which generate a set of states of the system with different adsorption energies.

Natter, Hempelmann and co-workers [163–168] have developed a method for electrosynthesis of compact nanocrystalline metals and alloys with the controlled size of nanocrystals in aqueous and non-aqueous electrolyte solutions by applying high-density current pulses to the electrochemical cell. Varying the current density changes the overpotential that determined the nucleus size. After a short pulse of metal deposition, the circuit was opened for a 5–100 ms period. In this period, the initial solution concentration near the substrate is restored and also the coalescence of nanoparticles is possible, *i.e.*, the length of open-circuit period affects the crystal size. The additional options for controlling the crystal size are offered by the introduction of various compounds to the solution and variation of the temperature and hydrodynamic conditions. The studies in this field have been surveyed.[169] The pulse electrodeposition was also used in other studies for synthesizing metal nanocrystals (see, *e.g.*, Refs 170–173). Under certain conditions, nanocrystalline compact deposits can be synthesized also by the uninterrupted direct-current procedure.[174]

Specific problems are faced in the electrosynthesis of other types of nanomaterials. Thus, in the electrosynthesis of continuous nanofilms, the important role is played by coalescence of nanoislets. The latter grow mainly by the isotropic mechanism and the nanofilm thickness is determined by the islet height at the moment of their coalescence. In the thin-film technology, it is important that high density can be reached for nanoislets having small thickness.[175, 176]

At present, the nanowires have gained in popularity, which led to the development of a method for electrodeposition of materials of this type. An important charac-

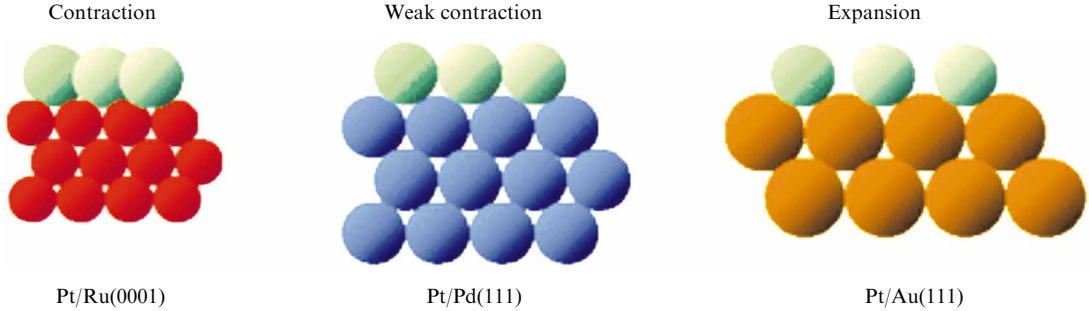


Figure 5. Models of pseudomorphous Pt layers on different surfaces.

teristic of nanowires is the aspect ratio. The researchers focus on electrosynthesis of nanowires with not only the desired diameter but also the specified aspect ratio.

Penner and co-workers [177–179] proposed two methods for electrosynthesis of Mo, Cu, Ni, Au and Pd nanowires, which were both based on the preferential electrodeposition of nanoparticles on the edges of steps of the HOPG basal face (Fig. 6) and were given the name of the electrochemical step edge decoration (ESED). One method consists of the direct electrodeposition of metal clusters on the steps. In the other method, the conducting metal oxide is the first to be deposited, which is followed by the reduction of the resulting metal oxide nanowire to the metal. It was shown that oxides are often deposited on the steps more efficiently than metals; hence, the latter method may be more advantageous. Figure 7 shows the SEM images of copper nanowires grown on HOPG by the step edge decoration method.

The idea of decoration as such is not new. It was used in the physical vapour deposition (PVD) of nanowires. Clavilier, Feliu and Aldaz [180] interpreted the peaks in the Pt(332) voltammograms in solutions containing bismuth ions as the result of ESED on this face. Nichols, Kolb and Behm [181] provided a direct substantiation of the decoration based on the data of scanning tunnelling microscopy.

A special method for electrodeposition of nanowires of palladium and conducting polymers in specially designed microcells was developed.[182, 183] Polymer nanowires are very promising, particularly, for sensor applications.[184] The three-pulse method which included an activating oxidative pulse, a nucleation pulse, and a growth pulse was used for the preparation of arrays of Pd–Ni nanowires on

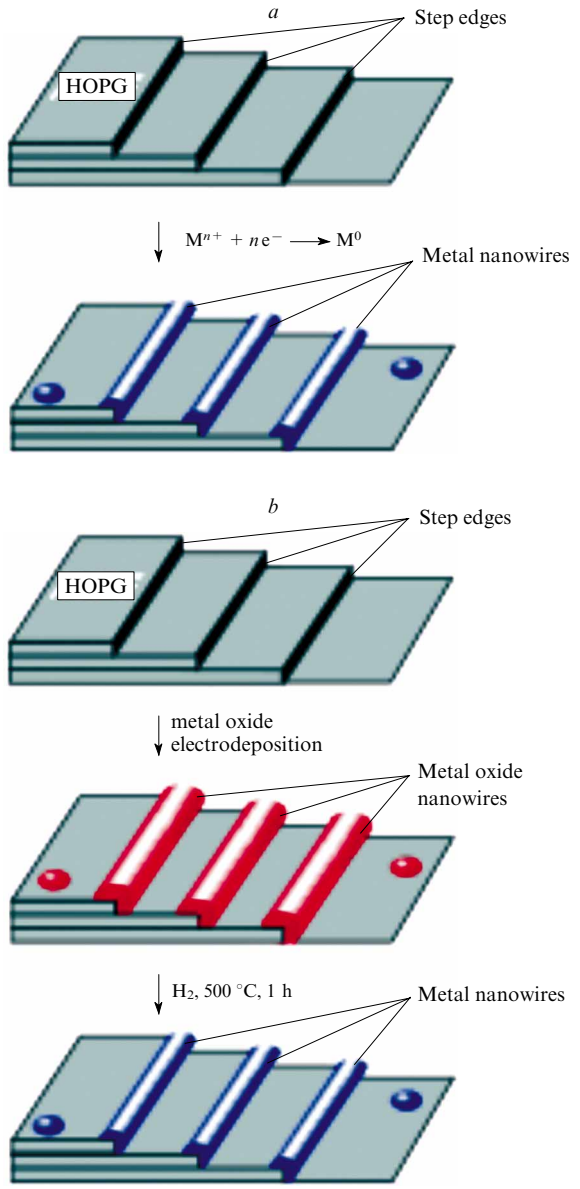


Figure 6. Illustration of two ways of deposition (*a*, *b*) of metal nanowires on HOPG, based on electrochemical decoration of steps.[177]

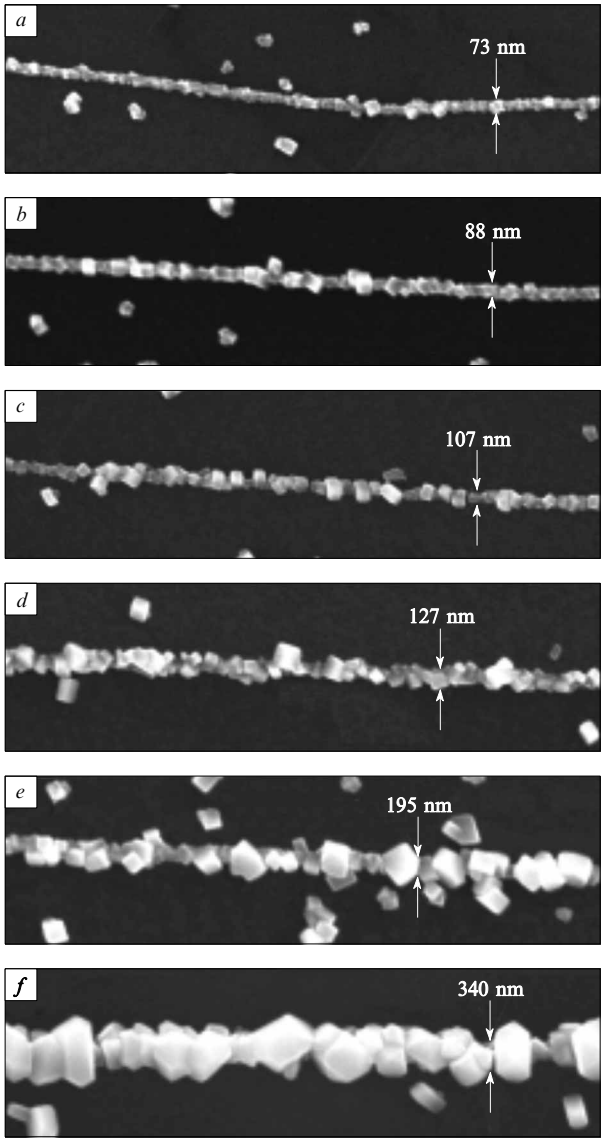


Figure 7. SEM images of copper nanowires deposited on HOPG at the nucleation potential of −0.8 V *vs.* normal calomel electrode and the growth potential of −5 mV.[177]
The time of nanowire growth /s (*a*) 120, (*b*) 180, (*c*) 300, (*d*) 600, (*e*) 900, (*f*) 2700.

HOPG.[185] The formation of nanoparticles on the terraces was avoided due to the correct choice of the nucleation and growth pulses.

The cathodic deposition of metals from aqueous solutions is often accompanied by the evolution of molecular hydrogen. This phenomenon was shown [70] to narrow down the size distribution of certain metal nanoparticles. This was ascribed to the template effect of hydrogen microbubbles, which screen a part of the surface thus preventing nucleation on it. The formation of metal foams upon the hydrogen evolution was demonstrated.[186–188] Gas microbubbles not only serve as the templates but also promote the nanoparticle detachment from the surface and flotation. Foams are open highly porous structures with pore walls formed by the fractal (dendrite) deposits. It was proposed to use copper–tin foam as the negative electrode in lithium cells.

Copper nanopowders easily detachable from the copper electrode were synthesized by the electrodeposition at a constant current.[189] It cannot be ruled out that this electrosynthesis was accompanied by hydrogen evolution.

Other processes accompanied by gas evolution were also used in the synthesis of nanostructures. Thus, it was shown [190] that the yttrium oxide nanotube material can be manufactured with simultaneous nitrous oxide reduction process to afford nitrogen microbubbles.

The electrochemical evolution of hydrogen is accompanied by pH change in the near-electrode layer. This undesired complication may be beneficial for the electrosynthesis of self-assembled oxide and hydroxide nanostructures. Thus, this electrochemically generated acid-base catalysis was used in the sol–gel deposition of zirconium oxide films.[191] Yet another example is the electrosynthesis of ZnO nanofilms (nanowalls, nanodisks, nanospikes, nanocolumns) on ITO from zinc nitrate solutions.[192] The pH variation was achieved by the parallel electroreduction of nitrate anions. The synthesized materials were crystalline wurtzite structures totally analogous to those observed in the vapour deposition of ZnO, although the coating of nanoparticles consisted of the $Zn(OH)_2$ layer. The pH variations were used in the deposition of α-Fe_2O_3 doped with molybdenum or chromium, which was destined for photoanodes of water decomposition.[193]

Attention is drawn to the use of ultrasound during electrodeposition. This favours the formation of fine metal particles and their detachment from the substrate. Such sonoelectrochemical method is analogous to the sonochemical synthesis of nanoparticles and nanopowders.[194–196] The modified sonoelectrochemical synthesis represents the pulse electrodeposition accompanied by the pulse sonication. The cathode called here the sonotrode simultaneously provides the current and ultrasonic pulses. This made it possible to obtain pure zinc nanopowders without adding any stabilizers and to prepare magnetic nanopowders of binary and even ternary alloys containing iron, cobalt and nickel. Supersonic treatment provides the removal of nanomaterials from the surface. The device developed by Reisse and coworkers [196] was used in electrosynthesis of nanoparticles of cadmium selenide [197] and lead selenide (12 nm in diameter).[198]

The electrodeposition is widely used for the synthesis of nanostructures of conducting polymers. Studies along this line have been surveyed.[199] It is known that at sufficiently positive electrode potentials, certain monomers such as aniline and pyrrole are electrooxidized to form radical cations and other active species, which initiate the polymerization process and, as a consequence, give rise to polymer films on the electrode. At the proper choice of electrosynthetic conditions, one can obtain polymer nanoparticles, nanowires or arrays of nanowires. Polymer films can be synthesized with the use of cyclic voltammetry (CV) and also by potentiostatic, galvanostatic or pulse potentiostatic methods.

The electrochemical fractal growth of the polyaniline (PANI) layer on pyrolytic graphite was accomplished.[200] Measuring current transients in the millisecond range revealed the presence of instantaneous nucleation in the region of more positive potentials. The polypyrrole–Fe nanocomposite which combined the specific properties of polypyrrole with magnetic properties of iron was synthesized [201] by the co-deposition of components under galvanostatic conditions with square-wave potential pulses.

The electrophoretic deposition, which is widely used for deposition of colloids on substrates,[202] was adapted to the preparation of thin films of nanocomposites.[203] This method was used for synthesizing the conducting polymer–metal oxide nanocomposite with the core–shell structure.[204]

To conclude this section, it should be noted that in addition to the electrodeposition, the reverse method, the anodic dissolution, was also used to prepare nanostructures. The latter method is usually referred to as etching. In particular, the nanowires [205] and nanoelectrodes [206] were thus synthesized. The controlled reduction of arsenic, gold and Bi_2O_3 nanowire diameters by electrochemical etching was described.[207]

III. Template, quasitemplate and epitaxial electrodeposition

The advantages of template-assisted electrodeposition methods over the other methods of synthesis of nanomaterials and porous structures and also over conventional electrodeposition (see above) are as follows: the process is carried out under mild conditions (at ambient temperatures and pressures) and requires no expensive equipment, the reaction rates are relatively high, the material morphology is unambiguously determined by the shape of template pores, the parameters of the material are dictated by the size of these pores and the quantity of electricity passed; moreover, two (or more) components can be deposited in a membrane to form multisegmented material. The template electrosynthesis is suitable for preparation of nanowires with the desired aspect ratio.

Ozin [208] surveyed the early template-assisted methods (with reference to nanoelectrochemistry). Mirkin and coworkers [16] analyzed in detail the template-assisted methods including those using electrodeposition. The latter review reflected the progress in the development of template-assisted methods and noted the considerable increase in the number of template types. A special review [209] was devoted to the template electrosynthesis of nanomaterials and porous structures. Examples of template electrodeposition of nanomaterials from conducting polymers can be found in paper by Malinauskas *et al.*[199] Jackowska *et al.*[210] discussed the use of so-called hard templates for the chemical synthesis and electrosynthesis of nanostructures of conducting polymers.

At present, the template electrodeposition makes use of a large number of various templates; the main types are discussed below.

The commercially available track membranes of polycarbonate and polyester or thin mica films with metal sputtered on one side were used to grow metal nanowires and nanotubes by electrodeposition.[209, 211 – 214] A method of electrosynthesis of SnO_2 nanotubes with a controlled diameter and length in porous polycarbonate membranes (pore diameter of 50 or 100 nm, pore density of 6×10^8 cm^{-2}) was proposed.[215] A solution of tin chloride and sodium nitrate acidified with nitric acid was used as the electrolyte. Insofar as the reduction of nitrate anions consumes hydrogen ions, the solution becomes alkaline and SnO_2 is deposited on the pore walls to afford nanotubes. The aspect ratio of nanotubes is controlled by varying the duration of electrolysis. The template-assisted electrosynthesis of $Ag(Ag_3O_4)_2NO_3$ nanowires in a polycarbonate matrix[216] can be considered as an example of the anodic template-assisted electrodeposition. The synthesized nanowires exhibited a high antibiotic activity due to the high oxidation state of silver and the large surface-to-volume ratio.

Another frequently used template is anodic aluminium oxide (AAO) or nanoporous alumina which has been known for more than 100 years; however, it is in the past decade that this material became so popular.[217] In a certain respect, this template is perfect, because the channels of its pores are perpendicular to the surface. Moreover, aluminium is easily dissolved and removed from the nanomaterial. This highly porous self-assembled structure can be synthesized by the two-step anodization technique.[218] The uniform cylindrical channels in AAO are arranged according to the hexagonal pattern. The pore diameters, the distance between them and the porous layer thickness can be controlled by varying the electrolyte composition for anodization, the potential and the time.

Template-assisted synthesis with anodized aluminium was used for potentiostatic deposition of platinum (Fig. 8), Pt – Ru (Ref. 219) and Ni (Ref. 220). The aluminium template was used[221] to prepare multisegmented nanowires gold – polypyrrole – nickel – gold which have found application in photonic devices and gas sensors. CoPt nanowires with different aspect ratios were electrodeposited into membranes of polycarbonate and AAO and the evolution of the nanowires with the deposition time was followed.[222] The magnetic properties of the wires were shown to depend on the aspect ratio and the membrane type.

Whitesides and co-workers[223] have developed the electrosynthesis of core – shell (PANI – Au) nanostructures and multisegmented (Au – PANI and Ni – Au – PANI) nanostructures with the use of AAO membranes.

Recently, attempts were undertaken to develop the theory of metal electrodeposition in AAO pores. Thus, Bograchev, Volgin and Davydov[224, 225] have developed the model of electrochemical growth of nanowires in AAO, which takes into account the ion transfer in the varying diffusion layers inside and above the pores and also the kinetics of electrochemical discharge of ions. With certain simplifications, one can obtain analytical equations for calculating the current *vs.* time dependences, the time it takes for the pores to be filled and other parameters. It was shown that the results of calculations adequately match the experimental data.

The possibility of electrosynthesizing self-assembled TiO_2 nanotubes was demonstrated.[226] Schmuki and co-workers[227, 228] have found the conditions for electrochemical synthesis of TiO_2 nanotubes with a high aspect ratio, which can be used as templates in the synthesis of nanostructures. The arrays of nanotubes with smooth walls and the titanium dioxide membranes were synthesized by electrochemical methods.[229] The use of various dopants made it possible to electrosynthesize modified nanotubes of TiO_2 with a wide range of applications.[230] The methods were developed for synthesizing nanotube materials from other valve metals (metals capable of forming the barrier oxide layers on their surface) and alloys.[231] The use of these materials opens up new prospects for template-assisted electrosynthesis. Nanotubes of TiO_2 were filled with CdS

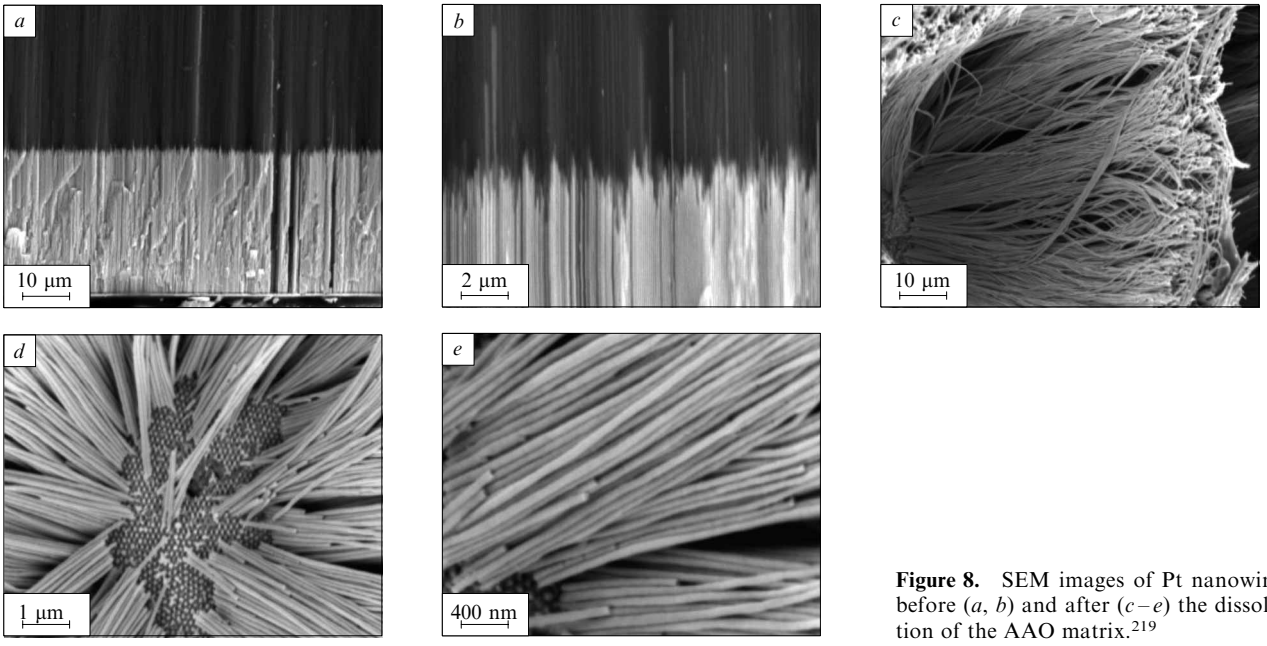


Figure 8. SEM images of Pt nanowires before (*a*, *b*) and after (*c* – *e*) the dissolution of the AAO matrix.[219]

nanoparticles by using both the conventional electrochemical method and its combination with the sonoelectrochemical method.[232]

Hepel *et al.*[233] used the oxide layer thermally prepared on titanium; the layer was electrochemically treated[234] in order to deposit a Pt—Ru catalyst. This catalyst exhibited the enhanced electrocatalytic activity with respect to methanol electrooxidation, being present in extremely low amounts.

The specific features of zeolites such as the presence of open pores and cavities make them suitable for template-assisted electrodespotion.[235] Dryfe and co-workers[236] proposed the electrochemical method for incorporating 1 nm platinum clusters into zeolite membranes and demonstrated the efficiency of this approach for optimizing electrocatalysts.

Mesoporous layers of silicon dioxide with vertically oriented mesochannels were used[237] as the templates for electrosynthesis of polycrystalline gold nanowires.

Among the templates used in electrosynthesis of ordered porous structures, mention should be made of colloid crystals, *i.e.*, regular and periodic arrays of particles with translational symmetry.[238] Usually, these are the spherical SiO_2 particles[239] or polymers.[240] The former are often prepared by, *e.g.*, hydrolysis of tetraalkylorthosilicates, while the latter are synthesized by the emulsion polymerization. Assemblies of colloid crystals were deposited on substrates by the methods of sedimentation and vertical deposition, sometimes with sonication. After evaporation of the solvent, these templates are ready for the deposition of nanomaterial into their pores.

Mandler and co-workers[241] proposed a method for electrodeposition of a sol–gel template on ITO or steel by using variations of the the local solution pH near the electrode during the electrolysis (the pH varied as a result of discharge of hydrogen ions and water molecules, the reduction of nitrate anions and other processes). The pH variations triggered the processes of hydrolysis and condensation of organic silicon derivatives to afford the sol–gel matrix on the electrode surface. Later this method was used in the co-deposition of a sol–gel matrix and metal nanoparticles.[242, 243] In the latter cases, the deposition on the electrode surface was initiated by pH variations caused by electroreduction of added protic solvents. To obtain uniform defect-free layers, tetramethylsiloxane should be added to the solution. It was shown that the potential value, the concentration ratio of tetramethylsiloxane and nanoparticles and also the nature of substrate substantially affect the nanoparticle aggregation and density in the nanocomposite. Applying a positive potential to the nanocomposite layer led to the dissolution of metal nanoparticles to form cavities and channels in the layer and changed its permeability.

Attard, Bartlett, *et al.*[244] proposed using lyotropic liquid-crystalline mesophases as the templates in electrosynthesis of nanostructures and later used them in a series of studies.[245–252] The lyotropic mesophases are divided into the following main categories: hexagonal (H_1), cubic ($Ia3d$) and lamellar (L_α). A template based on the hexagonal mesophase was used to prepare a platinized platinum microelectrode with the uniquely high real surface area and palladium deposits with real surface area reaching 91 $m^2\ g^{-1}$ (assessed with respect to oxygen adsorption).[252] During hydrogen adsorption, this deposit undergoes $\alpha-\beta$ phase transitions without loss of the nanostructure.

Mesophases of all three types of lyotropic liquid crystals built from block copolymers (polystyrene–polyethylene oxide) were used[253] to synthesize platinum nanocrystals. Mesoporous Pt–Au alloy was synthesized[254] in a liquid-crystalline template; in the process, the phase segregation typical of this system was avoided.

A liquid-crystalline template was employed[255] for the deposition of Pt–Ru nanoparticles on carbon paper. The time evolution of the mesostructure was followed and its mechanism was proposed, which allows the use of this method in the template deposition of other bimetallic systems.

A strategy based on electrostatic binding of the precursor to the template followed by the electrochemical transformation of the resulting complex extends the possibilities of nanoparticle synthesis. As the templates, it is possible to use DNA molecules[256] adsorbed on a self-assembled thiol layer. The addition of aniline to the solution and its electrochemical polymerization made it possible to synthesize PANI nanowires. A PANI monolayer was deposited by anodic polymerization on the hydroxylated surfaces of quartz, glass, ITO and silica.[257] The surfaces were preliminarily covered with a mercaptoethanesulfonate monolayer, to which aniline was electrostacally linked, and then the layer was subjected to electrochemical polymerization.

The synthesis of nanowires by the photolithography technique in combination with electrodeposition was proposed[258] and further developed.[259, 260] This method served to prepare nanowires of Au, Ag, Bi, Pd, Pt,[261] PdTe and CdSe (Refs 262, 263) and also of polyethylenedioxythiophene (PEDOT).[264] Complex micro/nanostructures were synthesized by a combination of the electrodeposition method, the lithographic techniques (including 'soft lithography'[265]), the template techniques and by forming self-assembled monolayers on the surfaces.[266–271]

Carbon nanotubes attract attention of scientists due to their unique structural, mechanical and electronic properties.[272] In certain studies they were used as the substrates in electrodeposition of nanoparticles to be used for electrocatalysis and sensors. According to the results of several studies,[273–277] single-walled carbon nanotubes can serve as the templates in electrodeposition, which was confirmed, among other factors, by the analysis of microscopic data, current transients for the potentiostatic deposition of Ag, Au, Pt, Pd and size distributions of nanoparticles. Carbon paper based on carbon nanotubes was used[278] as the substrate in the electrodeposition of MnO_2 nanowires. The synthesis was carried under CV conditions. The synthesized composite exhibited a high specific capacity and cyclability, which makes it a suitable meterial for flexible electrodes in supercapacitors.

A pulse electrodeposition procedure was proposed[279] in which the concentration was levelled off in the periods between pulses. This allowed nanowires to be synthesized in self-assembled single-walled carbon nanotubes. This method was used to obtain continuous gold nanowires with different geometry (parallel arrays, serpentines, spirals) and also Bi_2Te_3. The proposed procedure was named 'drawing with nanotubes'. A group of authors[280] succeeded in deposition of arrays of CdSe nanowires, serpentines and loops. Such nanowires exhibited considerable photolumi-

nescence and photoconductivity and, hence, they are the candidates for the use in photodetectors.

A homogeneous graphene–polypyrrole nanocomposite was synthesized by pulse electrochemical polymerization.[281] It exhibited high characteristics as the electrode in a supercapacitor.

The method in which the nanomaterials and the matrix are co-deposited is sometimes referred to as the assisted electrodeposition. It should be stressed that in some cases, it is difficult to draw a borderline between the template electrodeposition and, *e.g.*, the molecular-assisted electrodeposition. Thus, several studies were devoted to electrodeposition of nanoparticles on films of conducting polymers.[257, 282 – 284] In certain cases, it was noted that the polymer layer plays not only the role of the conducting substrate but also catalyzes the discharge of the precursor. Furthermore, the pores in the conducting polymer film could determine the deposit structure.

The method of quasitemplate deposition with the use of the polymer matrix furnished a palladium deposit with a high specific surface area.[285]

The electrochemical deposition of the Ni/montmorillonite composite on steel and copper and the structural analysis of resulting deposits were carried out.[286] Template deposition with the use of clays to afford a platinum catalyst was described.[287] In this case, the term 'quasitemplate' seems to be more appropriate, because the negatively charged precursor (a Pt^{IV} chloride complex) can hardly penetrate into inner voids of the clay structure, which is also negatively charged.

Comparison of the electrodeposition of platinum on glassy carbon and polycrystalline platinum in the presence of Keggin type heteropoly acids has shown [288] that the layer of heteropolytungstate anions exhibits template properties. For various tungstates, it was demonstrated [289] that the comparative study of the behaviour of isopolytungstate-modified smooth and platinized platinum allows more in-depth analysis of the porous structure and the properties of pores of diameter $< 1.5 – 2$ nm.

The strategy of electrochemical co-deposition of a matrix-forming polymer with semiconductor nanoparticles (CdS, CdTe) was used.[290]

In electrodeposition, in addition to template-forming substances, the surfactants with shape-inducing properties were used. Thus, in micelles, in the presence of a shape-inducing additive, gold nanorods with different aspect ratios and different light absorption spectra were synthesized by the electrochemical procedure.[291] Silver nanoparticles were synthesized [125] by electrodeposition in the presence of poly(*N*-vinylpyrrolidone) and sodium dodecylbenzenesulfonate. On stirring of the solution (or sonication), a stable colloid solution of silver nanoparticles was formed.

Palladium nanostructures with a controlled morphology were synthesized by the sonoelectrochemical method in the presence of polyvinylpyrrolidone and hexadecyltrimethylammonium [292] and then used in ethanol electrooxidation. The sonoelectrochemical synthesis of copper nanoparticles in the presence of polyvinylpyrrolidone, polyvinyl alcohol and cetyltrimethylammonium bromide was described.[293] Zinc oxide was synthesized [294] in the presence of sodium dodecyl sulfate and cetyltrimethylammonium bromide from a nitrate bath (the alkalization method). A mesoporous WO_3 film was electrodeposited [295] from a tungsten peroxo complex in the presence of sodium dodecyl sulfate (the structure-forming agent).

Abdelmoti and Zamborini [296] studied the electrodeposition of gold nanorods from a solution containing $AuCl_4^-$ with an addition of cetyltrimethylammonium bromide on the ITO surface functionalized with mercaptopropylmethoxysilane. It was demonstrated that such structures deposited directly on the surface substantially differ from those obtained after the preliminary deposition of gold nanoparticles. The nanoparticles served as the nuclei of the new phase. This method was proposed with the aim of optimizing the structure of nanorods to be used in optical and electrochemical devices.

The quasitemplate electrosynthesis in the presence of several additives is very promising; however, its mechanism is still unclear and should be studied further.

It was mentioned above that attention of scientists is attracted by the ordered UPD monolayers formed by metal atoms on single-crystal faces and also by the synthesis of epitaxial nanofilms based on them. The growth of these nanofilms can be considered as an example of template-assisted deposition in which the single-crystal face serves as the template. Certain research groups are successfully developing the method of epitaxial electrodeposition of complex nanomaterials (*e.g.*, see Refs 297 – 306). Thus, Switzer and co-workers carried out epitaxial electrodeposition of Bi_2O_3,[297] PbS,[299] ZnO,[302] SnS,[304] Co_3O_4 [305]) on gold single-crystal faces. Single-crystalline Co_3O_4 is of interest as a catalyst of the oxygen electroevolution reactions. Stickney and co-workers [306] demonstrated the possibility of epitaxial deposition of $CuInSe_2$, Cu_2Se and InSe on the gold surface.

IV. Methods of electroless deposition and galvanic displacement. Synthesis of core – shell nanostructures

The methods related to electrodeposition, namely, the electroless plating/deposition (also called the autocatalytic deposition) [§] and the galvanic displacement are now widely used to synthesize nanostructures.

The electroless deposition has long been used for deposition of metal films on surfaces of dielectric or catalytically inactive materials from the properly chosen solutions of precursors. The catalytic sites are preliminarily formed on the substrate (the surface activation step). In the classical version, these sites represent palladium clusters obtained by, *e.g.*, the reduction of Pd^{II} by tin(II) salts. Then, on the activated surface, the required metal is deposited from a solution containing its salt and a salt of tin(II) or some other reducing agent. Relatively recently it was shown [307] that the clusters formed in the $Pd^{II} + Sn^{II}$ reaction have the core – shell structure: the core consists of the $Pd_{1-x}Sn_x$ alloy ($x = 0.6 – 1$) and the shell has a higher tin content (up to pure tin). Palladium serves as the universal catalyst in electroless deposition. In certain cases, other nanoparticles can also be used as the catalysts. Thus, for catalyzing the electroless deposition of copper on dielectrics, Vaskelic *et al.*[308] used silver nanoparticles obtained by the reduction of Ag^+ cations with Sn^{2+} ions. These clusters consisted of silver atoms and SnO_2.

§ In the Russian literature, the term 'chemical deposition' is often used for this method.

Different versions of electroless deposition were used in many studies. Thus, the procedure of two-step sensitization–activation was proposed [309] for electroless deposition of platinum nanoparticles on multiwalled carbon nanotubes. Osaka and co-workers [310] developed the procedure of electroless deposition of nickel in a liquid-crystalline matrix. An original method was proposed [311] for synthesizing Ag/MnO_x nanodomains on a carbon substrate in which MnO_4^- ions were reduced in their reaction with carbon and the resulting nanosized MnO_x particles served as the deposition sites for silver nanoparticles.

In its conventional form, the method of galvanic displacement is based on a redox process like the following:

$$M(1) + \frac{n}{z} M(2)^{z+} \longrightarrow M(1)^{n+} + \frac{n}{z} M(2)$$

where M(1) and M(2) are different metals, $M(1)^{n+}$ and $M(2)^{z+}$ are the corresponding ions. This method was long known and used (sometimes under the name 'cementation') for M(1) in the bulk (3D) form. The galvanic displacement, like electroless deposition, requires no external current source but in contrast to the latter method, it does not require a reducing agent either.

The driving force of the galvanic displacement is the positive difference between redox potentials of the deposited [M(2)] and sacrificial [M(1)] metals.

The solution composition and concentration are important factors. By using tables of standard redox potentials and the Nernst equation for the potential drop at the interface, it is possible to obtain the criteria for selecting participants for the galvanic displacement process.

Brancovic, Wang and Adzic [312, 313] and also Weaver and co-workers [314] put forward a version of galvanic displacement restricted to the M(1) monolayer [M(1) in the 2D form]. In this procedure, the sacrificial element M(1) is applied as a UPD monolayer on a conducting substrate; subsequently, this monolayer is spontaneously displaced by the M(2) monolayer in a solution containing $M(2)^{z+}$ ions, the electric circuit being open. The authors [312, 313] used copper UPD on the Au(111) surface for the deposition of a platinum submonolayer, a palladium monolayer and a silver bilayer. Weaver and co-workers [314] used roughened (SERS-active) gold as the substrate, where copper (or lead) served as the sacrificial metal, the transition metal precursors were H_2PtCl_6, K_2PtCl_4, $PdCl_2$, and also Rh^{III} and Ir^{IV} salts. The redox displacement of copper which utilized Pt^{IV} furnished incomplete platinum coatings so that almost eight displacement cycles were needed to obtain a continuous platinum film. At the same time, the use of Pt^{II} afforded a more uniform continuous monolayer as soon as in the first displacement cycle. Platinum and palladium synthesized by the displacement method demonstrated the enhanced Raman responses exceeding those collected for electroplates of platinum metals.

Weaver and co-workers [315] used galvanic displacement for the deposition of platinum and palladium on colloid gold particles synthesized by the standard procedure. The nanoparticles were deposited on the ITO modified with 3-aminopropyltriethoxysilane. The resulting particles with the core–shell structure exhibited a voltammetric response typical of platinum and palladium and were SERS-active. The galvanic displacement was also applied by other authors,[316, 317] who used a copper electroplate deposited (with coulometric control) on gold nanoparticles.

Dong and co-workers [318] utilized an analogous procedure [315] of galvanic displacement of copper adatoms for the deposition of an ultrathin platinum layer on gold colloid particles synthesized by the liquid-phase chemical method and grafted on the ITO surface, in order to optimize the oxygen electroreduction catalyst.

Adzic and co-workers [319] employed the phenomenon of spontaneous deposition of platinum on ruthenium they had discovered and also the deposition and galvanic displacement of a copper adlayer by platinum with the aim of synthesizing ruthenium nanoparticles covered with an ultrathin platinum layer. Later,[320] they used galvanic displacement for the deposition of a platinum monolayer on carbon-supported palladium nanoparticles. In fact, the aforementioned studies [318–320] can be considered as examples of the use of galvanic displacement for synthesizing nanomaterials consisting of core–shell nanoparticles.

Platinum [321] and palladium [322] were deposited on several well-characterized substrates [Ru(0001), Rh(111), Ir(111), Pt(111), Au(111) faces] by the galvanic displacement technique and then tested in the reaction of oxygen electroreduction. The highest activity was observed for the Pd/Pt(111) pair. A platinum monolayer or mixed monolayers of platinum with other transition metals (Au, Pd, Ir, Ru, Rh, Re, Os) deposited on the Pd(111) surface were used [323] in oxygen electroreduction. Some of these alloys demonstrated a 20-fold increase in the activity as compared with conventional totally platinum catalysts.

Adzic and co-workers [324] developed a method for deposition of Pt–Ru plates on the carbon substrate pretreated by special procedures (oxidation by ammonium persulfate, dipping into a solution containing Pb^{2+} to form the adsorbed layer of lead ions and the cathodic reduction of these ions). After this, the electrode was immersed into a solution of platinum and ruthenium salts in order to replace fine-grain lead by these noble metals. The $Ru_{ML}/Pt/C$ (ML is the monolayer) catalyst, which was also prepared by the galvanic displacement of copper adatoms, exhibited a very high activity in the methanol electrooxidation reaction.

Dimitrov and co-workers [325, 326] have developed a method in which a sacrificial lead layer was used for the deposition of epitaxial silver nanofilms (35 adlayers thick) on the surface of Au(111) and also of copper nanofilms (up to 100 atomic layers) on the surfaces of Ag(111) and Au(111). In these processes, the sacrificial monolayers were successively deposited and displaced. The reaction of galvanic displacement was analyzed by taking into account the difference in the atomic sizes of the sacrificial metal and the metal to be deposited, for instance,

$$Pb^0 + k\,(2/1)\,Ag^+ \longrightarrow Pb^{2+} + k\,(2/1)\,Ag^0$$

where 1 and 2 are the oxidation states of elements before and after the displacement for Ag and Pb, respectively. The coefficient $k = d_{Ag}/d_{Pb}$ takes into account the difference in the numbers of adatoms (d) that can fit 1 cm^2 for the elements (Ag and Pb) involved in the displacement reaction; in the case under consideration, k lies in the range of 0.74 – 0.79, *i.e.*, the limiting amount of silver that can be deposited in one run of displacement of the lead monolayer is $\sim$ 1.6 monolayers.

Dimitrov and co-workers [327] deposited platinum on single-crystalline and polycrystalline gold by utilizing copper and lead adatoms. They have found that the layer roughness did not increase after the deposition of 10 platinum layers and that the crystallographic orientation remained unchanged. Even the first platinum layer behaved as pure platinum in voltammetric measurements. Spectroscopic methods revealed the presence of up to 4 at.% Pb and up to 13 at.% Cu in the deposits. The peculiarities caused by the formation of Cu^+ ions and the effect of traces of dissolved oxygen on the galvanic displacement process were revealed. It was concluded that lead adatoms may be more favourable for the galvanic displacement.

Stickney and co-workers [328] also employed successive cycles of galvanic displacement of copper adatoms in order to grow an epitaxial platinum nanofilm on the Au(111) surface. For this method, the name 'electrochemical atomic layer epitaxy' was proposed and the galvanic displacement of the sacrificial metal monolayer is now called the 'surface-limited redox replacement reaction'. It was found that the preliminary formation of an I^- layer on gold makes easier the growth of a uniform copper layer and its subsequent complete replacement by the platinum monolayer with the adsorbed I^- monolayer on the top. Later, this method was also developed by several scientific groups.[325–336]

The process of galvanic displacement involves the following succession of operations:

— electrode pretreatment;

— washing of the system from the solution in which the pretreatment was carried out;

— introduction of the solution for deposition of the sacrificial monolayer;

— washing of the system from this solution;

— introduction of the solution containing ions of the substituent metal;

— washing of the system.

The works mentioned above [325–336] employed a special flow-through electrochemical cell which provided the automated standardized run of the mentioned operations and the thorough cleaning of solutions from oxygen, which might have affected the results of galvanic displacement. Such a setup can be considered as a part of the process flow diagram for the synthesis of nanofilms by galvanic displacement.

The automated flow-through system was used by Cukrowski and co-workers [337] to manufacture multilayer Pt–Ru catalysts on glassy carbon with high characteristics in methanol electrooxidation. The possibility of synthesizing multilayer catalysts provided by the galvanic displacement method was used [338] to fabricate the layered Au/Pt/Au catalyst of formic acid electrooxidation.

The galvanic displacement method was used in a series of studies performed by the research group of Kokkinidis and Sotiropoulos.[339–345] Myung and co-workers have developed the synthesis of films of Bi, Te [346] and Bi_xTe_y intermetallic [347] on the $Pt/Ti/SiO_2/Si$ substrate covered with thin sacrificial layers of Ni, Co and Fe. The synthesis was accompanied by simultaneous monitoring of the open-circuit potential. They observed the strong dependences of the film morphology and crystal structure on the nature of the sacrificial metal. Galvanic displacement was used [348] in the deposition of silver on the aluminium alloy with a low copper content, the preparation of a nanoporous copper layer on the nickel substrate [349] and the deposition of palladium on copper-modified graphite.[350] In the latter case, the galvanic displacement was carried out with the simultaneous analysis of potential transients.

Brankovic and co-workers [351, 352] discussed in detail the stoichiometry of displacement of a metal monolayer in the galvanic displacement reaction. Particularly, they have shown that under certain conditions, the oxidation of copper adatoms to Cu^I is preferable to its oxidation to Cu^{II}, the latter affecting the stoichiometry of this process. A model describing the kinetics of galvanic displacement and the transients of open-circuit potential was proposed.

Generally, the reactions of galvanic displacement pertain to the class of reactions for which mechanism has to be detailed. It is essential that such processes may generate nanostructures with a wide diversity of shapes, for instance, boxes, cages, frames, shells, rattles or tubes. Several fundamental studies along this line were carried out by the research group of Xia (*e.g.*, see publications [31, 353–355]). The scheme shown in Fig. 9 illustrates the synthesis of certain types of nanostructures by the galvanic displacement. The reaction of galvanic displacement between palladium nanocrystals and $PtCl_6^{2-}$ was studied systematically.[355] It was shown that the addition of Br^- ions to the solution promotes this reaction and enhances the reaction selectivity with respect to Pd(100) facets; as a result, concave Pd–Pt nanocrystals are formed. The reason is the preferential adsorption of Br^- on the Pd(100) facets and their complexation with the ions involved in the reaction. The concave nanocubes were four times more active in the oxygen reduction reaction as compared with commercial Pt/C catalysts.

The following special trick was used in the galvanic displacement:[356] a layer of a ferrocene derivative was deposited on HOPG and stimulated deposition of nano-

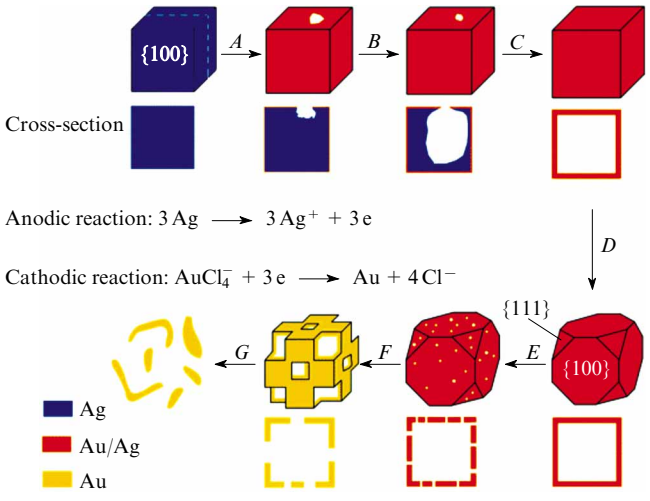


Figure 9. Illustration of the morphological and structural modifications during the galvanic displacement reaction between an Ag nanocube and an aqueous $HAuCl_4$ solution;[354]
(*A*) initiation of the displacement reaction in high surface energy sites; (*B*) formation of partly hollow nanostructures; (*C*) formation of nanoboxes with homogeneous walls of the Ag–Au alloy; (*D*) selective dissolution of the alloy and reconstruction of nanoboxes; (*E*, *F*) further selective dissolution to form pores in the walls; (*G*) fragmentation of porous Au nanoboxes.

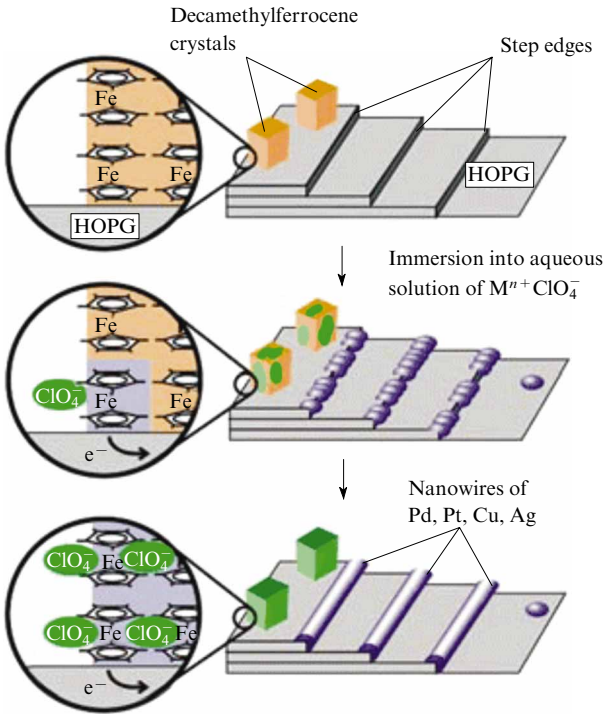


Figure 10. Illustration of mechanisms of spontaneous metal electrodeposition and the competing incorporation of anions into decamethylferrocene crystals.[356]

particles predominantly on the steps. This resulted in the formation of palladium nanowires because the terraces were already occupied by the organic substance (Fig. 10). Thus the Cu-, Pt-, Ag- and Au nanowires were deposited. The authors failed to deposit nanowires of Cd, Ni, Pb and MoO_2, because in accordance with the table of standard potentials shown in their study, the processes involving these substances are impossible for thermodynamic reasons.

Myung and co-workers[357] applied galvanic displacement to copper nanowires which were immersed in a H_2PtCl_6 solution. The increase in the H_2PtCl_6 concentration eventually led to the decoration of nanowires with platinum nanoparticles and the formation of core (Cu)–shell (Pt) structures, nanowires and dense and porous platinum nanotubes. A special procedure has been developed for synthesizing pod-like multicomponent nanotubes by galvanic displacement combined with template-assisted electrodeposition.[358] Transformation of cobalt nanotubes to Te nanotubes with controlled diameter, wall thickness and length was carried out[359] by the galvanic displacement according to the following reaction:

$$HTeO_2^+ + 3H^+ + 2Co \longrightarrow Te + 2H_2O + 2Co^{2+}$$

Nanotubes of Pt and PtPd were synthesized by galvanic displacement with the use of silver nanowires and tested in the oxygen electroreduction reaction.[360] Such non-contacting nanostructures were weakly affected by the Ostwald ripening and agglomeration and also by the anodic dissolution.

Single-crystalline copper nanowires were used as the sacrificial template in the galvanic displacement synthesis of bimetallic porous CuPd and CuPt nanotubes in dimethyl sulfoxide.[361] It was found that the residual content of copper in CuPd nanotubes somewhat exceeded 2%, whereas in CuPt nanotubes it was > 30%. The authors attributed the difference in the behaviours of these two systems to the Kirkendall effect, *i.e.*, the different diffusion rates of copper adatoms through the platinum and palladium layers. The role of this effect on the nanoscale level was discussed.[362]

The interest in the concentric multilayer nanoparticles (core–shell nanostructures) was aroused back in the 1990s. Since then, a lot of materials have been synthesized differing in the nature of cores and shells (totally inorganic, mixed, totally organic), containing cores of several materials (the nesting doll type), several shells, *etc*. The core–shell nanostructures can be successfully synthesized by using electrodeposition and galvanic displacement methods. This approach proved to be particularly in demand in designing electrocatalysts of nanoparticles on different substrates (mainly carbon) for fuel cells. This method makes it possible to reach a high degree of utilization of the catalytically active material, which is often expensive. The catalyst activity can be increased (decreased) by the core-induced deformations (lattice extension or contraction) combined with the ligand effect (electronic factor); the catalyst stability can be controlled by the appropriate choice of core materials. The use of core–shell systems makes it possible to develop a new area in electrocatalysis, namely, the establishment of correlations between the catalytic activity and the physical properties of the shell and the core.

This approach was developed most consistently by Adzic and co-workers[363–379] with the aim of synthesizing both the model (for solving fundamental problems of electrocatalysis) and practice-destined electrocatalysts. Figure 11 shows the synthesis of core–shell nanoparticles with the use of preliminary segregation of one component at an elevated temperature, which is followed by the growth of the new shell by the galvanic displacement.

To explain the enhanced electrocatalytic activity of multilayer catalysts and core–shell nanoparticles, the calculations were carried out by the electronic density functional technique.[321, 322, 366, 371, 372, 379]

The research group headed by Adzic[373] has developed a setup for synthesizing gramme amounts of platinum catalysts. The modern electron microscopic HAADF–STEM¶ method for visualization of interfaces/localizations between different elements using *Z*-contrast images served to characterize the catalyst particles at the atomic level (*Z* is the atomic number of the element) (Fig. 12).

An important problem of catalysis with the use of core–shell nanostructures is the stability of these systems. Their instability can be associated with either the phenomena of segregation and dissolution of components or their diffusion deep into nanoparticles and back.[381] Table 1 shows certain core–shell nanostructures synthesized using the galvanic displacement and their applications.

To understand the nature of catalytic activity of core–shell nanostructures, it is essential to elucidate the role of their parameters such as the shell thickness and the core size, which have been studied so far only for some systems. Thus, it was shown[379] that in the oxygen electroreduction

¶ High-resolution scanning transmission electron microscopy with the high angle annular dark field (HAADF) detector.[380]

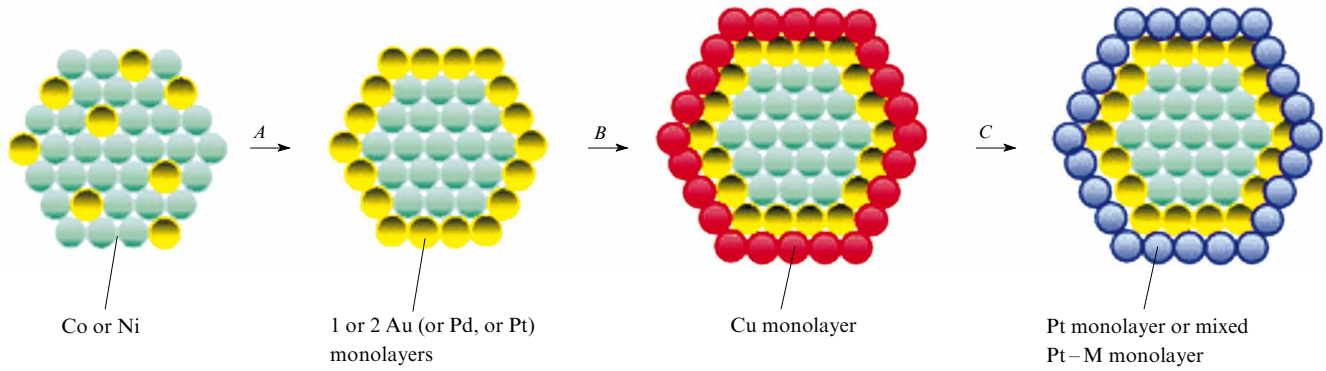


Figure 11. Scheme of the synthesis of core – shell nanoparticles by a combination of high-temperature segregation with subsequent galvanic displacement of copper adatoms;[366]
(*A*) segregation at elevated temperature; (*B*) formation of the copper layer; (*C*) displacement of copper by platinum.

reaction, the highest activity was exhibited by the catalyst with two platinum monolayers, namely,

$$Pt_{2ML}Ru/C > Pt_{3ML}Ru/C > Pt_{1ML}Ru/C > Ru/C$$

It was found[390] that the activity of the Au-supported platinum shell with respect to formic acid oxidation increased as the size of gold nanoparticles decreased from 14 to 2 nm. This effect was probably associated with the specific features of the electronic structure of clusters due to the Au substrate effect.

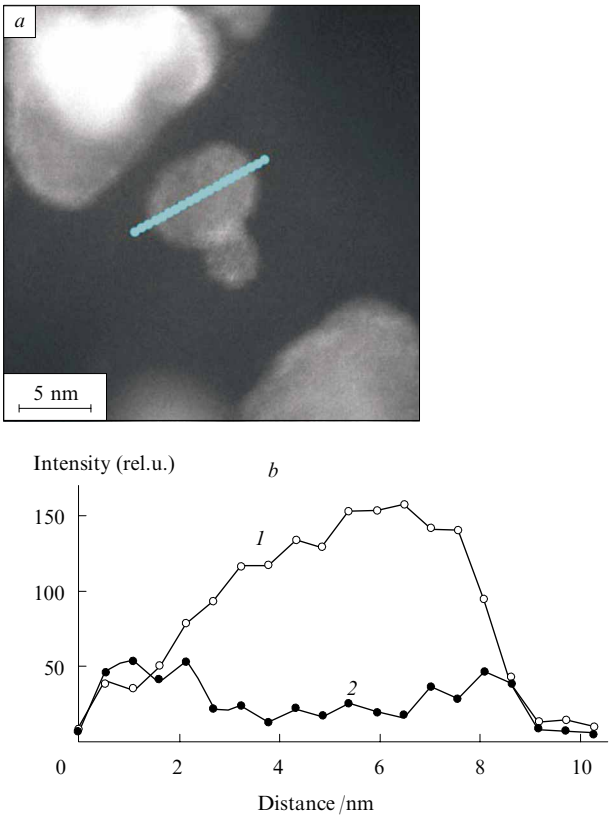


Figure 12. SEM image of a $Pt_{ML}/Pd/C$ nanoparticle (*a*) and concentration profiles of palladium (*1*) and platinum (*2*) plotted using data of energy dispersive X-ray spectrometry (*b*).[373]

In relation to the development of the galvanic displacement method, Russell and co-workers[391] studied the structure of Pt/Pd/C and Pd/Pt/C catalysts by the EXAFS method. For Pd/Pt/C, the core – shell structure was confirmed and for Pt/Pd/C, the penetration of platinum inside the palladium shell was observed. The copper adlayers were studied[392] in sulfuric acid solutions on carbon-supported gold nanoparticles. The measurements have shown that in the absence of copper adatoms, the gold nanoparticles had a potential-dependent shape, representing mainly spheres at negative potentials (in the copper deposition region) and flattened spheres at the positive potentials. In contrast to

Table 1. Examples of core – shell nanostructures synthesized with the use of galvanic displacement.

Substrate	Core	Shell	Applications	Ref.
ITO + 3-APTEMS [a]	Au	Pt	SERS	315
ITO + 3-APTEMS	Au	Pt	OR [b]	318
Au(111)	Ru	Pt	HE,[c] OR	319
Au(111)	Au	Pt	HE, OR	319
Glassy carbon	Co	Pt	EO [d] of CO and MeOH	382
C	Pt	Au	OR	364
C	PdCo	Pt	OR	367
C	Ir_3Co	Pt_{ML}/Pd_{ML}	OR	372
C	IrCo	Pt_{ML}/Pd_{ML}	OR	379
C	Pd	Pt	OR	373
C	Pd	PdAu/Pt	OR	374
C	Pd	Pt	OR	375
C	IrFe	Pt	OR	377
ITO + 3-APTEMS	Au	Ag		383
Carbon nanotubes	Cu	Pt	MeOH EO	384
PdCo/Pd/C	Pt	PdCo	OR	385
C	$PdCu_5$	Pt	OR	386
C	Pd	Pt	OR	373
C	PtCu	Pt	MeOH EO	387
C	Co	Pt	OR	388
C	PdCu	PtRu	MeOH EO	389

[a] 3-APTEMS is 3-aminopropyltri(ethoxymethyl)silane.
[b] OR is oxygen reduction.
[c] HE is hydrogen evolution.
[d] EO is electrooxidation.

the deposition on gold single-crystal faces, neither the mixed copper sulfate layers were formed on the substrate, nor the complete coverage with copper adatoms was reached. Thus the UPD copper is unsuitable for producing a uniform shell of a noble metal by the subsequent galvanic displacement.

Studying the structure of shells in nanostructures on the atomic level is a challenging problem. The shells are neither perfect nor continuous; hence, in the general case, it is more correct to speak of structures resembling the core–shell system.[393]

It was shown[394, 395] that the correct choice of the deposition conditions makes it possible to synthesize the core–shell structures by the direct electrodeposition without using the galvanic displacement. Thus the model Cu(core)–Pt(shell) structures were synthesized[394] by electrodeposition of platinum on copper nanoparticles prepared by two-pulse deposition on glassy carbon. The electrocatalytic activity of these materials in the oxygen electroreduction proved to be comparable with the activities found for the other analogous systems.

The core–shell nanostructures Pt/Pd/C of the ETEK type with an ultralow platinum content (0.5–15 μg cm^{-2}) were synthesized[395] by platinum electrodeposition on a commercial palladium catalyst. The catalysts were characterized by the HAADF–STEM method. The catalyst activity in the oxygen electroreduction reaction was shown to sharply increase as the platinum content decreased down to values corresponding to its mono- and submonolayer coverage. The authors attributed this to the effect of palladium on the electronic properties of platinum.

V. Selective dissolution of alloys

The selectivity of dissolution plays an important role in the corrosion of alloys both at the open circuit potential and under polarization from an external power source. Under certain conditions, the selective dissolution of homogeneous alloys affords nanoporous materials, which makes it possible to form the highly porous ultrathin layers for catalysis/electrocatalysis, sensors, optical devices and other applications. This process consists in the selective removal of, as a rule, the less noble metal (metals) from the alloy. If the alloy nanoparticles serve as the precursors, then the method under consideration makes it possible to obtain the porous core–shell nanostructures and also tune the nanoparticle shell.

The selective dissolution of alloys can be carried out by both chemical and electrochemical methods. The most widely known example is the selective dissolution of aluminium alloys, which underlies the preparation of the Raney catalysts. Nanoporous layers of Cu, Ag, Au with great true specific surface areas were synthesizied[396] on the corresponding bulk metals, which involved the electrodeposition of zinc on the metal surface, heat treatment at 150 °C in the nitrogen atmosphere (to form the alloy) followed by the chemical dissolution of zinc.† Nanoporous copper with a controlled pore size distribution was prepared[398] by the chemical dissolution of an Al–Cu alloy. Nanoporous copper was also synthesized by the dissolution of a Cu–Zn film in a HCl solution.[399]

† Note that Burshtein, Korovin and co-workers[397] used an analogous procedure to synthesize surface skeletal electrocatalysts back in the 1960.

Electrochemical selective dissolution is carried out either at a constant potential or at the potential cycling under certain conditions. The alloy dissolves selectively if the equilibrium potentials of its components differ by a sufficient value (>0.1 V). Optimization of the process is achieved by varying the alloy composition, by selecting the appropriate electrolyte, potential (or the potential range), dissolution time and temperature.

The question of what is the mechanism of chemical dissolution remains open. If the reagent reacts with the active metal in one elementary step and in one and the same surface site, one can speak of the classical chemical dissolution. At the same time, if the active metal dissolves and the liberated electrons migrate to the sites occupied by the noble component to take part in the reagent reduction (for instance, hydrogen ions and water molecules), then we deal with the electrochemical mechanism of alloy dissolution.

Erlebacher, Dimitrov and co-workers[400–415] considered the fundamental problems of selective dissolution in the context of formation of nanoporous materials. Silver–gold alloys were chosen as the model systems for studying the nature and evolution of nanoporosity. First of all, this was due to the similar atomic radii of these elements, their similar crystal structure, the wide difference of their equilibrium potentials and the wide range of single-phase alloys. Silver dissolution from such alloys affords nanoporous gold.

The key points of the theory of nanoporosity evolution are as follows:

— dissolution of silver atoms, formation of gold clusters under the effect of surface diffusion and the appearance of pits;

— as the pits grow, the formation of new gold clusters and the destruction of pits to daughter pits;

— reproduction of daughter pits and their penetration into the bulk to afford the totally porous 3D structure.

Thus, the model of selective dissolution should consider the dissolution kinetics, the phenomena of surface diffusion and transport through the alloy bulk and the solution. To simulate the process of silver dissolution from the Ag–Au alloy, the Monte Carlo method was used. The pores were formed because the atoms of the more noble component aggregated to afford two-dimensional clusters at the interface with the electrolyte. A number of problems were considered such as the roles played by the critical dissolution potential and the alloy composition, the effect of the pH of the medium, the possibility of using the Pourbaix diagrams for predicting the process, the mechanism of formation of a passive layer of the noble metal. The atomistic theory of the formation and evolution of nanoporosity was put forward. The phenomenon of lead UPD was used for characterizing the material porosity.[412] It was found that nanoporous gold exhibits high catalytic activity with respect to electroreduction of oxygen and H_2O_2.[413] Small amounts of platinum added into the original Ag–Au alloy were shown to stabilize the nanoporous material morphology and decrease the pore size down to nearly atomic size.[414, 415]

The alloy potential is the key parameter for selective electrochemical dissolution.[403] If the applied potential far exceeds the overpotential of dissolution of the less noble component but is lower than the overpotential of dissolution of the noble component, then the less noble component rapidly dissolves to afford the nanoporous structure in the

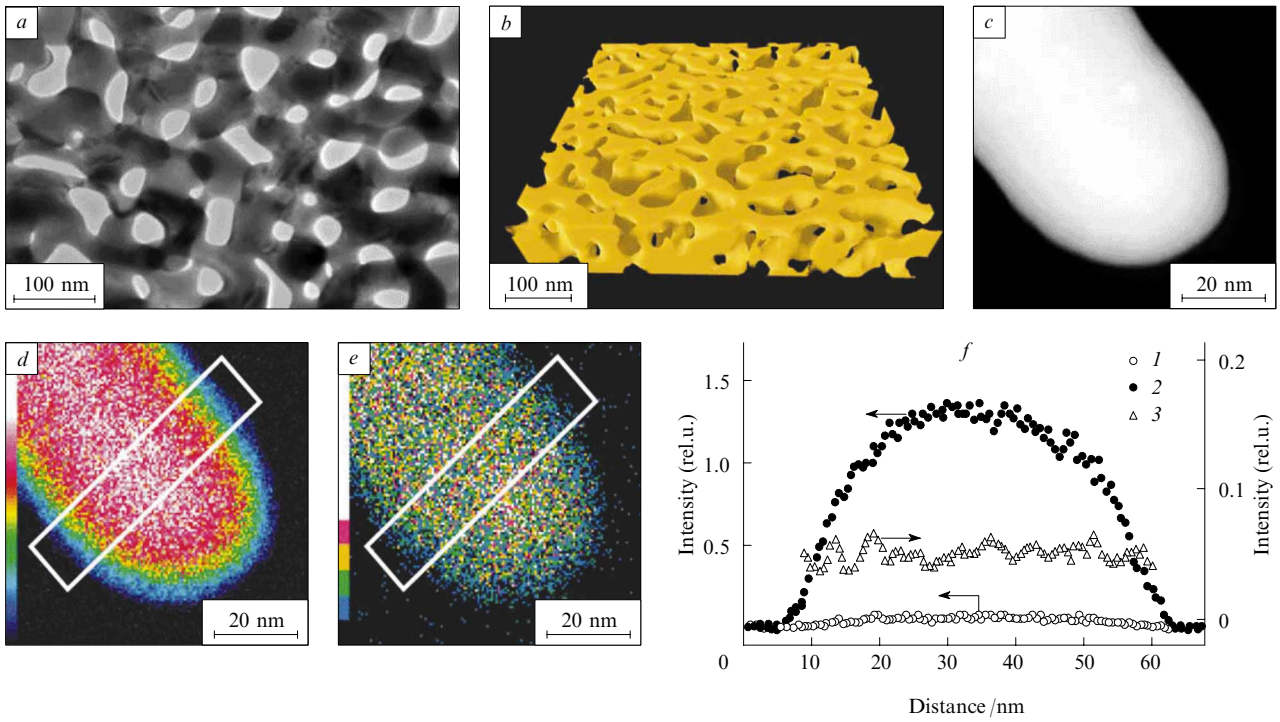


Figure 13. TEM images and the results of chemical analysis of nanoporous gold (NPG) synthesized by selective electrochemical dissolution of Au–Ag alloy.[416]
(*a*) Representative low-resolution light-field TEM image of NPG; (*b*) 3D scan of NPG (electron imaging data); (*c*) HAADF image of a gold ligament; (*d*) Au M_α map of the gold ligament; (*e*) Ag L_α map of the gold ligament; (*f*) overall intensity profile (*3*) obtained by integrating the Au M_α (*2*) and Ag L_α (*1*) intensities.

noble component. At the same time, if the applied potential is low but exceeds the dissolution overpotential of the less noble component, then the noble component is accumulated on the surface and inhibits (passivates) the dissolution. The potential between the regions of passivation and selective dissolution (the critical potential) depends on the alloy composition and the potential scan rate.

The structure of nanoporous gold was studied in detail[416] by the method of spherical aberration-corrected transmission electron microscopy in the mode of scanning electron microscopy with the HAADF detector (Fig. 13). As a result, the atomic surface structure of nanoporous gold was represented and this allowed the authors to gain a deeper insight into the nature of catalytic activity of gold nanoparticles with the characteristic size of >30 nm.

A combination of the method of selective dissolution of Ag–Au alloys and the template-assisted deposition was used[417] in the synthesis of gold nanowires.

Sun and Xia[418] combined the galvanic displacement process with the selective dissolution to prepare gold and silver nanostructures containing voids and highly crystalline walls.

The results of studes of the mechanical strength of nanoporous gold synthesized by selective dissolution of the Ag–Au alloy[419] suggest that the size and surface effects play the substantial role in the mechanism of deformation of this material.

Dimitrov and co-workers[420] proposed a scheme of the totally electrochemical preparation of nanoporous gold electrodes for formic acid electrooxidation with the high mass activity and stability, which included the following three stages:

— dissolution of the Au–Ag alloy;
— deposition of lead atoms;
— galvanic displacement of lead by platinum.

Abruna and co-workers[421] have shown, in relation to intermetallic Cu_3Pt/C nanoparticles, that core–shell nanostructures can be prepared by using the methods of chemical (immersion into 1 M HNO_3) and electrochemical dissolution of copper from the surface layer (Fig. 14). The electrochemical dissolution was carried out by cycling the electrode potential in the interval from $+0.05$ to $+1.0$ V *vs.* the reversible hydrogen electrode in 0.1 M $HClO_4$. The electrochemical dissolution induced the formation of an ordered platinum layer with the thickness of 1 nm on the surface of nanoparticles, whereas the chemical dissolution produced a disordered sponge-like structure of nanoparticles containing numerous voids. Both materials exhibited the enhanced catalytic activity in the oxygen electroreduction and higher stability as compared with Pt/C.

Usually, it is the electrochemically most active alloy components that undergo the selective etching. The method of preparation of nanoporous structures by removing the more noble component of the alloy was discussed[422] for the dissolution of the homogeneous single-phase material Ni_xCu_{1-x}. The possibility of transfering nickel into the passive state in sulfamate solutions was considered, which would create the conditions for dissolution of the more noble copper. Such strategy may be especially efficient for the synthesis of nanoporous structures of transition metals; however, it is not practically used so far.

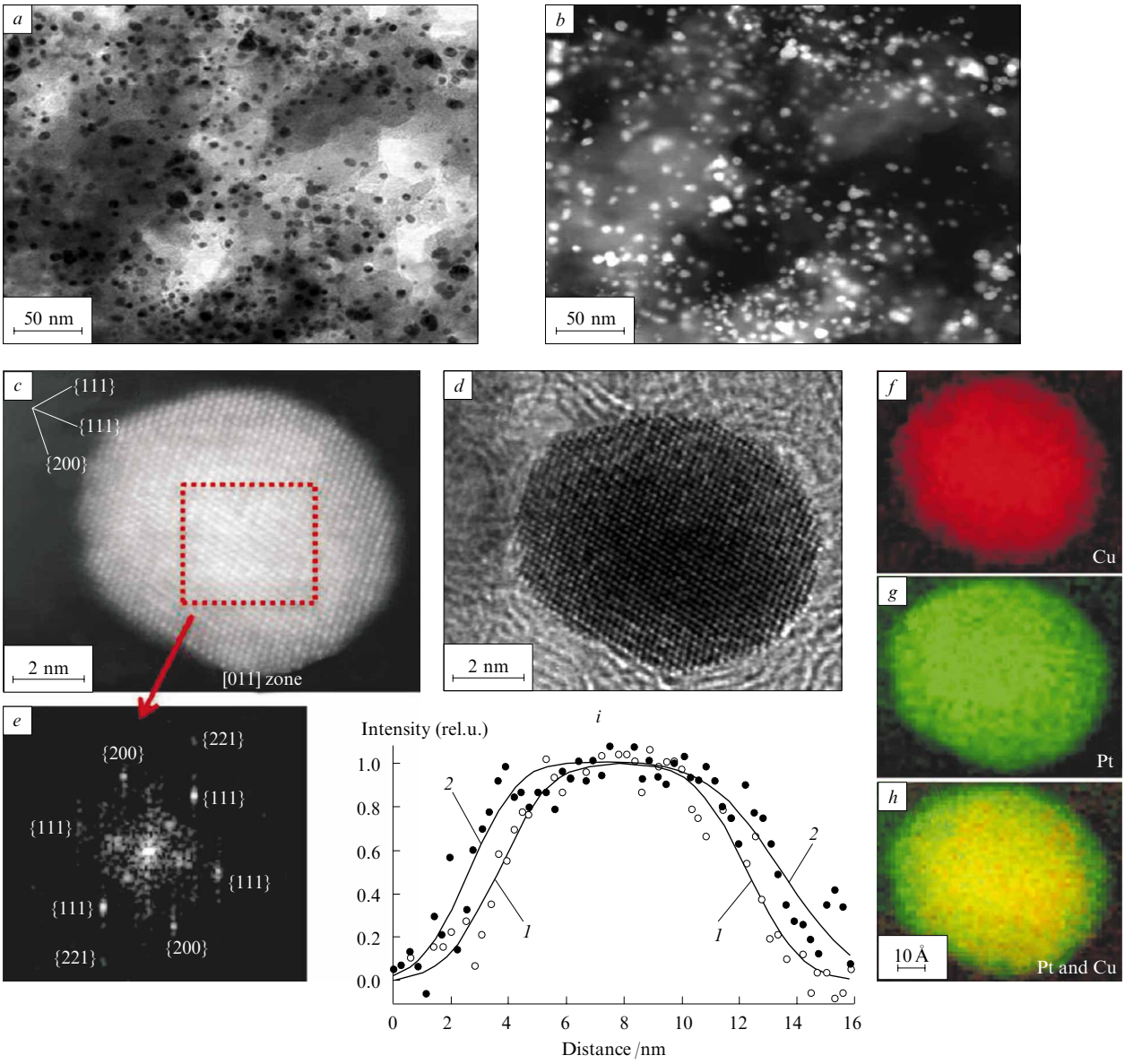


Figure 14. Electron microscopic images of intermetallic nanoparticles Cu_3Pt/C after the electrochemical selective dissolution.[421] Light-field (*a*) and dark-field (*b*) dissolution; (*c*, *d*) atomic-resolution images of a single nanoparticle along the [011] axis of the zone illustrating the ordered structure in the light field; (*e*) the lightest region singled out in Fig. *c*, which was studied by fast Fourier transformation; (*h*) combination of images *f* and *g* showing the Pt shell; (*i*) concentration profiles of Cu (*1*) and Pt (*2*) in the Pt shell.

Nanoporous copper was synthesized from the $Mn_{0.7}Cu_{0.3}$ alloy by the selective dissolution method.[423, 424] For pores with the optimal size, the SERS signals reached a value comparable with the signals of nanoporous gold.

Stratmann and co-workers [425] carried out an *in situ* STM study of the selective dissolution of Au_3Cu and Cu_3Au in the sulfuric acid solution containing hydrochloric acid. Attention was focused on the initial stage of dissolution. It was found that the dissolution started from the terraces and resulted in surface loosening. Chloride ions accelerated the dissolution due to the increase in the rate of surface diffusion of metal atoms.

Nanoporous palladium was synthesized by the selective dissolution of a Pd–Co alloy.[426] The hydrogen solubility in the nanoporous palladium α-phase was shown [427] to be analogous to that in bulk palladium but in the β-phase the solubility was close to the values found for other nanostructured palladium materials (nanocrsytalline palladium and palladium nanoparticles). This was apparently due to the specific features of the lattice of this material rather than to the presence of cobalt traces in nanoporous palladium.

In recent years, attention was drawn to the processes of selective dissolution of platinum alloys with various transition metals (Cu, Co, Ni, Mn, Fe, *etc.*) in connection with the development of the oxygen electrode for fuel cells. The functioning of sputtered films of these alloys was studied by Watanabe and co-workers [428] and Dahn and co-workers.[429]

The selective dissolution of copper from compact Pt–Cu alloys of different composition in sulfuric acid solutions was studied.[430] A correlation with the Ag–Au system was drawn. The difference between these systems was discussed based on the different rates of surface

diffusion for platinum and gold. The critical potentials in these systems were discussed.

For oxygen electroreduction, a nanoporous NiPt composite impregnated with a hydrophobic ionic liquid with the high oxygen solubility was proposed.[431] The nanoporous NiPt nanoparticles were synthesized by the selective dissolution method and used to fabricate the oxygen electrode.[432] The role of the initial nanoparticle size for the subsequent selective dissolution and evolution of nanoporosity was demonstrated. The conditions were found for the development of hierarchical nanoporosity inside the nanoparticles. The resulting catalyst represented skeletal platinum that covered the NiPt alloy core containing voids.

Strasser and co-workers[433 – 447] systematically used the chemical and electrochemical (CV mode) selective dissolution of platinum alloy nanoparticles with the aim of enhancing the activity of catalysts in oxygen electroreduction. First, a platinum – copper alloy and later copper alloys with cobalt and nickel served as the investigation objects in these works.

It was demonstrated that after acid treatment of the Pt_3Co (Ref. 448) and Pt – Cu (Ref. 449) alloys, coarse particles and some of medium-sized particles acquired numerous voids (as in Swiss cheese), while the fine particles retained their core – shell structure.

The complete removal of the active component is virtually impossible so that one has to take account of its presence in the catalyst. Mukerjee and co-workers[450] arrived at the conclusion that residual copper in the nanoparticles may be liberated during catalyst operation and adversely affect the performance of both the anode and the cathode of the fuel cell.

In a study by Markovic and co-workers,[451] platinum alloys with cobalt, nickel and iron the surfaces of which represented a Pt coating generated by heat treatment (Pt-Skin) were compared with the same alloys subjected to the acid treatment (Pt-Skeleton). Both catalysts were more active than polycrystalline platinum in oxygen electroreduction. However, Pt-Skin catalysts were somewhat more active; the authors attributed this to the stronger electronic effect of their core enriched with the transition metal. Later, it was demonstrated by the example of Pt – Ni nanoparticles that the surface composition of the skeletal layer depended strongly on the precursor composition. Stamenkovic, Markovic and co-workers[452] carried out a detailed study of Pt – Ni nanoparticles which included the simulation of their structure by the Monte Carlo method.

Recently, using the methods of erosion and subsequent annealing, highly crystalline polymetallic nanoframework catalysts with electrocatalytically active surfaces were synthesized based on $PtNi_3$.[453] According to detailed studies, the framework edges consisted of Pt_3Ni, *i.e.*, they were substantially enriched with platinum. Such catalysts demonstrated 36-fold increase in their mass activity and 22-fold increase in the specific activity in oxygen electroreduction.

Electrochemical treatment was used for synthesizing the Pt-Skin structures from PtCo nanocubes of the controlled composition.[454] The highest activity in the oxygen electroreduction was exhibited by a catalyst prepared by selective dissolution of Pt_3Co.

The ternary alloy $Pd_{20-y}Au_yNi_{80}$ was chosen[455] as the precursor for the preparation of a nanoporous catalyst of ethanol electrooxidation by selective nickel dissolution.

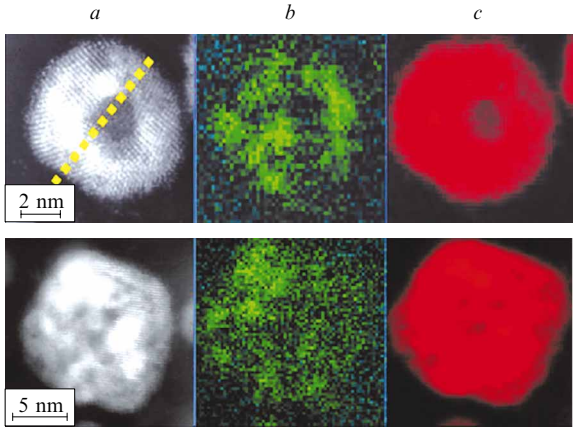


Figure 15. HAADF images of $PtCo_3/C$ nanoparticles (*a*) and low electron energy loss spectroscopy maps of cobalt (*b*) and platinum (*c*), which demonstrate the multiple Pt – Co nuclei.[459]

The stability and activity of FePt and CoPt nanowires after their acid treatment have been studied.[456]

A synthesis of oxygen electroreduction catalyst formed by core – shell nanoparticles with a porous/hollow Pd – Cu alloy core and a monolayer platinum shell was described.[457]

Recently, Wagner and Muller and co-workers[458 – 460] carried out a thorough study of different aspects in the synthesis and structure of nanoporous catalysts. Figure 15 shows some of their results. The most spectacular images were those obtained[460] by low electron energy loss spectroscopy (LEELS) for nanoparticles in their original state and

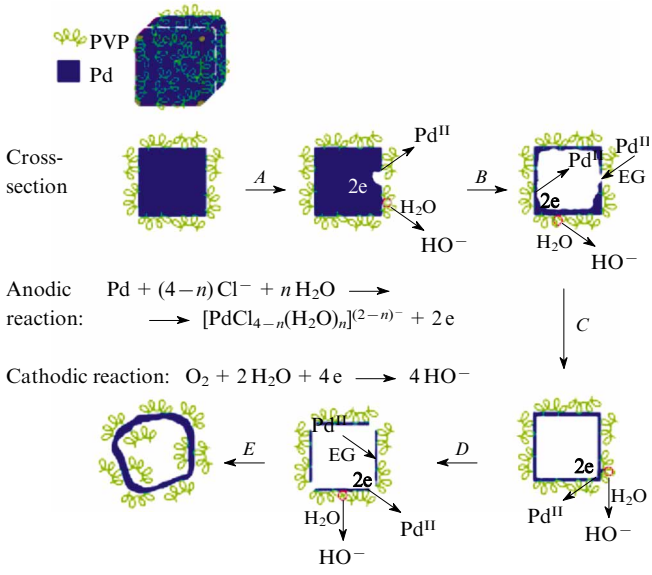


Figure 16. Scheme of synthesis of Pd nanoboxes and nanocages by corrosion etching in a solution of ethylene glycol (EG) + water + poly(vinylpyrrolidone) (PVP) in the presence of oxygen.[461]
(*A*) formation of pits in specific sites of the nanocube surface with generation of Pd^{2+} and HO^- ions; (*B*) formation of voids during further dissolution of palladium; (*C*) formation of a hollow nanobox with the continuous palladium shell; (*D*) removal of palladium atoms from the corners of nanoboxes; (*E*) nanoframework reconstruction and wall thickening.

after potential cycling. These images can serve for development of the views on the nature of processes occurring during the cycling.

The above information demonstrates that the phenomenon of selective dissolution can be successfully used in electrosynthesis of highly efficient nanomaterials.

The selective dissolution was considered above by the example of alloys. However, it can also be used in modifying single-component materials. The latter method is referred to as controlled corrosion. The corrosion of palladium in the presence of oxygen in solution to afford single-crystalline nanoboxes and nanocages without using templates can serve as an example (Fig. 16).[461]

VI. Electrochemical modification of nanoparticles

This Section is largely devoted to advances in the synthesis of metal nanocrystals of controlled shape by electrochemical methods. The studies on the role the nanoparticle shape plays in electrocatalysis of processes occurring in fuel cells have been surveyed.[462]

Arvia and co-workers[463 – 465] were the first to systematically use the electrochemical treatment of bulk electrodes of platinum metals and gold by applying fast potential pulses, which was aimed at their electrochemical faceting and the development of the preferential crystallographic orientation of the electrode surface.

Watanabe and co-workers[466] made an attempt to study *in situ* the surface morphology of Pt(111) during its cycling in a hydrofluoric acid solution by the STM method. A highly interesting result of their study is that in each cathodic scan starting from 1.3 V, they observed the formation and growth of platinum islets in the vicinity of 0.5 V *vs*. the reversible hydrogen electrode, *i.e*., at the potential where the reduction of the surface oxide had virtually stopped.

Sun and co-workers[467] have extended Arvia's approach to Pt microelectrodes and then to the presynthesized metal nanoparticles with the aim of electrochemical synthesis of nanoparticles of a desired shape (Fig. 17). Nanoparticles of the unusual tetrahexahedral shape were synthesized in high yield from platinum nanospheres with a diameter of $\sim$ 750 nm electroplated on glassy carbon.[468] For this purpose, in a solution of 0.1 M H_2SO_4 + 30 mM ascorbic acid, the predeposited nanospheres were subjected to square-wave pulses. It was assumed that at the maximum positive pulse potential, platinum partially dissolved and at the minimum pulse potential, the platinum ions were deposited to form new nanocrystals. Their size could be varied in the range from 20 to 220 nm by controlling the growth time. The standard deviation from the average value was 10% – 15%. The nanoparticle surface was mainly formed by facets with the Miller index {730}. These electrodes exhibited higher activity as compared with commercial Pt/C catalysts in the processes of formic acid electrooxidation and NO electroreduction. The presence of ascorbic acid was not obligatory, the chief role being played by the periodic oxidation – reduction of the platinum surface. In the absence of this additive, the nanoparticles were also shaped as tetrahexahedrons but were less perfect. At the same time, the replacement of ascorbic acid by sodium citrate in the same concentration led to the synthesis of intricate concave polyhedral nanoparticles. Citrate ions promoted the

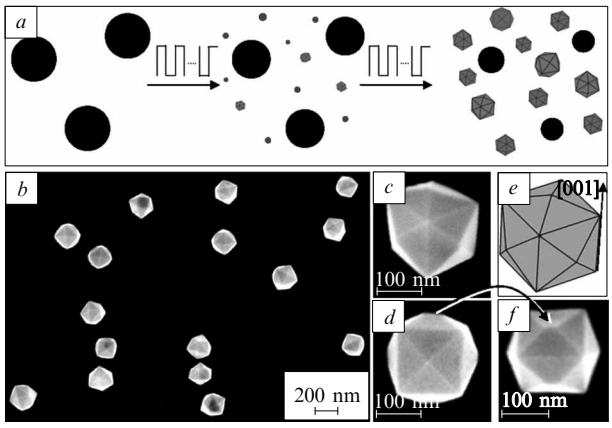


Figure 17. Scheme of the electrosynthesis of Pt tetrahexahedra from nanospheres by applying square-wave potential pulses (*a*), low-resolution TEM images of nanoparticles after 60 min of the synthesis (*b*), high-resolution TEM images showing the shape of nanoparticles (*c*, *d*), geometrical model of the ideal tetrahexahedron (*e*) and high-resolution TEM image showing the vertices deformed due to unequal size of neighbouring facets (*f*).[468]

formation of {111} microfacets. It is known that sodium citrate is used in the chemical synthesis of nanoparticles as the reducing agent, the stabilizer and the pH mediator. An attempt was made to study the adsorption of citrate on low-index faces of platinum[469] aimed at elucidating the role of citrate in the synthesis of nanoparticles with the desired shape.

The appropriate choice of nucleation conditions can provide, besides well-developed single-crystalline surfaces, twin crystals with high-index facets.[470, 471] Thus, on the surface of nanospheres, one can grow platinum nanobars of the nonuniform shape, namely, thick in the middle and thinning to the ends.

An unusual precursor, namely, the insoluble Cs_2PtCl_6 salt was used in electrodeposition of platinum nanoparticles on a carbon substrate with a well-developed surface, which was followed by potential cycling. This made it possible to synthesize high-index faceted platinum nanoparticles measuring 2 – 10 nm, which were comparable with the commercial Pt/C catalysts as regards their size but exhibited higher activity in ethanol electrooxidation and higher selectivity with respect to ethanol electrooxidation to CO_2.[472]

The electrochemical methods (with certain modifications) were used to prepare Pd nanocrystals with high-index facets.[470, 471] Palladium was electroplated from a 0.2 mM $PdCl_2$ + 0.1 M $HClO_4$ solution by the stepwise potentiostatic procedure combined with square-wave potential pulses[473] to afford platinum single crystals with a monomodal particle size distribution. The increase in the palladium salt concentration induced the appearance of twin Pd nanorods. The formation of various kinds of facets upon the electrochemical synthesis was attributed to the different susceptibility of different facets to the reconstruction induced by electrochemical adsorption/desorption of oxygen.[474]

Cubiform nanoparticles of iron with the average size of $\sim$171 nm were synthesized on glassy carbon.[475] The nanoparticle shape transformations and the nature of their facets

were described in another publication.[476] These nanoparticles exhibited electrocatalytic activity in the nitrate anion electroreduction.

In a review[17] devoted to the synthesis of high surface energy materials, which include nanoparticles with the high-index faces, the electrochemical methods were compared with the liquid-phase chemical methods. The authors noted the analogy between the electrochemical method which employs square-wave potential pulses and the chemical method which involves the periodic redox reactions and was discussed in another review.[31] The structure and the stability of platinum nanocrystals represented by both low- and high-index facets were simulated.[477]

Burges and co-workers[478] have shown that the electrochemical measurements (impedance and open-circuit potential) on gold single-crystalline faces in the presence of 4-dimethylaminopyridine make it possible to elucidate the causes for the growth of anisotropic gold particles and its mechanism.

Nanostructured silver was synthesized[479] by the cyclic voltammetry method from silver foil in concentrated KOH solutions.

The cycling of the palladium electrode potential in the HCl solution containing cetyltrimethylammonium bromide was studied[480] in combination with the *in situ* Raman spectroscopic measurements. The cycling was shown to result in the formation of the micronanostructured surface that proved to be SERS active for the adsorption of pyridine as the test molecule.

Cyclic voltammetry in a potassium hydroxide solution was used[481] as an alternative to the chemical method for cleaning single-walled carbon nanotubes.

Finally, it should be stressed that the cyclic voltammetry technique offers unique possibilities for characterization of the surface structure of nanoparticles.[482]

VII. Electrochemical nanodispersion

Dispersion of bulk electrode materials during their electrolysis is a long-known phenomenon. It was described by Haber more than 100 years ago by the example of several metals (*e.g.*, see Ref. 483).

In the 1960s – 1970s, the interest in cathodic dispersion was stimulated by the idea of cathodic incorporation of alkali and alkaline earth metals during electrolysis stated by Kabanov.[484, 485] This idea was utilized in explaining the platinum dispersion during ac electrolysis in alkaline solutions.[486, 487] It was also noted that in solutions containing strontium and barium chlorides, the dispersion can proceed not only under the effect of alternating current but also upon the cathodic polarization by direct current of sufficiently high density.

The interest in the cathodic dispersion of electrode materials was revived recently. Thus, the cathodic dispersion of Bi, Pb and Sn[488, 489] and also of Pt and Rh[490, 491] in alkaline solutions was described. Dispersion of Bi, Pb and Sn at strong cathodic polarization was explained by the formation of hydrides of these elements and their subsequent decomposition to form clusters; the evolving hydrogen was considered as the dynamic template. For the cathodic dispersion of Pt and Rh, it was noted that the potentials of oxygen adsorption on these metals should be reached in the periodic potential variations, although the hydrosols are formed in the cathodic cycle at the simultaneous hydrogen evolution. In all cases, porous 3D structures arise on the surface.

The cathodic corrosion of Pt, Au, Cu, Ag, Ni, Rh, Si, Nb and Ru was studied in alkaline solutions of various composition;[492] the formation of PtRh, PtRu, PtNi, AuCo, AuCu, FeCo alloy nanoparticles was demonstrated.[493] It was stressed that for dispersing platinum group metals, the attainment of the oxygen adsorption potentials is unnecessary. The dispersion was observed at high negative potentials (-7.2 V *vs.* mercury oxide reference electrode)‡ and could also occur in tetraalkylammonium hydroxide solutions and in NaOH melts. The nanoparticle size varied from 3 to 30 nm. It was assumed that at high negative potentials, a layer devoid of water molecules was formed near the cathode surface, the cations were reduced to anions to be stabilized by the metal lattice cations. On contact with water (during the anodic potential cycle), these anionic metal intermediates were reoxidized to the metallic state and the resulting metal atoms agglomerated to afford nanoparticles.

The electrochemical dispersion of platinum by alternating current was accomplished in alkaline solutions with simultaneous addition of Vulcan XC72 carbon powder, which allowed the authors to obtain a Pt/C catalyst.[494] Figure 18 shows the scheme of this process. The chief role in the platinum destruction was attributed[494] to intercalation of alkali metal cations into platinum lattice defects. At the same time, the anodic intercalation of oxygen was also important because this favoured the formation of defects. The structure of nanoparticles was characterized by synchrotron X-ray diffraction.

The mechanism of dispersion of platinum group metals in alternating current was also the subject for discussion.[495] However, it still needs to be further clarified.

The electrosynthesis of Pd nanoparticles in TiO_2 nanotubes with the use of anodic-cathodic potential pulses was described.[496] This allowed the dispersion of nanoparticles to be carried out simultaneously with their faceting. As a result, an active electrocatalyst for ethanol electrooxidation in alkaline solutions was synthesized.

When trying to explain the dispersion of metals, one should take into account the appreciable decrease in the work of formation for solid surfaces with the potential deviation from the zero free (or total) charge potential.[497]

The fundamentals of the dispersion method proposed by Reetz and Helbig[498] were developed much more thoroughly. The latter method provides size-selective electrochemical synthesis of nanostructured clusters of transition metals. The authors used a two-electrode electrochemical cell with a palladium anode and a platinum cathode (Fig. 19). Tetraoctylammonium bromide (0.1 M) in a mixture of actonitrile and tetrahydrofuran (4 : 1) was used as the electrolyte. When electric current was passed, palladium served as the sacrificial anode and dissolved. Palladium ions diffused to the platinum cathode to be reduced there to afford nanoparticles. The latter were stabilized by tetraoctylammonium cations and precipitated as a powder to the bottom of the electrochemical cell. Depending on the current density, the particles with the average size from 1.4 to 4.8 nm were synthesized, the particle size decreasing with the increase in the current density. This method proved to

‡ The attainment of such negative potentials in aqueous solutions is non-trivial and needs to be additionally confirmed.

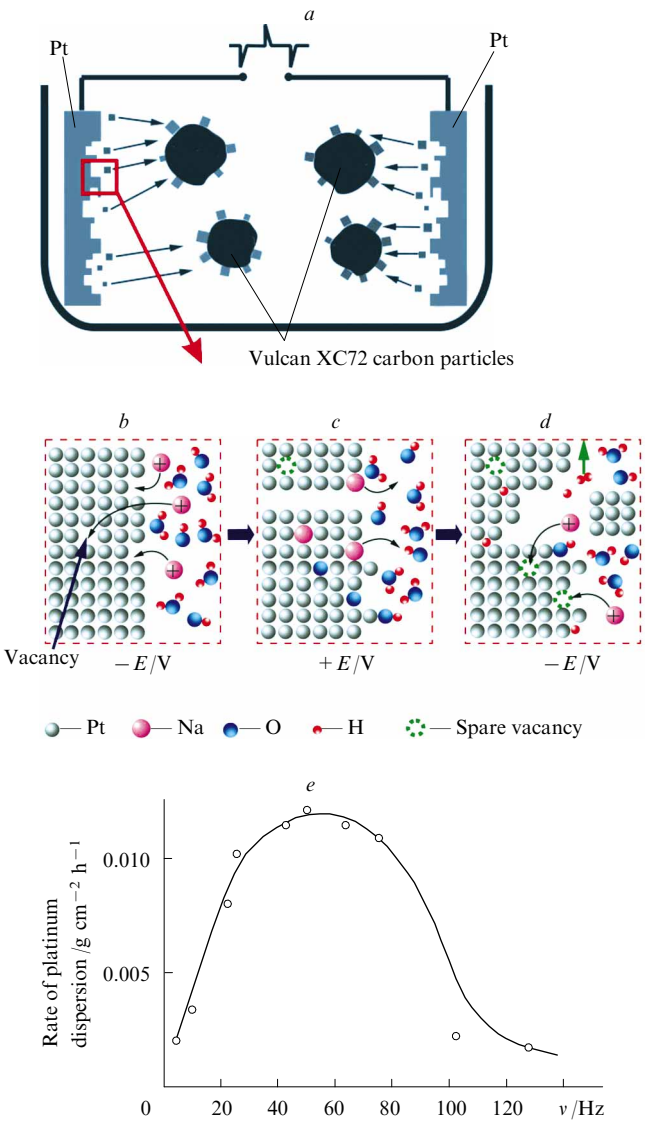


Figure 18. Illustration of electrochemical synthesis of the Pt/C catalyst (*a*–*d*) and dependence of the rate of Pt dispersion on the ac frequency (*e*).[494]

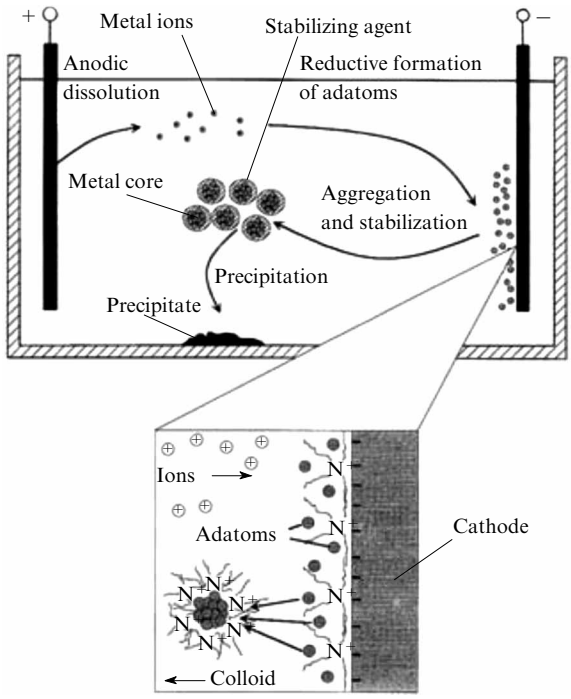


Figure 19. General scheme of electrosynthesis of metal nanoparticles stabilized by NR_4^+ cations.[498]

be efficient for several tetraalkylammonium and phosphonium salts (*e.g.*, tetrabutylhexadecylphosphonium bromide). The deposits could be dissolved in, *e.g.*, dimethylformamide, and even in nonpolar solvents (*e.g.*, in pentane) when the quaternary salts with longer hydrocarbon chains were used. The solubility in water was achieved when sulfobetaine 3-(dimethyldodecylammonium)propane sulfonate and LiCl (for clusters of 8 nm size) were used. In the presence of carbon powder in solution, clusters immobilized on the surface of carbon particles can be obtained; moreover, the cluster size will be the same as in the absence of the substrate.

The method described above was also used to synthesize Ni clusters with the average size of 2.2 and 4.5 nm. The nanoparticles were formed in high yields and no by-products were formed (*e.g.*, hydrides or boron-containing compounds, which would contaminate the material in the chemical methods of synthesis), the material was easily isolated and the particle size was controlled by varying the current density. It is probable that the changes in the current density induced the changes in the cathode potential. This can be ascertained in special experiments carried out in a three-electrode cell. The thus synthesized nanoparticles were characterized by the combination of STM and HRTEM methods.[499]

The Reetz–Helbig method is largely based on the achievements of the liquid-phase chemical methods of synthesis and stabilization of nanoparticles, as was noted by its authors.[500] A basically similar method was used[501] for synthesizing active zinc nanoparticles in dimethylformamide to be later used directly in a catalytic process.

Reetz *et al.*[502] adapted this method to the synthesis of bimetallic Pt–Pd clusters. The method was also used for synthesizing superparamagnetic cobalt clusters,[503] Ti nanoparticles,[504] Pd clusters stabilized by propylene carbonate[505] (the specific character of the isotherms of hydrogen sorption by Pd clusters was also demonstrated[506]).

At attempt was undertaken[500] to optimize the synthesis with the sacrificial anode by varying the factors such as the nature of solvent, the electrolysis time (the passed charge), the current density (for different times of electrolysis), the interelectrode spacing, the nature of ammonium salt, the synthesis temperature and also by varying simultaneously any two of these parameters.

The Reetz–Helbig method was used[291,507] in the electrochemical synthesis of gold nanorods with different aspect ratios by using a sacrificial Au anode, a platinum cathode and also hexadecyltrimethylammonium bromide as a surfactant additive promoting the formation of nanorods and also functioning as a stabilizer preventing the further growth. The synthesis was carried out under the action of

ultrasound, with the temperature control and in the presence of acetone.

El-Sayed and co-workers [507] studied the stability of gold nanorods and observed the appearance of fine gold clusters with a narrow size distribution. These clusters increased in their volume as the temperature increased but remained the same in number. It was assumed that these clusters grew by the Ostwald ripening mechanism.

The Reetz–Helbig method (including some modifications) was used to synthesize silver [489, 508–510] and copper [511] nanoclusters.

The shape- and size-selective synthesis of Ag_2O micro- and nanoparticles with the use of a sacrificial silver anode was developed.[512] The synthesis involved two stages, namely, the anodic dissolution of silver in an alkalified sulfate solution and the deposition of Ag_2O according to the reaction

$$2\,Ag^+ + 2\,OH^- \longrightarrow Ag_2O + H_2O$$

The changes in the particle shape were dictated by the variations of the anode potential.

Is was demonstrated [513] that the sacrificial anode method can be used for synthesizing the Pd–Ni alloy clusters and core–shell nanostructures. In the latter case, the Ni nanorods are first synthesized by the Reetz–Helbig process and then palladium acetate is added to the suspensions of particles. As a result, the galvanic displacement of the Ni-core layer takes place to form the core–shell structure.

The Reetz–Helbig method has attracted the attention of scientists because it is suitable for the synthesis of nanoparticles unattached to the electrode surface on which they are formed. As was shown,[514] such nanoparticles can be prepared by mediated electroreduction. In the above study, Pd nanoparticles were synthesized using $PdCl_4^{2-}$ ions as the precursor and tetraviologen calix[4]resorcine as the mediator.

VIII. Electrosynthesis of nanostructures in melts

As an example of the electrosynthesis of nanoporous nickel in classical melts, consider the study by Katagiri and Nakata.[515] A nickel electrode was kept in a $ZnCl_2-NaCl$ melt at the zinc deposition potential. Then its potential was shifted to the region of the anodic dissolution of zinc. As a result, a nanoporous nickel electrode with the roughness factor of >200 was obtained.

The electrodeposition from ionic liquids can be considered as a new trend in the electrosynthesis of nanostructures. Ionic liquids represent fused salts with the melting point below 100 °C. They are usually composed of organic cations (substituted imidazolium or pyridinium ions, tetraalkylammonium cations, *etc.*) and also of inorganic or organic anions [$AlCl_4^-$, BF_4^-, PF_6^-, SbF_6^-, $CF_3SO_3^-$, $(CF_3SO_2)_2N^-$, $(CF_3SO_2)_3C^-$, *etc.*]. In principle, ionic liquids can be divided into three groups according to the type of constituting anions (although their detailed classification is still to be developed):

— chloroaluminate systems;

— systems with inorganic fluoride anions;

— systems with organofluorine anions.

The history of discovery, examples, properties, purification methods and purity control of ionic liquids, the reference electrodes used, handling rules, and application fields were discussed in many studies (*e.g.*, see Refs 516–525). The ionic liquids attracted attention of electrochemists, first of all, due to the wide interval of potentials of their electrochemical inactivity (the wide electrochemical window), which in certain systems exceeds 6 V (Fig. 20), and their good conductivity. They can be used in the deposition of nanocrystalline materials of less noble elements or the compounds that cannot be electrodeposited from aqueous or organic media. The majority of metals that can be deposited from aqueous solutions can also be deposited from ionic liquids. At the same time, the use of the latter makes it possible to avoid the parallel evolution of hydrogen and its dissolution in the deposits, which often affects their properties. Moreover, the use of ionic liquids allows the temperature ranges to be extended, which can substantially affect the kinetics of deposition. The majority of ionic liquids have very low vapour pressure and some of them are thermally stable up to 450 °C. The studies of ionic liquids were especially expanded after the discovery of systems stable in contact with moisture and air. In contrast to classical fused salts, which have very high melting points and are corrosive (and, hence, require electrochemical cells resistant to corrosive media), the ionic liquids are easier to handle. The fine tuning of properties of ionic liquids is possible by changing the nature of substituents. At present, ionic liquids are considered as an alternative to volatile organic solvents, very promising as regards the environmental issues.

The cations and anions of ionic liquids represent complex structures in which the charges are mostly localized on the side groups and(or) screened by them. This is one of the main reasons for the low melting points of ionic liquids.

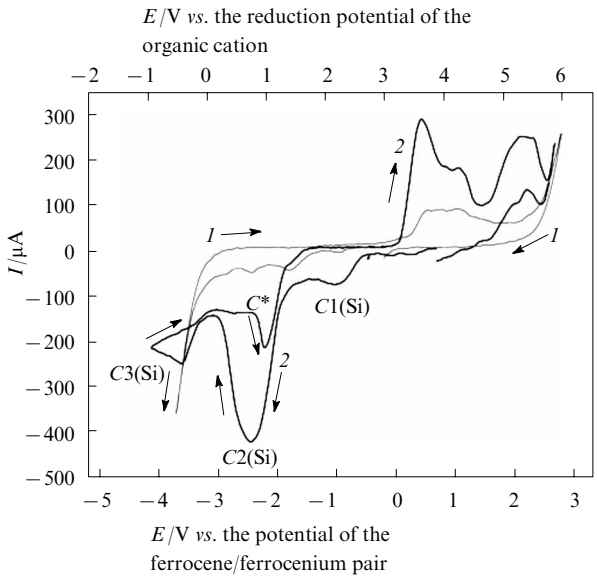


Figure 20. Voltammograms of Au(111) in the 1-n-butyl-1-methylpyrrolidinium bis(trifluoromethylsulfonyl)imide ionic liquid (*1*) and in the presence of $SiCl_4$ (0.1 M) (*2*) at the potential scan rate of 10 mV s^{-1} (Ref. 526).
Peaks *C*1, *C*2, *C*3, *C** are associated with the silicon deposition processes. The maxima in the anodic scan at potentials of >0 correspond to oxidation of the reduction products of silicon and gold cations.

The studies of electrodeposition of metals and semiconductors from ionic liquids date back to the end of the 20th century and were first carried out in chloroaluminate systems and later in ionic liquids of the next generations. Reviews of the early studies in this field are available.[518, 522, 527, 528] A fairly complete list of metals deposited from ionic liquids has been reported.[522] In many cases, nanocrystalline deposits were synthesized. The electrochemical *in situ* versions of STM and STS methods gained in importance for elucidating the specific features of electrodeposition from ionic liquids; they were used in studying the electrodeposition of nickel, cobalt and their alloys with aluminium and also of germanium on the Au(111) and Si(111):H surfaces.[529] Nanosized films of Si, Ge and Si_xGe_{1-x} were deposited at room temperature from 1-n-butyl-1-methylpyrrolidinium bis(trifluoromethylsulfonyl)amide containing $GeCl_4$ and $SiCl_4$ as the precursors.[530]

The possibility of controling the electrodeposition by changing the nature of the ionic liquid cation was demonstrated[531, 532] for the synthesis of nanocrystalline aluminium (from $AlCl_3$ precursor) under potentiostatic conditions in the absence of any additives directly from 1-n-butyl-1-methylpyrrolidinium bis(trifluoromethylsulfonyl)imide, 1-methyl-3-ethylimidazolium bis(trifluoromethylsulfonyl)imide and trihexyltetradecylphosphonium bis(trifluoromethylsulfonyl)imide. Aluminium was deposited on gold substrate at various temperatures. In the pyrrolidinium-based ionic liquid in the temperature range of 25–100 °C, nanocrystalline deposits were obtained, whereas in the imidazolium-based liquids the deposits were microcrystalline in the same temperature interval. The authors attributed this to different adsorption activities of the cations. As the temperature rose, the particle size increased. In trihexyltetradecylphosphonium, the crystals of ~20 nm size were synthesized at 25 °C. Homogeneous thin tantalum layers were deposited under potentiostatic conditions onto the surfaces of Au(111) and platinum from 1-n-butyl-1-methylpyrrolidonium bis(trifluoromethanesulfonyl)imide at different temperatures;[533] TaF_5 served as the precursor. The film quality improved with the addition of LiF into the electrolyte. The same ionic liquid was used for synthesizing nanoscale silicon films on the surfaces of gold and HOPG from solutions saturated with $SiCl_4$.[526] The STM method made it possible to study the processes of gold surface restructuring/reconstruction upon polarization.

Porous polycarbonate membranes were used for the template-assisted electrosynthesis of Si_xGe_{1-x} nanowires in 1-n-butyl-1-methylpyrrolydinium bis(trifluoromethylsulfonyl)amide and 1-ethyl-3-methylpyrrolidinium bis(trifluoromethylsulfonyl)amide to afford nanowires with the average diameter of 100 nm and the length reaching 2.5 μm.[534]

Photonic crystals with high dielectric constant were synthesized by electrodeposition of germanium (with $GeCl_4$ as the precursor) using templates of polystyrene colloid crystals and 1-hexyl-3-methylimidazolium tris(pentafluoroethyl)triphosphate and 1-ethyl-3-methylimidazolium (trifluoromethylsulfonyl)amide.[535]

To synthesize nanowires, titanium deposition ($TiCl_4$ as the precursor) was carried out[536] from 1-n-butyl-3-methylimidazolium bis(trifluoromethylsulfonyl)amide on HOPG by the method proposed by Penner.[50] Wires with the length of >100 nm were synthesized with a narrow diameter distribution (10 ± 2 nm).

The initial stages of titanium deposition on Au(111) from 1-methyl-3-butylimidazolium bis(trifluoromethylsulfone)imide using $TiCl_4$ as the precursor were studied[537] by electrochemical methods and also by *in situ* electrochemical STM. It was concluded that a layer of 1–2 nm titanium clusters and a Ti–Au alloy were formed. However, these conclusions were questioned in another publication[538] in which it was found that the use of $TiCl_4$ as the precursor in various ionic liquids leads most probably to the deposition of a thin $TiCl_x$ layer. Thus, the synthesis of titanium nanowires described above[536] requires more evidence.

Silver was deposited on glassy carbon in the potentiostatic mode by using $AgBF_4$ as the precursor and two ionic liquids, one hydrophobic (1-n-butyl-3-methylimidazolium hexafluorophosphate) and one hydrophilic (1-n-butyl-3-methylimidazolium tetrafluoroborate); the transients of currents were analyzed.[539] The formation of silver nanolayers with a high SERS response was observed.

The electroplating of Pt nanoparticles (with H_2PtCl_6 as the precursor) on multiwalled carbon nanotubes with the use of 1-n-butyl-3-methylimidazolium hexafluorophosphate was proposed.[540] The resulting nanocomposite demonstrated good electrocatalytic activity in the reaction of methanol electrooxidation.

In addition to the nature of ionic liquid and the temperature, characteristics of nanostructured deposits are determined by other factors, particularly, by the introduction of typical diluents (benzene, toluene), organic solvents and the metal salts with small inorganic cations such as Li^+. All these factors have already been summarized[522] and discussed.[541] The effect of UPD phenomenon on the character of electrodeposition was noted.[542] The need for more detailed studies of the structure of the ionic liquid/electrode interface is apparent if we take into account the effects of the ionic-liquid type, the small-sized cation and the UPD phenomenon on the electrodeposition of nanostructures.[522, 541–547] Recently, this line of research has been actively developed.[547–549]

Owing to their extremely low vapour pressure and the wide electrochemical window, ionic liquids can be successfully used for the plasma-chemical synthesis of nanoparticles, as was demonstrated[550, 551] for the synthesis of silver and copper nanoparticles, respectively. In the latter case, the effect of the ionic liquid on the nanoparticle size was noted. One of the electrodes of the vertical gas-discharge tube was immersed into an ionic liquid while the other was left in the gas atmosphere (*e.g.*, in argon). Nanoparticles were formed on the surface of the precursor-containing ionic liquid (due to interaction of the plasma electrons with the precursor ions). The stability of ionic liquids in the plasma discharge was demonstrated[552] for 1-n-butyl-3-methylimidazolium tetrafluoroborate during the synthesis of palladium and gold nanoparticles.

IX. Electrosynthesis of nanoparticles on the liquid/liquid interface

The first study in the field of electrochemical deposition of metal nanoparticles at the interface of two immiscible liquids was published in 1975.[553] Its authors have found that the electric current flowing across the 1,2-dichloroethane/water interface with $CuSO_4$ in the aqueous phase

and tetrabutylammonium hexacarbonylvanadate in dichloroethane produced a copper film at the interface.

However, it was only in 1996 that Cheng and Schiffrin [554] demonstrated that this method can produce nanoparticles. Using a four-electrode potentiostat which allowed the correct control over the interface potential, the colloid nanoparticles of gold were deposited at the 1,2-dichloroethane/water interface as a result of electrochemical reduction of tetraoctylammonium tetrachloroaurate (in the organic phase) by hexacyanoferrate (in the aqueous phase). The electrodeposition at the boundary of two phases can be considered as the electrochemical analogue of the synthesis of nanoparticles by the Brust – Schiffrin method.[555, 556]

The design of electrochemical cells and the instruments used in studying the liquid/liquid interfaces are described elsewhere.[557]

When the deposition takes place at the boundary of two immiscible liquids, the interaction with the substrate is altogether absent (or weakly pronounced), which distinguishes this process from the deposition on the solid electrode surface. Furthermore, the interface is free from sites with preferential nucleation, thus being rather simple for studying. When modelling the phenomena of nucleation and growth at the liquid/liquid interface, one must consider the diffusion in the contacting media, because the electron transfer across the interface is accompanied by the transport of electroactive species in both media.[558, 559] Such a simulation is based on the concepts of Scharifker *et al.*[71, 72] It was demonstrated that the important role in the nucleation at the interface of two liquids is played by nanoparticle agglomeration; spontaneous nucleation at the liquid/liquid interface was also observed.

Konturri and co-workers [560] have shown that the surface activity of nuclei plays an important role in the phase formation at the liquid/liquid interface. The critical size is determined by the values of interfacial tension and linear tension of the three-phase boundary. These conclusions were confirmed by experiments on the deposition of palladium nanoparticles.

Cyclic voltammetry and chronoamperometry were used [561] in studying the platinum deposition at the water/1,2-dichloroethane interface during the reduction of Pt^{II} in water by 1,1′-dimethylferrocene in dichloroethane. The shape of current transients was described in terms of the nucleation – growth theory. However, the initial rates of platinum deposition on the freshly formed interfaces had a spread within two orders of magnitude. The authors assumed this unusual phenomenon to be due to fluctuations in the rate of formation of the nuclei with the critical size necessary for their further growth. The authors simulated the electrodeposition process and their results confirmed this assumption.

The role of the potential in the formation of gold nanoparticle assemblies stabilized by mercaptosuccinic acid was studied at the water/1,2-dichloroethane interface.[562] It was demonstrated that the density of particles in the assembly can be reversibly changed and tuned by varying the potential drop at the interface of these immiscible liquids.

A method was proposed for electrosynthesizing silver nanoparticles [Ag_2SO_4 as the precursor and tetraphenylarsonium tetrakis(pentafluorophenyl)borate as the organic reagent] and polyphenylpyrrole at the water/1,2-dichloroethane interface.[563] It cannot be ruled out that nanostructures with the core – shell structure were thus synthesized.

A liquid/liquid interface can be modified by molecular assemblies, mesoporous (or microporous) particles or mesoporous membranes, which may endow it with new properties. Such template-assisted synthesis makes it possible to avoid agglomeration of nanoparticles at this interface.[564] Palladium nanoparticles were synthesized upon interface modification with an alumina membrane.[565, 566] The design of electrochemical cells and the process of template-assisted electrodeposition have been reported.[567] The size of nanoparticles depends on the interface position which, in turn, is determined by the wetting properties of the liquids in contact.

Dryfe and co-workers [568] compared the deposition of platinum and palladium on the bare and templated water/1,2-dichloroethane interfaces and characterized in detail the nanoparticles synthesized. They noted that the nucleation rate was lower for platinum and the particle size was in the range of 3 – 5 nm being somewhat smaller for platinum. The possibility of co-deposition of platinum and palladium on the alumina-membrane-modified liquid/liquid interface was demonstrated.[569]

Chronoamperometric deposition of palladium at the water/1,2-dichloroethane interface (ammonium tetrachloropalladate as the precursor; butylferrocene as the organic reagent) was studied [570] at different overpotentials. A high concentration of the organic electron donor was chosen, which simplified the analysis of results because the diffusion limitation in the organic medium could be ignored.

Spectroelectrochemistry in the UV and visible regions offers great possibilities in studying the liquid/liquid interface.[571] The spatial scanning spectroelectrochemistry method was proposed for studying the electrodeposition of palladium nanoparticles at the water/1,2-dichloroethane interface.[572] The method makes it possible to acquire information on the processes that occur on both sides of the liquid/liquid interface. For electrodeposition of palladium nanoparticles, it was found that small palladium clusters were desorbed from the surface to the aqueous phase. It was noted that the overpotential affects the size of aggregates of Pd nanoparticles.

Functionalization of the interface between two immiscible liquids by nanoobjects is a way of preparation of new types of electrooptical devices.[573]

The introduction of porous membranes actually transforms the liquid/liquid interface into an assembly of smaller surfaces. Unwin and co-workers [574] studied the formation of silver nanoparticles at micro- and nano-sized liquid/liquid interfaces formed without introducing any membranes. These interfaces are convenient because they make it possible to avoid the multiple and spontaneous nucleation that complicates the electrodeposition on macroscopic boundaries. Micro and nanointerfaces were formed at the ends of tapered pipettes with the orifice radius of several fractions of micrometre. These pipettes were introduced into practice by Taylor and Girault [575] for studying the charge transfer across the liquid/liquid interface. It was found that for pipettes with the radius below 0.5 μm, the current transients reflect the deposition of a single silver nanoparticle. The nanoparticle size was controlled by changing the electrolysis time.

The great advantage in the development of two-phase electrochemistry is offered by the method of electrode sur-

face modification with immobilized microdrops of water-insoluble liquids.[576, 577] The consideration of this actively developing trend is beyond the scope of the present review. It only deserves mention that in such systems, the three-phase interfaces solid electrode/liquid/liquid are formed, which makes it possible to synthesize, *e.g.*, metal strips from nanoparticles.[578]

X. Electrosynthesis of nanomaterials in the probe microscope configuration

The nanodesign in the chamber of a tunnelling microscope under electrochemical conditions was first reported by Li, Virtanen and Penner.[579, 580] The surface defects on HOPG were generated by the tunnelling microscope tip and then served as the nucleation sites for metal (Cu and Ag) electrodeposition. This method was used in the nanodesign involving conducting polymers.[581] The first stage of such nanodesign has been surveyed.[582]

Kolb *et al.*[583] put forward the method of precision positioning of copper clusters with the height reaching four atomic layers on the surface of Au(111). Copper was electrochemically deposited on the tunnelling microscope tip and then transferred to the surface under controlled approach of the tip to the substrate. This method is called 'jump-to-contact' and includes the following stages:

— metal electrodeposition on the tip while the substrate potential is maintained in the UPD region of the metal being deposited;

— the controlled approach of the tip to the substrate surface during which the tip–substrate connecting bridge is formed;

— the removal of the tip, which breaks the bridge to form a nanocluster on the surface.

Kolb and co-workers described application of this method for the deposition of Pd clusters[584] and also Cu clusters[585] on the bare and thiol-coated Au(111) surfaces. The method was used for the deposition of small Ag clusters on Au(111). The attempts to decorate the gold surface with nickel clusters led to the formation of breaks in the coating continuity due to the detachment of gold atoms upon withdrawal of the tip. This was explained by high cohesion of nickel.

A similar mechanism of formation of Ag nanoclusters can probably be realized in humid air.[586] An example of electrochemical atomic force nanolithography in humid air has been reported.[587]

It was stressed[588] that copper clusters synthesized on the Au substrate by the 'jump-to-contact' method exhibit remarkable stability with respect to anodic dissolution: they survive even a 200 mV potential shift from its equilibrium value in the Cu/Cu^{2+} system, although small clusters are usually unstable due to the large number of surface atoms. It was assumed that the energy levels in clusters are discrete rather than continuous as in the bulk metal and are separated by an energy barrier from the electronic levels of the underlying metal, which accounts for the stability of clusters. However, Schmickler and co-workers[589] noted that this energy barrier is very low and cannot affect the cluster stability. Molecular dynamic calculations have shown that the stability of clusters can be explained only by the formation of copper and gold alloys.

The concept of possible formation of alloy clusters was confirmed in further experiments and calculations.[590–592] The deposition of Pd, Cu, Ag and Pb on Au(111) and Cu on Ag(111) was analyzed in detail and the Monte Carlo calculations were carried out.[592] It was predicted that the Cu/Pd(111) system should be a good candidate for the formation of stable clusters. The cohesion and the heat of formation of alloys proved to be the main factors that determine the behaviour of metals when the nanodesign is carried out in a tunnelling microscope chamber in the jump-to-contact mode.

It was shown[593] that the deposition of Cd clusters on the Au support produced the Cd–Au alloy. The alloy composition depended on the substrate potential and determined the corrosion resistance of clusters and the kinetics of their dissolution.

The local formation of alloys at the atomic contact of the tip with the substrate surface was anticipated[594] for the copper deposition on the surfaces of Pt(111) and Au(111) and also for the palladium deposition on gold.

It was demonstrated[595] that the cobalt deposition on Au(111) and the lead deposition on the thoroughly pretreated n-Si(111) surface [sometimes designated as n-Si(111):H] can produce clusters with a controlled aspect ratio. This situation is especially interesting in connection with the fact that sufficiently stable nanoclusters can thus be deposited on a semiconducting substrate with a low surface energy. Factors that should be taken into account when simulating the processes on the tunnelling microscope tip were also considered. Schindler *et al.*[596] proposed the following method for the localized electrodeposition of cobalt clusters: first, cobalt was deposited on the tip and then it was dissolved upon the application of an anodic pulse. As a result, a high cobalt concentration was created in the vicinity of the surface under the tip, which led to deposition of clusters measuring up to 15 nm on the substrate.

The jump-to-contact method was successfully used in the nanodesign in ionic liquids where experiments on the deposition of iron[597] and zinc[598] nanoclusters were carried out. The possibility of nanostructuring of bare and ethylene-modified Pt(111) surfaces by scanning with a closely positioned tip in the presence of copper ions in solution was demonstrated.[599] Certain problems of growing nanostructures in chambers of probe microscopes were also discussed.[45, 600, 601]

Zhdanov and Kasemo[602] mentioned the possibility of designing model nanocatalysts in the chamber of a tunnelling microscope. Seo and Borguet[603] have developed a special procedure of electrodeposition with the use of an atomic force microscope. The methods of nanodesign in the tunnelling microscope chamber were systematized and it was demonstrated that nanostructures can be formed under the conditions where both the substrate and the tip are coated with a layer of the deposited metal, in particular, atomic scale scratching takes place.[604]

Xie and Kolb[605] have discovered an interesting phenomenon, namely, the copper dissolution under a tunnelling microscope tip when the copper potential is more negative than the reversible potential of the Cu/Cu^{2+} system and the tip potential is more positive than this value. A similar phenomenon was also observed for the Ag dissolution.[600] The reasons for this are still unclear. According to the results obtained,[600] the local tip-induced dissolution produces negatively charged nanostructures on the substrate surface. The dissolution is associated with the local decrease in

the concentration of potential-determining ions, their electrostatic repulsion from the positively charged tip and hindering of the mass transfer due to the screening effect of the tip. Probably, account should be taken of the effect of oxygen traces on the behaviour of electrodes in the probe microscope chamber, which was noted in many studies. Thus, Mirkin and co-workers [606] observed the dissolution of platinum in aqueous and organic media in the potential region where hydroxyl radicals could appear during the oxygen electroreduction but the platinum dissolution was not still expected.

The different ways of formation of metal nanoparticles and their detection by the electrochemical scanning microscopy were discussed.[607] The authors used carbon fibre as the tip on which individual nanoparticles of platinum and nickel were electrodeposited.

Tao and co-workers [608] used an electrochemical scanning tunnelling microscope for preparation of atomic metal wires. In the original version, the tip was fixed at a distance of 10 – 150 nm from the substrate in a solution of 1 mM $CuSO_4$ + 0.1 M H_2SO_4. The substrate potential was maintained more positive than the tip potential so that copper was deposited only on the tip and gradually filled the gap between the tip and substrate. Once the growing copper layer reached the substrate, the contact (or a wire) was formed between them and the conductivity of the tip – substrate system increased jumpwise. The further copper deposition led to the stepwise increase in conductivity in accordance with the theory of conduction of thin films. When dissolving copper by shifting the tip potential in the positive direction, one could observe a stepwise increase in the resistance. The electrochemical synthesis of atomic wires was modified so that at present one can synthesize arrays of such wires and also nanoelectrodes separated by molecular-scale gaps to be used in studying the electron transport through molecules, measuring the conductivity of single molecules and designing molecular electronics devices.[609, 610]

XI. Conclusion

The presented material illustrates the wide diversity and the great potentials of electrochemical methods in synthesizing nanostructures and nanomaterials and the increasing use of these methods in nanochemistry and nanotechnology. At the same time, it is true that the possibilities of electrosynthesis of nanostructures are far from being exhausted.[21] Different lines of research in this field have been elaborated to different extents and the new electrosynthetic methods can also appear to satisfy the arising demands in new nanomaterials.

The nanoscale studies made it possible to take a new view on certain classical concepts and parts of electrochemistry and also on the phenomena and processes which were long in the focus of attention of electrochemists. In such studies, new and sometimes unexpected experimental and theoretical approaches were generated.

The development of efficient electrochemical methods for synthesizing and modifying nanoparticles opened up the possibility of preparing electrocatalysts that resemble their model analogues applied in fundamental research. However, the conclusions on higher activity of one or another type of nanoparticles often lack substantiation by measurements under steady-state (or quasisteady-state) conditions. The problems of stability of synthesized nanomaterials under practical conditions are still topical as well as the problems of cleanness of surfaces and the possible presence of impurities in the systems studied.[462, 611]

It should be emphasized that the past decade was characterized by the deep integration of nanoelectrochemistry with the other branches of nanoscience.[612] Such integration was beneficial for the progress in new areas of science and technology, in particular, in the field of photoelectrochemical conversion of solar energy.[613]

References

1. H Bonnemann, R M Richards *Eur. J. Inorg. Chem.* 2455 (2001)
2. A Roucoux, J Schulz, H Patin *Chem. Rev.* **102** 3757 (2002)
3. K Philippot, B Chaudret *C. R. Chimie* **6** 1019 (2003)
4. M A El-Sayed *Acc. Chem. Res.* **37** 326 (2004)
5. M-C Daniel, D Astruc *Chem. Rev.* **104** 293 (2004)
6. C Burda, X Chen, R Narayanan, M El-Sayed *Chem. Rev.* **105** 1025 (2005)
7. Y Yin, A P Alivisatos *Nature (London)* **437** 664 (2005)
8. P Wilcoxon, B L Abrams *Chem. Soc. Rev.* **35** 1162 (2006)
9. L S Ott, R G Finke *Coord. Chem. Rev.* **251** 1075 (2007)
10. S Guo, E Wang *Anal. Chim. Acta* **598** 181 (2007)
11. L D Pachon, G Rothenberg *Appl. Organomet. Chem.* **22** 288 (2008)
12. R Ferrando, J Jellinek, R L Johnston *Chem. Rev.* **108** 845 (2008)
13. X Hu, S Dong *J. Mater. Chem.* **18** 1279 (2008)
14. D R Rolison, J W Long, J C Lytle, A E Fischer, C P Rhodes, T M McEvoy, M E Bourg, A M Lubers *Chem. Soc. Rev.* **38** 226 (2009)
15. R Sardar, A M Funston, P Mulvaney, R W Murray *Langmuir* **25** 13840 (2009)
16. M R Jones, K D Osberg, R J Macfarlane, M R Langille, C A Mirkin *Chem. Rev.* **111** 3736 (2011)
17. Z-Y Zhou, N Tian, J-T Li, I Broadwell, S-G Sun *Chem. Soc. Rev.* **40** 4167 (2011)
18. R G Chaudhuri, S Paria *Chem. Rev.* **112** 2373 (2012)
19. J N Tiwari, R N Tiwari, K S Kim *Prog. Mater. Sci.* **57** 724 (2012)
20. S M Oja, M Wood, B Zhang *Anal. Chem.* **85** 473 (2013)
21. O A Petrii, G A Tsirlina *Russ. Chem. Rev.* **70** 285 (2001)
22. R W Murray *Chem. Rev.* **108** 2688 (2008)
23. H Gleiter *Acta Mater.* **48** 1 (2000)
24. A S Arico, P Bruce, B Scrosati, J-M Tarascon, W van Schalkwijk *Nat. Mater.* **4** 366 (2005)
25. A B Yaroslavtsev, Yu A Dobrovolsky, N S Shaglaeva, L A Frolova, E V Gerasimova, E A Sanginov *Russ. Chem. Rev.* **81** 191 (2012)
26. S Ya Istomin, E V Antipov *Russ. Chem. Rev.* **82** 686 (2013)
27. M P Pileni *J. Phys. Chem. C* **111** 9019 (2007)
28. T S Ahmadi, Z Y Wang, T C Green, A Henglein, M A El-Sayed *Science* **272** 1924 (1996)
29. V P Ananikov, N V Orlov, I P Beletskaya, V N Khrustalev, M Yu Antipin, T V Timofeeva *J. Am. Chem. Soc.* **129** 7252 (2007)
30. G A Somorjai, J Y Park *Top. Catal.* **49** 126 (2008)
31. Y Xia, Y Xiong, B Lim, S E Skrabalak *Angew. Chem., Int. Ed.* **48** 60 (2009)
32. C Wang, N M Markovic, V R Stamenkovic *ACS Catal.* **2** 891 (2012)
33. Y Kang, M Li, Y Cai, M Cargnello, R E Diaz, T R Gordon, N L Wieder, R R Adzic, R J Gorte, E A Stach, C B Murray *J. Am. Chem. Soc.* **135** 2741 (2013)
34. M E Baumgartner, C J Raub *Platinum Met. Rev.* **32** 188 (1988)

35. P L Cavallotti *Electrochim. Acta* **50** 4523 (2005)
36. *Electrochemical Dictionary* (Eds A J Bard, G Inzelt, F Scholz) (Heidelberg, Dordrect, London, New York: Springer, 2013)
37. E Budevski, G Staikov, W J Lorenz *Electrochemical Phase Formation and Growth* (New York: VCH, 1996)
38. A Milchev *Electrocrystallization: Fundamentals of Nucleation and Growth* (Boston: Kluwer, 2002)
39. M Paunovic *Fundamental of Electrochemical Deposition* (New York: Wiley, 2006)
40. *Electrocrystallization in Nanotechnology* (Ed. G Staikov) (Weinheim: Wiley-VCH, 2007)
41. W Plieth *Electrochemistry for Materials Science* (Amsterdam: Elsevier, 2008)
42. Y D Gamburg, G Zangari *Theory and Practice of Metal Electrodeposition* (New York: Springer, 2011)
43. A I Danilov *Russ. Chem. Rev.* **64** 767 (1995)
44. E Budevski, G Staikov, W J Lorenz *Electrochim. Acta* **45** 2559 (2000)
45. W J Lorenz, G Staikov, W Schindler, W Wiesbeck *J. Electrochem. Soc.* **149** K47 (2002)
46. M E Hyde, R G Compton *J. Electroanal. Chem.* **549** 1 (2003)
47. G B Sergeev, K J Klabunde *Nanochemistry* (Amsterdam: Elsevier, 2013)
48. V K LaMer, R H Dinegar *J. Am. Chem. Soc.* **72** 4847 (1950)
49. H Reiss *J. Chem. Phys.* **19** 482 (1954)
50. R M Penner *J. Phys. Chem. B* **106** 3339 (2002)
51. K Shimazu, D Weisshaar, T Kuwana *J. Electroanal. Chem.* **223** 223 (1987)
52. J V Zoval, R M Stiger, P R Biernacki, R M Penner *J. Phys. Chem.* **100** 837 (1996)
53. J V Zoval, P Biernacki, R M Penner *Anal. Chem.* **68** 1585 (1996)
54. G Hsiao, M G Anderson, S Gorer, D Harris, R M Penner *J. Am. Chem. Soc.* **119** 1439 (1997)
55. M Anderson, S Gorer, R M Penner *J. Phys. Chem.* **101** 5895 (1997)
56. R M Nyffeneger, B Craft, M Shaahan, S Gorer, R M Penner *Chem. Mater.* **10** 1120 (1998)
57. J V Zoval, J Lee, S Gorer, R M Penner *J. Phys. Chem. B* **102** 1166 (1998)
58. I Lee, K Y Chan, D L Phillips *Appl. Surf. Sci.* **136** 321 (1998)
59. H Liu, R M Penner *J. Phys. Chem. B* **104** 9131 (2000)
60. P Shen, N Chi, K-Y Chan, D L Phillips *Appl. Surf. Sci.* **172** 159 (2001)
61. S N Pron'kin, G A Tsirlina, O A Petrii, S Yu Vassiliev *Electrochim. Acta* **46** 2343 (2001)
62. K Marquez, G Staikov, J W Schultze *Electrochim. Acta* **48** 875 (2003)
63. J A Bennett, Y Show, S Wang, G M Swain *J. Electrochem. Soc.* **152** E184 (2005)
64. M M E Duarte, A S Pilla, J M Sieben, C E Mayer *Electrochem. Commun.* **8** 159 (2006)
65. A A Isse, S Gottardello, C Maccato, A Gennaro *Electrochem. Commun.* **8** 1707 (2006)
66. L Komsiyska, G Staikov *Electrochim. Acta* **54** 168 (2008)
67. T Brulle, U Stimming *J. Electroanal. Chem.* **636** 10 (2009)
68. M Bayati, J M Abad, R J Nichols, D J Schiffrin *J. Phys. Chem. C* **114** 18439 (2010)
69. W Plieth, H Dietz, G Sandmann, A Meixner, M Weber, P Moyer, J Schmidt *Electrochim. Acta* **44** 3659 (1999)
70. M P Zach, R M Penner *Adv. Mater.* **12** 878 (2000)
71. B Scharifker, G Hills *Electrochim. Acta* **28** 879 (1983)
72. R Scharifker, J Mostany *J. Electroanal. Chem.* **177** 13 (1984)
73. M V Mirkin, A P Nilov *J. Electroanal. Chem.* **283** 35 (1990)
74. L Heerman, A Tarallo *Electrochem. Commun.* **2** 85 (2000)
75. A N Correia, S A S Machado, L A Avaca *J. Electroanal. Chem.* **488** 110 (2000)
76. M Sluyters-Rehbach, J H O J Wijenberg, E Bosco, J H Sluyters *J. Electroanal. Chem.* **236** 1 (1987)
77. A Milchev, W S Kruijt, M Sluyters-Rehbach, J H Sluyters *J. Electroanal. Chem.* **350** 89 (1993)
78. V A Isaev, A N Baraboshkin *J. Electroanal. Chem.* **377** 33 (1994)
79. A Milchev *J. Electroanal. Chem.* **457** 35 (1998)
80. L Heerman, A Tarallo *J. Electroanal. Chem.* **470** 70 (1999)
81. J Fransaer, R M Penner *J. Phys. Chem. B* **103** 7643 (1999)
82. L Heerman, E Matthijs, S Langerjck *Electrochim. Acta* **47** 905 (2001)
83. Y Cao, A C West *J. Electroanal. Chem.* **514** 103 (2001)
84. Y Cao, P Searson, A C West *J. Electrochem. Soc.* **148** C376 (2001)
85. R M Penner *J. Phys. Chem. B* **105** 8672 (2001)
86. L Guo, A Radisic, P C Searson *J. Phys. Chem. B* **109** 24008 (2005)
87. M Y Abyaneh, M Fleischmann, E Del Giudice, G Vitiello *Electrochim. Acta* **54** 879 (2009)
88. J Ustarroz, X Ke, A Hubin, S Bals, H Terryn *J. Phys. Chem. C* **116** 2322 (2012)
89. A Serruya, J Mostany, B R Scharifker *J. Electroanal. Chem.* **464** 39 (1999)
90. G Oskam, P Searson *J. Electrochem. Soc.* **147** 2199 (2000)
91. C Ehlers, U Konig, G Staikov, J W Schultze *Electrochim. Acta* **47** 379 (2001)
92. C Li, G Oskam, P C Searson *J. Electrochem. Soc.* **148** C476 (2001)
93. A Radisic, J C Long, P M Hoffman, P C Searson *J. Electrochem. Soc.* **148** C41 (2001)
94. A Radisic, P M Vereecken, J B Hannon, P C Searson, F M Ross *Nano Lett.* **6** 238 (2006)
95. A Radisic, F M Ross, P C Searson *J. Phys. Chem. B* **110** 7862 (2006)
96. A Radisic, P M Vereecken, P C Searson, F M Ross *Surf. Sci.* **600** 1817 (2006)
97. T Zapryanova, A Hrussanova, A Milchev *J. Electroanal. Chem.* **600** 311 (2007)
98. A Serruya, J Mostany, B Scharifker *J. Chem. Soc., Faraday Trans.* **89** 255 (1993)
99. A Serruya, B Scharifker, I Gonzalez, M T Oropeza, M Palomar-Pardave *J. Appl. Electrochem.* **26** 451 (1996)
100. J Vermurugan, J-M Noel, W Nogala, M V Mirkin *Chem. Sci.* **3** 3307 (2012)
101. A R Kucernak, P B Chowdhury, C P Wilde, G H Kelsall, Y Y Zhu, D E Williams *Electrochim. Acta* **45** 4483 (2000)
102. D Grujicic, B Pesic *Electrochim. Acta* **47** 2901 (2002)
103. M E Hyde, R Jacobs, R G Compton *J. Phys. Chem. B* **106** 11075 (2002)
104. S Chen, A Kucernak *J. Phys. Chem. B* **107** 8392 (2003)
105. A O Summ, X B Ji, C E Banks, M Ehyde, R G Compton *ChemPhysChem* **7** 704 (2006)
106. E Sheridan, J Hjelm, R J Forster *J. Electroanal. Chem.* **608** 1 (2007)
107. M J Williamson, R M Tromp, P M Vereecken, R Hull, F M Ross *Nat. Mater.* **21** 532 (2003)
108. J Ustarroz, U Gupta, A Hubin, S Bals, H Terryn *Electrochem. Commun.* **12** 1706 (2010)
109. H M Zheng, R K Smith, Y W Jun, C Kisielowski, U Dahmen, A P Alivisatos *Science* **324** 1309 (2009)
110. V N Richards, S P Shields, W E Buhro *Chem. Mater.* **23** 137 (2011)
111. S Gorer, J Ganske, J C Hemminger, R M Penner *J. Am. Chem. Soc.* **120** 9584 (1998)
112. H Liu, F Favier, K Ng, M P Zach, R M Penner *Electrochim. Acta* **47** 671 (2001)
113. A Scheludko, M Todorova *Bull. Acad. Bulg. Sci. Phys.* **3** 61 (1952)
114. G Sandmann, H Dietz, W Plieth *J. Electroanal. Chem.* **491** 78 (2000)
115. M Ueda, H Dietz, A Anders, H Kneppe, A Meixner, W Plieth *Electrochim. Acta* **48** 377 (2002)

116. W Plieth, H Dietz, A Anders, G Sandmann, A Meixner, M Weber, H Kneppe *Surf. Sci.* **597** 119 (2005)
117. G Lu, G Zangari *J. Phys. Chem. B* **109** 7998 (2005)
118. G Lu, G Zangari *Electrochim. Acta* **51** 2531 (2006)
119. K L Norrod, K L Rowlen *Anal. Chem.* **70** 4218 (1998)
120. A N Patel, M G Collingtnon, M A O'Connell, W O Y Hung, K McKelvey, J V Macpherson, P R Unwin *J. Am. Chem. Soc.* **134** 20117 (2012)
121. Y-B He, G-R Li, Z-L Wang, Y-N Ou, Y-X Tong *J. Phys. Chem. C* **114** 19175 (2010)
122. F Montilla, E Morallon, I Duo, C Comninellis, J L Vazquez *Electrochim. Acta* **48** 3891 (2003)
123. P S Ruvinsky, S N Pronkin, V I Zaikowskii, P Bernhardt, E R Savinova *Phys. Chem. Chem. Phys.* **10** 6665 (2008)
124. J N Richardson, A J Osisek, A L Dyer *Electroanalysis* **15** 1567 (2003)
125. B Yin, H Ma, S Wang, S Chen *J. Phys. Chem. B* **107** 8898 (2003)
126. D H Dahanayaka, J X Wang, S Hossain, I A Bumm *J. Am. Chem. Soc.* **128** 6052 (2006)
127. X Dai, R C Compton *Anal. Sci.* **22** 567 (2006)
128. J Yu, S Li, J Li, F Zhao, B Zeng *J. Solid State Electrochem.* **11** 1211 (2007)
129. L Wang, W Mao, D Ni, J Di, Y Wu, Y Tu *Electrochem. Commun.* **10** 673 (2008)
130. Y Ma, J Di, X Yan, M Zhao, Z Lu, Y Tu *Biosens. Bioelectron.* **24** 1480 (2009)
131. H Zhang, W Zhou, Y Du, P Yang, C Wang *Electrochem. Commun.* **12** 882 (2010)
132. G Oskam, J G Long, A Natarajan, P C Searson *J. Phys. D: Appl. Phys.* **31** 1927 (1998)
133. A Radisic, A C West, P C Searson *J. Electrochem. Soc.* **149** C94 (2002)
134. A Radisic, Y Cao, P Taephaisitphongse, A C West, P C Searson *J. Electrochem. Soc.* **150** C362 (2003)
135. Q Huang, H Deligianni, L T Romankiw *J. Electrochem. Soc.* **153** C332 (2006)
136. E Herrero, L J Buller, H D Abruna *Chem. Rev.* **101** 1897 (2001)
137. L A Kibler, A M El-Aziz, D M Kolb *J. Mol. Catal., Int. Ed.* **199** 57 (2003)
138. L A Kibler, A M El-Aziz, R Hoyer, D M Kolb *Angew. Chem., Int. Ed.* **44** 2080 (2005)
139. L A Kibler *ChemPhysChem* **7** 985 (2006)
140. M E Quaym, S Ye, K Uosaki *J. Electroanal. Chem.* **520** 126 (2002)
141. T Kondo, J Morita, K Hanaoka, S Takakusagi, K Tamura, M Takahasi, J Mizuki, K Uosaki *J. Phys. Chem. C* **111** 13197 (2007)
142. S Takakusagi, K Kitamura, K Uosaki *Electrochim. Acta* **54** 5137 (2009)
143. M Shibata, N Hayashi, T Sakurai, A Kurokawa, H Fukumitsu, T Masuda, K Uosaki, T Kondo *J. Phys. Chem. C* **116** 26464 (2012)
144. A I Danilov, E B Molodkina, Yu M Polukarov, V Climent, J Feliu *Electrochim. Acta* **46** 3137 (2001)
145. A I Danilov, E B Molodkina, A A Baitov, I V Pobelov, Yu M Polukarov *Russ. J. Electrochem.* **38** 743 (2002) [*Elektrokhimiya* **38** 836 (2002)]
146. A I Danilov, E B Molodkina, A V Rudnev, Yu M Polukarov, J M Feliu *Electrochim. Acta* **50** 5032 (2005)
147. P L Redmond, A J Hallock, L E Brus *Nano Lett.* **5** 131 (2005)
148. P A Thiel, M Shen, D J Liu, J W Evans *J. Phys. Chem. C* **113** 5047 (2009)
149. P V Dudin, P R Unwin, J V Macpherson *J. Phys. Chem. C* **114** 13241 (2010)
150. R Ouyang, J-X Liu, W-X Li *J. Am. Chem. Soc.* **135** 1760 (2013)
151. C R K Rao, D C Trivedi *Coord. Chem. Rev.* **249** 613 (2005)
152. J J Whalen III, J D Weiland, P C Searson *J. Electrochem. Soc.* **152** C738 (2005)
153. S V Mentus *Electrochim. Acta* **50** 3509 (2005)
154. L M Plyasova, I Yu Molina, A N Gavrilov, S V Cherepanova, O V Cherstiouk, N A Rudina, E R Savinova, G A Tsirlina *Electrochim. Acta* **51** 4477 (2006)
155. O V Cherstiouk, A N Gavrilov, L M Plyasova, I Yu Molina, G A Tsirlina, E R Savinova *J. Solid State Electrochem.* **12** 497 (2008)
156. H M Yasin, G Denuault, D Pletcher *J. Electroanal. Chem.* **633** 327 (2009)
157. H Jeon, J Joo, Y Kwon, S Uhm, J Lee *J. Power Sources* **195** 5929 (2010)
158. A N Gavrilov, L M Plyasova, N A Rudina, I Yu Molina, G A Tsirlina, T Ya Safonova *Russ. J. Electrochem.* **40** 981 (2004) [*Elektrokhimiya* **40** 1134 (2004)]
159. A N Gavrilov, O A Petrii, A A Mukovnin, T V Levchenko, G A Tsirlina *Electrochim. Acta* **52** 2775 (2007)
160. O A Petrii *J. Solid State Electrochem.* **12** 609 (2008)
161. O A Petrii, T Ya Safonova, G A Tsirlina, M Yu Rusanova *Electrochim. Acta* **45** 4117 (2000)
162. P Liu, J K Norskov *Phys. Chem. Chem. Phys.* **3** 3814 (2001)
163. H Natter, R Hempelmann *J. Phys. Chem.* **100** 19525 (1996)
164. H Natter, T Krajewski, R Hempelmann *Ber. Bunsen. Ges. Phys. Chem.* **100** 55 (1996)
165. H Natter, M Schmelzer, R Hempelmann *J. Mater. Res.* **13** 1186 (1998)
166. H Natter, M Schmelzer, M-S Loffler, C E Krill, A Fitch, R Hempelmann *J. Phys. Chem. B*, **104** 2467 (2000)
167. R Przenioslo, R Winter, H Natter, M Schmelzer, R Hempelmann, W Wagner *Phys. Rev. B* **63** 054408 (2001)
168. H Natter, R Hempelmann *Electrochim. Acta* **49** 51 (2003)
169. H Natter, R Hempelmann *Z. Phys. Chem.* **222** 319 (2008)
170. A M El-Sherik, U Erb *J. Mater. Sci.* **30** 5743 (1995)
171. R T C Choo, J M Toguri, A M El-Sherik, U Erb *J. Appl. Electrochem.* **25** 384 (1995)
172. B Yu, P Woo, U Erb *Scr. Mater.* **56** 353 (2007)
173. Z-J Tian, D-S Wang, G F Wang, L D Shen, Z-D Liu, Y-H Huang *Trans. Nonferr. Met. Soc. China* **20** 1037 (2010)
174. A M Rashidi, A Amadeh *J. Mater. Sci. Technol.* **26** 82 (2010)
175. L Guo, P C Searson *Langmuir* **24** 10557 (2008)
176. T W Cornelius, J Brotz, N Chtanko, D Dobrev, G Miehe, R Neumann, M E T Mollares *Nanotechnology* **16** S246 (2005)
177. E C Walter, M P Zach, F Favier, B J Murray, K Inazu, J C Hemminger, R M Penner *ChemPhysChem* **4** 131 (2003)
178. M P Zach, R H Ng, R M Penner *Science* **290** 2120 (2000)
179. F Favier, E C Walter, M P Zach, T Benter, R M Penner *Science* **293** 2227 (2001)
180. J Clavilier, J M Feliu, A Aldaz *J. Electroanal. Chem.* **243** 419 (1988)
181. R J Nichols, D M Kolb, R J Behm *J. Electroanal. Chem.* **313** 109 (1991)
182. M Yun, N V Myung, R P Vasquez, C Lee, E Menke, R M Penner *Nano Lett.* **4** 419 (2004)
183. K Ramanathan, M A Bangar, M Yun, W Chen, A Muchandani, N V Myung *Nano Lett.* **4** 1237 (2004)
184. H Liu, J Kameoka, D A Czaplewski, H G Craighead *Nano Lett.* **4** 671 (2004)
185. Y Xiao, G Yu, J Yuan, J Wang, Z Chen *Electrochim. Acta* **51** 4218 (2006)
186. H-C Shin, J Dong, M Liu *Adv. Mater.* **15** 1610 (2003)
187. H-C Shin, M Liu *Chem. Mater.* **16** 5460 (2004)
188. H-C Shin, M Liu *Adv. Funct. Mater.* **15** 582 (2005)
189. M Raja, J Subha, F B Ali, S H Ryu *Mater. Manufact. Proc.* **23** 782 (2008)
190. V V Rajasekharan, D A Buttry *Chem. Mater.* **18** 4541 (2006)
191. R Shachman, D Mandler, D Avnir *Chem. – Eur. J.* **10** 1936 (2004)
192. D Pradhan, K T Leung *Langmuir* **24** 9707 (2008)

193. A Kleiman-Shwarsctein, Y-S Hu, A J Forman, G D Stucky, E W McFarland *J. Phys. Chem. C* **112** 15900 (2008)
194. J Reisse, H Francois, J Vandercammen, O Fabre, A Kirsch-de Mesmaeker, C Maerschalk, J-L Delplancke *Electrochim. Acta* **39** 37 (1994)
195. A Durant, J L Delplancke, V Libert, J Reisse *Eur. J. Org. Chem.* 2845 (1999)
196. J-L Delplancke, J Dille, J Reisse, G J Long, A Mohan, F Grandjean *Chem. Mater.* **12** 946 (2000)
197. Y Mastai, R Polsky, Yu Koltypin, A Gedanken, G Hodes *J. Am. Chem. Soc.* **121** 10047 (1999)
198. J Zhu, S T Aruna, Yu Koltypin, A Gedanken *Chem. Mater.* **12** 143 (2000)
199. A Malinauskas, J Malinauskiene, A Ramanavicius *Nanotechnology* **16** R51 (2005)
200. D Bhattacharjya, I Mukhopadhyay *Langmuir* **28** 5893 (2012)
201. M Chipara, R Skomski, D J Sellmyer *Mater. Lett.* **61** 2412 (2007)
202. M Giersig, P Mulvaney *Langmuir* **9** 3408 (1993)
203. I Zhitomirsky *J. Mater. Sci.* **41** 8186 (2006)
204. Q-T Vu, M Pavlik, N Hebestreit, J Pfleger, U Rammelt, W Plieth *Electrochim. Acta* **51** 1117 (2005)
205. R M Penner, M J Heben, T L Longin, N S Lewis *Science* **250** 1118 (1990)
206. D W M Arrigan *Analyst* **129** 1157 (2004)
207. M A Thompson, E J Menke, C C Martens, R M Penner *J. Phys. Chem. B* **110** 36 (2006)
208. G A Ozin *Adv. Mater.* **4** 612 (1992)
209. M Lai, D J Riley *J. Colloid Interface Sci.* **323** 203 (2008)
210. K Jackowska, A T Biegunski, M Tagowska *J. Solid State Electrochem.* **12** 437 (2008)
211. T M Whitney, J S Jiang, P C Searson, C L Chien *Science* **261** 1316 (1993)
212. C R Martin *Science* **266** 1961 (1994)
213. C R Martin *Acc. Chem. Rev.* **28** 61 (1995)
214. C R Martin *Chem. Mater.* **8** 1739 (1996)
215. M Lai, J-H Lim, Y Rheem, A Mulchandani, M A Deshusses, N V Myung *Nanotechnology* **20** 185602 (2009)
216. E J B Rodijk, A W Maijenburg, M G Maas, D H A Blank, J E ten Elshof *Mater. Lett.* **65** 3374 (2011)
217. A M M Jani, D Losic, N H Voelcker *Prog. Mater. Sci.* **58** 636 (2013)
218. H Masuda, K Fukuda *Science* **268** 1466 (1995)
219. K S Napolskii, P J Barczuk, S Yu Vassiliev, A G Veresov, G A Tsirlina, P J Kulesza *Electrochim. Acta* **52** 7910 (2007)
220. K S Napolskii, I V Roslyakov, A A Eliseev, D I Petukhov, A V Lukashin, S-F Chen, C-P Liu, G A Tsirlina *Electrochim. Acta* **56** 2378 (2011)
221. M A Bangar, C M Hangarter, B Yao, Y Rheem, W Chen, A Mulchandani, N V Myung *Electroanalysis* **21** 61 (2009)
222. M Cortes, E Gomez, E Valles *J. Electroanal. Chem.* **689** 69 (2013)
223. M Lahav, E A Weiss, Q Xu, G M Whitesides *Nano Lett.* **6** 2166 (2006)
224. D A Bograchev, V M Volgin, A D Davydov *Electrochim. Acta* **96** 1 (2013)
225. D A Bograchev, V M Volgin, A D Davydov *Electrochim. Acta* **112** 279 (2013)
226. V Zwilling, M Aucouturier, E Darque-Ceretti *Electrochim. Acta* **44** 921 (1999)
227. J M Macak, H Tsuchiya, P Schmuki *Angew. Chem., Int. Ed.* **44** 2100 (2005)
228. J M Macak, H Tsuchiya, L Taveira, S Aldabergerova, P Schmiki *Angew. Chem., Int. Ed.* **44** 7463 (2005)
229. S P Albu, A Ghicov, J M Macak, R Hahn, P Schmuki *Nano Lett.* **7** 1286 (2007)
230. Y-C Nah, I Paramasivam, P Schmuki *ChemPhysChem* **11** 2698 (2010)
231. P Roy, S Berger, P Schmuki *Angew. Chem., Int. Ed.* **50** 2904 (2011)
232. C Wang, L Sun, H Yun, J Li, Y Lai, C Lin *Nanotechnology* **20** 295601 (2009)
233. M Hepel, I Kumarihamy, C J Zhong *Electrochem. Commun.* **8** 1439 (2006)
234. T Hepel, M Hepel, R Osteryoung *J. Electrochem. Soc.* **129** 2132 (1982)
235. D R Rolison *Chem. Rev.* **90** 867 (1990)
236. S Senthilkumar, A Adisa, R Saraswathi, R A W Dryfe *Electrochem. Commun.* **10** 141 (2008)
237. Y Kanno, T Suzuki, Y Yamauchi, K Kuroda *J. Phys. Chem. C* **116** 24672 (2012)
238. N V Dziomkina, G J Vansco *Soft Mater.* **1** 265 (2005)
239. L Xu, W L Zhou, C Frommen, R H Baughman, A A Zakhidov, L Malkinski, J-Q Wang, J B Wiley *Chem. Commun.* 997 (2000)
240. H Yan, Y Yang, Z Fu, B Yang, L Xia, S Fu, F Li *Electrochem. Commun.* **7** 1117 (2005)
241. R Shacham, D Avnir, D Mandler *Adv. Mater.* **11** 384 (1999)
242. R Toledano, R Shacham, D Avnir, D Mandler *Chem. Mater.* **20** 4276 (2008)
243. R Toledano, D Mandler *Chem. Mater.* **22** 3943 (2010)
244. G S Attard, P N Bartlett, N R B Coleman, J M Elliot, J R Owen, J H Wang *Science* **278** 838 (1997)
245. J M Elliott, G S Attard, P N Bartlett, N R B Coleman, D A S Merckel, J R Owen *Chem. Mater.* **11** 3602 (1999)
246. J M Elliott, P R Birkin, P N Bartlett, G S Attard *Langmuir* **15** 7411 (1999)
247. J M Elliott, J R Owen *Phys. Chem. Chem. Phys.* **2** 5653 (2000)
248. B Gollas, J M Elliott, P N Bartlett *Electrochim. Acta* **45** 3711 (2000)
249. P N Bartlett, P R Birkin, M A Ghanem, P de Groot, M Sawicki *J. Electrochem. Soc.* **148** C119 (2001)
250. I Nandhakumar, J M Eliot, G S Attard *Chem. Mater.* **13** 3840 (2001)
251. J M Elliott, L M Cabuche, P N Bartlett *Anal. Chem.* **73** 2855 (2001)
252. P N Bartlett, B Gollas, S Guerin, J Marwan *Phys. Chem. Chem. Phys.* **4** 3835 (2002)
253. A Takai, Y Yamauchi, K Kuroda *J. Am. Chem. Soc.* **132** 208 (2010)
254. Y Yamauchi, A Tonegawa, M Komatsu, H Wang, L Wang, Y Nemoto, N Suzuki, K Kuroda *J. Am. Chem. Soc.* **134** 5100 (2012)
255. Y-C Liang, Y-W Juan, K-T Lu, U-S Jeng, S-A Chen, W-T Chuang, C-J Su, C-L Liu, C-W Pao, J-F Lee, H-S Sheu, J-M Chen *J. Phys. Chem. C* **116** 26649 (2012)
256. Y Shao, Y D Jin, S J Dong *Electrochem. Commun.* **4** 773 (2002)
257. D K Sarkar, X J Zhou, A Tannous, K T Leung *J. Phys. Chem. B* **107** 2879 (2003)
258. E J Menke, M A Thompson, C Xiang, L C Yang, R M Penner *Nat. Mater.* **5** 914 (2006)
259. C Xiang, S-C Kung, D K Taggart, F Yang, M A Thompson, A G Guell, Y Yang, R M Penner *ACS Nano* **2** 1939 (2008)
260. C Xiang, J Y Kim, R M Penner *Nano Lett.* **9** 2133 (2009)
261. C X Xiang, Y G Yang, R M Penner *Chem. Commun.* 859 (2009)
262. Y A Yang, S C Kung, D K Taggart, C Xiang, F Yang, M A Brown, A G Guell, T J Kruse, J C Hemminger, R M Penner *Nano Lett.* **8** 2447 (2008)
263. S C Kung, W E van der Veer, F Yang, K C Donavan, R M Penner *Nano Lett.* **10** 1481 (2010)
264. J A Arter, D K Taggart, T M McIntire, R M Penner, G A Weiss *Nano Lett.* **10** 4858 (2010)
265. Y Xia, G M Whitesides *Angew. Chem. Int. Ed.* **37** 550 (1998)
266. A George, A W Maijenburg, M G Maas, D H A Blank, J E ten Elshof *ACS Appl. Mater. Interfaces* **3** 3666 (2011)
267. M G Maas, E J B Rodijk, A W Maijenburg, D H A Blank, J E ten Elshof *J. Mater. Res.* **26** 2261 (2011)
268. A R Halpern, R M Corn *ACS Nano* **7** 1755 (2013)

269. N S Pesika, A Radisic, K J Stebe, P C Searson *Nano Lett.* **6** 1023 (2006)
270. F Zhou, M Chen, W Liu, J Liu, Z Liu, Z Mu *Adv. Mater.* **15** 1367 (2003)
271. M Cavallini, M Facchini, C Albonetti, F Biscarini, M Innocenti, F Loglio, E Salvietti, G Pezzatini, M L Foresti *J. Phys. Chem. C* **111** 1061 (2007)
272. I Dumitrescu, P R Unwin, J V Macpherson *Chem. Commun.* 6886 (2009)
273. T M Day, P R Unwin, N R Wilson, J V Macpherson *J. Am. Chem. Soc.* **127** 10639 (2005)
274. B M Quinn, C Dekker, S G Lemay *J. Am. Chem. Soc.* **127** 6146 (2005)
275. B M Quin, S G Lemay *Adv. Mater.* **18** 855 (2006)
276. T M Day, P R Unwin, J V Macpherson *Nano Lett.* **7** 51 (2007)
277. P V Dudin, M E Snowden, J V Macpherson, P R Unwin *ACS Nano* **5** 12 10017 (2011)
278. S-L Chou, J-Z Wang, S-Y Chew, H-K Liu, S-X Dou *Electrochem. Commun.* **10** 1724 (2008)
279. T S Yarden, E Joselevich *Nano Lett.* **12** 4742 (2010)
280. X W Gu, N Shadmi, T S Yarden, H Cohen, E Joselevich *J. Phys. Chem. C* **116** 20121 (2012)
281. A Davies, P Audette, B Farrow, F Hassan, Z Chen, J-Y Choi, A Yu *J. Phys. Chem. C* **115** 17612 (2011)
282. V Tsakova, S Winkels, J W Schultze *J. Electroanal. Chem.* **500** 574 (2001)
283. X J Zhou, A J Harmer, N F Heinig, K T Leung *Langmuir* **29** 5109 (2004)
284. T Danieli, J Colleran, D Mandler *Phys. Chem. Chem. Phys.* **13** 20345 (2011)
285. G A Tsirlina, O A Petrii, T Ya Safonova, I M Papisov, S Yu Vassiliev, A E Gabrielov *Electrochim. Acta* **47** 3749 (2002)
286. R A Horch, N D Golden, N A D'Souza, L Riester *Chem. Mater.* **14** 3531 (2002)
287. E K Lavrentyeva, S Yu Vassiliev, E E Levin, A A Tsirlin, S N Polyakov, M Leoni, K S Napolskii, O A Petrii, G A Tsirlina *Electrochim. Acta* **61** 94 (2012)
288. M I Borzenko, M Chojak, P J Kulesza, G A Tsirlina, O A Petrii *Electrochim. Acta* **48** 3497 (2003)
289. E V Timofeeva, M I Borzenko, G A Tsirlina, E A Astaf'ev, O A Petrii *J. Solid State Electrochem.* **8** 778 (2004)
290. I Gorelikov, E Kumacheva *Chem. Mater.* **16** 4122 (2004)
291. Y-Y Yu, S-S Chang, C-L Lee, C R C Wang *J. Phys. Chem. B* **101** 6661 (1997)
292. Q Shen, Q Min, J Shi, L Jiang, J-R Zhang, W Hou, J-J Zhu *J. Phys. Chem. C* **113** 1267 (2009)
293. I Haas, A Gedanken *Chem. Mater.* **18** 1184 (2006)
294. K-S Choi, H C Lichtenegger, E W McFarland, G D Stucky *J. Am. Chem. Soc.* **124** 12402 (2002)
295. S-H Baeck, K-S Choi, T F Jaramillo, G D Stucky, E W McFarland *Adv. Mater.* **15** 1269 (2003)
296. L G Abdelmoti, F P Zamborini *Langmuir* **26** 13511 (2010)
297. J A Switzer, M G Shumsky, E W Bohannan *Science* **284** 293 (1999)
298. L P Colletti, J L Stickney *J. Electrochem. Soc.* **145** 1442 (1998)
299. A A Vertegel, M G Shumsky, J A Switzer *Angew. Chem., Int. Ed.* **38** 3169 (1999)
300. T Pauporte, R Cortes, M Froment, B Beaumont, D Lincot *Chem. Mater.* **14** 4702 (2002)
301. J A Switzer, H M Kothari, E W Bohannan *J. Phys. Chem. B* **106** 4027 (2002)
302. S J Limmer, E A Kulp, J A Switzer *Langmuir* **22** 10535 (2006)
303. J J Mallett, E B Svedberg, M D Vaudin, L A Bendersky, A J Shapiro, T P Moffat *Phys. Rev. B* **75** 085304 (2007)
304. S Boonsalee, R V Gudavarthy, E W Bohannan, J A Switzer *Chem. Mater.* **20** 5737 (2008)
305. J A Koza, Z He, A S Miller, J A Switzer *Chem. Mater.* **24** 3567 (2012)
306. D Banga, N Jarayaju, L Sheridan, Y-G Kim, B Perdue, X Zhang, Q Zhang, J Stickney *Langmuir* **28** 3024 (2012)
307. O Holderer, T Epicier, C Esnouf, G Fuchs *J. Phys. Chem. B* **107** 1723 (2003)
308. A Vaskelic, A Jagminiene, L Tamasauskaite-Tamasiunaite, R Juskenas *Electrochim. Acta* **50** 4586 (2005)
309. Z Liu, X Lin, J Y Lee, W Zhang, M Han, L M Gan *Langmuir* **18** 4054 (2002)
310. Y Yamauchi, T Momma, T Yokoshima, K Kuroda, T Osaka *J. Mater. Chem.* **15** 1987 (2005)
311. D A Slanac, A Lie, J A Paulson, K J Stevenson, K P Johnston *J. Phys. Chem. C* **116** 11032 (2012)
312. S R Brancovic, J X Wang, R R Adzic *Surface Sci.* **474** L173 (2001)
313. S R Brancovic, J X Wang, R R Adzic *J. Serb. Chem. Soc.* **66** 887 (2001)
314. M F Mrozek, Y Xie, M J Weaver *Anal. Chem.* **73** 5953 (2001)
315. S Park, P Yang, P Corredor, M J Weaver *J. Am. Chem. Soc.* **124** 2428 (2002)
316. M van Brussel, G Kokkinidis, I Vandendael, C Buess-Herman *Electrochem. Commun.* **4** 808 (2002)
317. M van Brussel, G Kokkinidis, I Vandendael, C Buess-Herman *Electrochim. Acta* **48** 3909 (2003)
318. Y Jin, Y Shen, S Dong *J. Phys. Chem. B* **108** 8142 (2004)
319. K Sasaki, Y Mo, J X Wang, M Balasubramanian, M Uribe, J McBreen, R R Adzic *Electrochim. Acta* **48** 3841 (2003)
320. J Zhang, Y Mo, M B Vukmirovic, R Klie, K Sasaki, R R Adzic *J. Phys. Chem. B* **108** 10955 (2004)
321. J L Zhang, M B Vukmirovic, Y Xu, M Mavrikakis, R R Adzic *Angew. Chem., Int. Ed.* **44** 2132 (2005)
322. M H Shao, T Huang, P Liu, J Zhang, K Sasaki, M B Vukmirovic, R R Adzic *Langmuir* **22** 10409 (2006)
323. M V Vukmirovic, J Zhang, K Sasaki, A U Nilekar, F Uribe, M Mavrikakis, R R Adzic *Electrochim. Acta* **52** 2257 (2007)
324. Y Ando, K Sasaki, R Adzic *Electrochem. Commun.* **11** 1135 (2009)
325. R Vasilic, N Dimitrov *Electrochem. Solid State Lett.* **8** C173 (2005)
326. L T Viyannalage, R Vasilic, N Dimitrov *J. Phys. Chem. C* **111** 4036 (2007)
327. M Fayette, Y Liu, D Bertrand, J Nutariya, N Vasiljevic, N Dimitrov *Langmuir* **27** 5650 (2011)
328. Y G Kim, J Y Kim, D Vairavapandian, J L Stickney *J. Phys. Chem.* **110** 17988 (2006)
329. J Y Kim, Y G Kim, J L Stickney *J. Electrochem. Soc.* **154** D260 (2007)
330. C Thambidural, Y-G Kim, J L Stickney *Electrochim. Acta* **53** 6157 (2008)
331. C Thambidural, Y-G Kim, N Jayaraju, V Venkatasamy, J L Stickney *J. Electrochem. Soc.* **156** D261 (2009)
332. C Thambidurai, D K Gebregziabiher, X H Liang, Q H Zhang, V Ivanova, P H Haumesser, J L Stickney *J. Electrochem. Soc.* **157** D466 (2010)
333. D K Gebregziabiher, Y G Kim, C Thambidurai, V Ivanova, P H Haumesser, J L Stickney *J. Cryst. Growth* **312** 1271 (2010)
334. L B Sheridan, J Czerwiniski, N Jayaraju, D K Gebregziabiher, J L Stickney, D B Robinson, M P Soriaga *Electrocatalysis* **3** 96 (2012)
335. N Jayaraju, D Vairavapandian, Y G Kim, D Banga, J L Stickney *J. Electrochem. Soc.* **159** D616 (2012)
336. L B Sheridan, D K Gebregziabiher, J L Stickney, D B Robinson *Langmuir* **29** 1592 (2013)
337. T S Mkwizu, M K Mathe, I Cukrowski *Langmuir* **26** 570 (2010)
338. R Wang, C Wang, W-B Cai, Y Ding *Adv. Mater.* **22** 1845 (2010)

339. G Kokkinidis, A Papoutsis, D Stoychev, A Milchev *J. Electroanal. Chem.* **486** 48 (2000)
340. G Kokkinidis, D Stoychev, A Lazarov, A Milchev *J. Electroanal. Chem.* **511** 20 (2001)
341. A Tegou, S Papadimitriou, E Pavlidou, G Kokkinidis, S Sotiropoulos *J. Electroanal. Chem.* **608** 67 (2007)
342. S Papadimitriou, A Tegou, E Pavlidou, S Armyanov, E Valova, G Kokkinidis, S Sotiropoulos *Electrochim. Acta* **53** 6559 (2008)
343. A Tegou, S Papadimitriou, E Pavlidou, S Armyanov, E Valova, G Kokkinidis, S Sotiropoulos *J. Electroanal. Chem.* **623** 187 (2008)
344. A Tegou, S Papadimitriou, G Kokkinidis, S Sotiropoulos *J. Solid State Electrochem.* **14** 175 (2009)
345. S Papadimitriou, S Armyanov, E Valova, A Hubin, O Steenhaut, E Pavlidou, G Kokkinidis, S Sotiropoulos *J. Phys. Chem. C* **114** 5217 (2010)
346. C H Chang, Y Rheem, Y-H Choa, D H Shin, D-Y Park, N V Myung *Electrochim. Acta* **55** 743 (2010)
347. C H Chang, Y Rheem, Y-H Choa, D-Y Park, N V Myung *Electrochim. Acta* **55** 1072 (2010)
348. D Brevnov, T S Olson, G P Lopez, P Atanassov *J. Phys. Chem. B* **108** 17531 (2004)
349. V Bansal, H Jani, J D Plessis, P J Coloe, S Bhargava *Adv. Mater.* **20** 717 (2008)
350. O Ghodbane, L Roue, D Belanger *Chem. Mater.* **20** 3495 (2008)
351. D Gokcen, S-E Bae, S R Brankovic *J. Electrochem. Soc.* **157** D582 (2010)
352. D Gokcen, S-E Bae, S R Brankovic *Electrochim. Acta* **56** 5545 (2011)
353. Y Sun, Y Xia *Science* **298** 2176 (2002)
354. Y Sun, Y Xia *J. Am. Chem. Soc.* **126** 3892 (2004)
355. H Zhang, M Jin, J Wang, W Li, P H C Camargo, M J Kim, D Yang, Z Xie, Y Xia *J. Am. Chem. Soc.* **133** 6078 (2011)
356. R A W Dryfe, E C Walter, R M Penner *ChemPhysChem* **5** 1879 (2004)
357. D-Y Park, H S Jung, Y Rheem, C M Hangarter, Y-I Lee, J M Ko, Y-H Choa, N V Myung *Electrochim. Acta* **55** 4212 (2010)
358. C M Hangarter, Y-I Lee, S C Hernandez, Y-H Choa, N V Myung *Angew. Chem.* **122** 7235 (2010)
359. Y Rheem, C H Chang, C M Hangarter, D-Y Park, K-H Lee, Y-S Jeong, N V Myung *Electrochim. Acta* **55** 2472 (2010)
360. Z Chen, M Waje, W Li, Y Yan *Angew. Chem., Int. Ed.* **46** 4060 (2007)
361. M Mohl, D Dobo, A Kukovecz, Z Konya, K Kordas, J Wei, R Vajtai, P M Ajayan *J. Phys. Chem. C* **115** 9403 (2011)
362. Y Yin, R M Riuox, C K Erdonmez, S Huges, G A Somorjai, A P Alivisatos *Science* **304** 711 (2004)
363. J Zhang, F H B Lima, M H Shao, K Sasaki, J X Wang, J Hanson, R R Adzic *J. Phys. Chem. B* **109** 22701 (2005)
364. J Zhang, K Sasaki, E Sutter, R R Adzic *Science* **315** 220 (2007)
365. K Sasaki, R R Adzic *J. Electrochem. Soc.* **155** B180 (2008)
366. R R Adzic, J Zhang, K Sasaki, M B Vukmirovic, M Shao, J X Wang, A U Nilekar, M Mavrikakis, J A Valerio, F Uribe *Top. Catal.* **46** 249 (2007)
367. M Shao, K Sasaki, N S Marinkovic, L Zhang, R R Adzic *Electrochem. Commun.* **9** 2848 (2007)
368. F H B Lima, J Zhang, M H Shao, K Sasaki, M B Vukmirovic, E A Ticianelli, R R Adzic *J. Solid State Electrochem.* **12** 399 (2008)
369. K Sasaki, L Zhang, R R Adzic *Phys. Chem. Chem. Phys.* **10** 159 (2008)
370. W Zhou, X Yang, M B Vukmirovic, B E Koel, J Jiao, G Peng, M Mavrikakis, R R Adzic *J. Am. Chem. Soc.* **131** 12755 (2009)
371. J X Wang, H Inada, L Wu, Y Choi, P Liu, W-P Zhou, R R Adzic *J. Am. Chem. Soc.* **131** 17298 (2009)
372. K Gong, W-F Chen, K Sasaki, D Su, M B Vukmirovic, W Zhou, E L Izzo, C Perez-Acosta, P Hirunsit, P B Balbuena, R R Adzic *J. Electroanal. Chem.* **649** 232 (2010)
373. K Sasaki, J X Wang, H Naohara, N Marinkovic, K More, H Inada, R R Adzic *Electrochim. Acta* **55** 2645 (2010)
374. Y Xing, Y Cai, M B Vukmirovic, W-P Zhou, H Karan, J X Wang, R R Adzic *J. Phys. Chem. Lett.* **1** 3238 (2010)
375. K Sasaki, H Naohara, Y Cai, Y M Choi, P Liu, M B Vukmirovic, J X Wang, R R Adzic *Angew. Chem., Int. Ed.* **49** 8602 (2010)
376. C Koenigsmann, A C Santulli, K Gong, M B Vukmirovich, W-R Zhou, E Sutter, S S Wong, R R Adzic *J. Am. Chem. Soc.* **133** 9783 (2011)
377. K Sasaki, K A Kuttiyiel, D Su, R R Adzic *Electrocatalysis* **2** 134 (2011)
378. M Li, P Liu, R R Adzic *J. Phys. Chem. Lett.* **3** 3480 (2012)
379. L Yang, M B Vukmirovic, D Su, K Sasaki, J A Herron, M Mavrikakis, S Liao, R R Adzic *J. Phys. Chem. C* **117** 1748 (2013)
380. P A Midley, M Weyland *Ultramicroscopy* **96** 413 (2003)
381. S-i Nagamatsu, T Arai, M Yamamoto, T Ohkura, H Oyanagi, T Ishizaka, H Kawanami, T Uriga, M Tada, Y Iwasawa *J. Phys. Chem. C* **117** 13094 (2013)
382. Q-S Chen, S-G Sun, Z-Y Zhou, Y-X Chen, S B Deng *Phys. Chem. Chem. Phys.* **10** 3645 (2008)
383. Y Hamasaki, N Nakashima, Y Niidome *J. Phys. Chem. C* **117** 2521 (2013)
384. B I Podlovchenko, V A Krivchenko, Yu M Maksimov, T D Gladysheva, L V Yashina, S A Evlashin, A A Pilevsky *Electrochim. Acta* **76** 137 (2012)
385. D Wang, H L Xin, Y Yu, H Wang, E Rus, D A Muller, H D Abruna *J. Am. Chem. Soc.* **132** 17664 (2010)
386. T Cochell, W Li, A Manthiram *J. Phys. Chem.* **117** 3865 (2013)
387. B I Podlovchenko, T D Gladysheva, A Yu Filatov, L V Yashina *Russ. J. Electrochem.* **46** 1189 (2010) [*Elektrokhimiya* **46** 1272 (2010)]
388. N Kristian, Y Yu, J-M Lee, X Liu, X Wang *Electrochim. Acta* **56** 1000 (2010)
389. P Wang, H Li, H Feng, H Wang, L Lei *J. Power Sources* **195** 1099 (2010)
390. G-R Zhang, D Zhao, Y-Y Feng, B Zhang, D S Su, G Liu, B-Q Xu *ACS Nano* **6** 2226 (2012)
391. P P Wells, E M Crabb, C R King, R Wiltshire, B Billsborrow, D Thompsett, A E Russell *Phys. Chem. Chem. Phys.* **11** 5773 (2009)
392. S W T Price, J D Speed, P Kannan, A E Russell *J. Am. Chem. Soc.* **133** 19448 (2011)
393. H Yang *Angew. Chem., Int. Ed.* **50** 2674 (2011)
394. C Kulp, K Gullmeister, W Widdra, M Bron *ChemPhysChem* **14** 1205(2013)
395. N A Majorova, O V Zhigalina, V G Zhigalina, O A Khazova *Russ. J. Electrochem.* **50** 223 (2014) [*Elektrokhimiya* **50** 251 (2014)]
396. F Jia, C Yu, K Deng, L Zhang *J. Phys. Chem. C* **111** 8424 (2007)
397. *Problemy Elektrokataliza* (The Problems of Electrocatalysis) (Ed. V S Bagotskii) (Moscow: Nauka, 1980)
398. W B Liu, S C Zhang, N Li, J W Zheng, Y L Xing *Microporous Mesoporous Mater.* **138** 1 (2011)
399. H-B Lu, Y Li, F-H Wang *Scr. Mater.* **56** 165 (2007)
400. J Erlebacher, M J Aziz, A Karma, N Dimitrov, K Sieradzki *Nature (London)* **410** 450 (2001)
401. Y Ding, J D Erlebacher *J. Am. Chem. Soc.* **125** 7772 (2003)
402. Y Ding, M W Chen, J Erlebacher *J. Am. Chem. Soc.* **126** 6876 (2004)
403. J Erlebacher *J. Electrochem. Soc.* **151** C614 (2004)
404. Y Ding, Y-J Kim, J Erlebacher *Adv. Mater.* **16** 1897 (2004)

405. J Rugolo, J Erlebacher, K Sieradzki *Nat. Mater.* **5** 946 (2006)
406. J Snyder, K Livi, J Erlebacher *J. Electrochem. Soc.* **155** C464 (2008)
407. J Erlebacher, R Seshardi *MRS Bull.* **34** 561 (2009)
408. Y Liu, S Bliznakov, N Dimitrov *J. Electrochem. Soc.* **157** K168 (2010)
409. J Erlebacher *Phys. Rev. Lett.* **106** 225504 (2011)
410. M Kamundi, L Bromberg, E Fey, C Mitchell, M Fayette, N Dimitrov *J. Phys. Chem. C* **116** 14123 (2012)
411. I McCue, J Snyder, X Li, Q Chen, K Sieradzki, J Erlebacher *Phys. Rev. Lett.* **108** 225503 (2012)
412. Y Liu, S Bliznakov, N Dimitrov *J. Phys. Chem. C* **113** 12362 (2009)
413. R Zeis, T Lei, K Sieradzki, J Snyder, J Erlebacher *J. Catal.* **253** 132 (2008)
414. R Zeis, A Mathur, G Fritz, J Lee, J Erlebacher *J. Power Sources* **165** 65 (2007)
415. J Snyder, P Asanithi, A B Dalton, J Erlebacher *Adv. Mater.* **20** 4883 (2008)
416. T Fujita, P Guan, K McKenna, X Lang, A Hirata, L Zhang, T Tokunaga, S Arai, Y Yamamoto, N Tanaka, Y Ishikawa, N Asao, Y Yamamoto, J Erlebacher, M Chen *Nat. Mater.* **11** 775 (2012)
417. S Ji, P C Searson *J. Phys. Chem. B* **107** 4494 (2003)
418. Y Sun, Y Xia *Nano Lett.* **3** 1569 (2003)
419. M Hakamada, M Mabuchi *Scr. Mater.* **56** 1003 (2007)
420. D A McCurry, M Kamundi, M Fayette, F Wahula, N Dimitrov *ACS Appl. Mater. Interfaces* **3** 4459 (2011)
421. D Wang, Y Yu, H L Xin, R Hovden, P Ercius, J A Mundy, H Chen, J H Richard, D A Muller, F J DiSalvo, H D Abruna *Nano Lett.* **12** 5230 (2012)
422. L Sun, C-L Chien, P C Searson *Chem. Mater.* **16** 3125 (2004)
423. J R Hayes, A M Hodge, J Biener, A V Hamza, K Sieradzki *J. Mater. Res.* **21** 2611 (2006)
424. L-Y Chen, J-S Yu, T Fujita, M-W Chen *Adv. Funct. Mater.* **19** 1221 (2009)
425. F U Renner, G A Eckstein, L Lymperakis, A Dakkouri-Baldauf, M Rohwerder, J Neugebauer, M Stratmann *Electrochim. Acta* **56** 1694 (2011)
426. M Hakamada, M Mabuchi *J. Alloys Compd.* **479** 326 (2009)
427. M Hakamada, H Nakano, T Furukawa, M Takahashi, M Mabuchi *J. Phys. Chem. C* **114** 868 (2010)
428. T Toda, H Igarashi, H Uchida, M Watanabe *J. Electrochem. Soc.* **146** 3750 (1999)
429. A Bonakdarpour, R Lobel, R T Atanasoski, G D Vernstrom, A K Schomoeckel, M K J Debe, J R Dahn *J. Electrochem. Soc.* **153** A1835 (2006)
430. D V Pugh, A Dursun, S G Corcoran *J. Electrochem. Soc.* **152** B455 (2005)
431. J Snyder, T Fujita, M W Chen, J Erlebacher *Nat. Mater.* **9** 904 (2010)
432. J Snyder, I McCue, K Livi, J Erlebacher *J. Am. Chem. Soc.* **134** 8633 (2012)
433. S Koh, P Strasser *J. Am. Chem. Soc.* **129** 12624 (2007)
434. P Mani, R Srivastava, P Strasser *J. Phys. Chem. C* **112** 2770 (2008)
435. P Strasser, S Koh, J Greeley *Phys. Chem. Chem. Phys.* **10** 3670 (2008)
436. S Koh, N Hahn, P Strasser *J. Electrochem. Soc.* **155** B1281 (2008)
437. C Yu, S Koh, J F Leisch, M F Toney, P Strasser *Faraday Discuss.* **140** 283 (2009)
438. P Strasser, S Koh, T Anniyev, J Greeley, K More, C Yu, Z Liu, S Kaya, D Nordlund, H Ogasawara, M F Toney, A Nilsson *Nat. Chem.* **2** 454 (2010)
439. R Yang, J Leisch, P Strasser, M F Toney *Chem. Mater.* **22** 4712 (2010)
440. F Hasche, M Oezaslan, P Strasser *Chem. Cat. Chem.* **3** 1805 (2011)
441. M Heggen, M Oezaslan, L Houben, P Strasser *J. Phys. Chem. C* **116** 19073 (2012)
442. M Oezaslan, M Heggen, P Strasser *J. Am. Chem. Soc.* **134** 514 (2012)
443. M Oezaslan, P Strasser *J. Power Sources* **196** 5240 (2011)
444. L Gan, M Heggen, S Rudi, P Strasser *Nano Lett.* **12** 5423 (2012)
445. C Cui, L Gan, H-H Li, S-H Yu, M Heggen, P Strasser *Nano Lett.* **12** 5885 (2012)
446. L Gan, M Heggen, R O'Malley, B Theobald, P Strasser *Nano Lett.* **13** 1131 (2013)
447. X Tuaev, S Rudi, V Petkov, A Hoell, P Strasser *ACS Nano* **7** 5666 (2013)
448. S Chen, P J Ferreira, W Sheng, N Yabuuchi, L F Allard, Y Shao-Horn *J. Am. Chem Soc.* **130** 13818 (2008)
449. I Dutta, M K Carpenter, M P Balogh, J M Ziegelbauer, T E Moylan, M H Atwan, N P Irish *J. Phys. Chem. C* **114** 16309 (2010)
450. Q Jia, D E Ramaker, J M Ziegelbauer, N Ramaswamy, A Halder, S Mukerjee *J. Phys. Chem. C* **117** 4585 (2013)
451. V R Stamenkovic, B S Mun, K J J Mayrhofer, P N Ross, N M Markovic *J. Am. Chem. Soc.* **128** 8813 (2006)
452. C Wang, M Chi, G Wang, D van der Vliet, D Li, K More, H H Wang, J A Schlueter, N M Markovic, V R Stamenkovic *Adv. Funct. Mater.* **21** 147 (2011)
453. C Chen, Y Kang, Z Huo, Z Zhu, W Huang, H I Xin, J D Snyder, J A Herron, M Mavrikakis, M Shi, K L More, N Markovic, G A Somorjai, P Yang, V R Stamenkovic *Science* **343** 1339 (2014)
454. S-I Choi, S-U Lee, W Y Kim, R Choi, K Hong, K M Nam, S W Han, J T Park *ACS Appl. Res. Mater. Interfaces* **4** 6228 (2012)
455. L Y Chen, N Chen, Y Hou, Z C Wang, S H Lv, T Fujita, J H Jang, A Hirata, M W Chen *ACS Catal.* **3** 1220 (2013)
456. S Guo, D Li, H Zhu, S Zhang, N M Markovic, V R Stamenkovic, S Sun *Angew. Chem., Int. Ed.* **52** 3465 (2013)
457. M Shao, K Shoemaker, A Peles, K Kaneko, L Protsailo *J. Am. Chem. Soc.* **132** 9253 (2010)
458. Z Liu, H Xin, Z Yu, Y Zhu, J Zhang, J A Mundy, D A Muller, F T Wagner *J. Electrochem. Soc.* **159** F554 (2012)
459. Z Yu, J Zhang, Z Liu, J M Zielgelbauer, H Xin, L Dutta, D A Muller, F T Wagner *J. Phys. Chem. C* **116** 19877 (2012)
460. H L Xin, J A Mundy, Z Y Liu, R Cabezas, R Hovden, L F Kourkoutis, J L Zhang, N P Subramanian, R Makharia, F T Wagner, D A Muller *Nano Lett.* **12** 490 (2012)
461. Y Xiong, B Wiley, J Chen, Z-Y Li, Y Yin, Y Xia *Angew. Chem., Int. Ed.* **44** 7913 (2005)
462. J Solla-Gullon, F J Vidal-Iglesias, J M Feliu *Annu. Rep. Prog. Chem., Sect. C: Phys. Chem.* **107** 263 (2011)
463. A Visitin, J C Canulo, W E Triaca, A J Arvia *J. Electroanal. Chem.* **239** 67 (1988)
464. W A Egli, A Visitin, W E Triaca, A J Arvia *Appl. Surf. Sci.* **68** 583 (1993)
465. F J R Neto, G Andreasen, M E Martins, F Castez, R C Salvarezza, A J Arvia *J. Phys. Chem. C* **107** 11452 (2003)
466. M Wakisaka, S Asizawa, H Uchida, M Watanabe *Phys. Chem. Chem. Phys.* **12** 4184 (2010)
467. H Gong, S G Sun, Y J Chen, S P Chen *J. Phys. Chem. B* **108** 11575 (2004)
468. N Tian, Z-Y Zhou, S-G Sun, Y Ding, Z L Wang *Science* **316** 732 (2007)
469. G A Attard, J-Y Ye, P Jenkins, F J Vidal-Iglesias, E Herrero, S-G Sun *J. Electroanal. Chem.* **688** 249 (2013)
470. Z-Y Zhou, N Tian, Z-Z Huang, D-J Chen, S-G Sun *Faraday Discuss.* **140** 81 (2009)
471. N Tian, Z-Y Zhou, S-G Sun *J. Phys. Chem. C* **112** 19801 (2008)

472. Z-Y Zhou, Z-Z Huang, D-J Chen, Q Wang, N Tian, S-G Sun *Angew. Chem., Int. Ed.* **49** 411 (2010)
473. N Tian, Z-Y Zhou, N-F Yu, L-Y Wang, S-G Sun *J. Am. Chem. Soc.* **132** 7580 (2010)
474. N Tian, Z-Y Zhou, S-G Sun *Chem. Commun.* 1502 (2009)
475. Y-X Chen, S-P Chen, Q-S Chen, Z-Y Zhou, S-G Sun *Electrochim. Acta* **53** 6938 (2008)
476. Y-X Chen, S-P Chen, Z-Y Zhou, N Tian, Y-X Jiang, S-G Sun, Y Ding, Z L Wang *J. Am. Chem. Soc.* **131** 10860 (2009)
477. R Huang, Y-H Wen, Z-Z Zhu, S-G Sun *J. Mater. Chem.* **21** 11578 (2011)
478. B R Danger, D Fan, J P Vivek, I J Burgess *ACS Nano* **12** 11018 (2012)
479. F Fathi, M Schlitt, D B Peresen, H-B Kraatz *Langmuir* **27** 12098 (2011)
480. S Chen, W Huang, J Zheng, Z Li *J. Electroanal. Chem.* **660** 80 (2011)
481. H-T Fang, C-G Liu, C Liu, F Li, M Liu, H-M Cheng *Chem. Mater.* **16** 5744 (2004)
482. F J Vidal-Iglesias, R M Aran-Ais, J Solla-Gullon, E Herrero, J M Feliu *ACS Catal.* **2** 901 (2012)
483. F Haber *Z. Anorg. Chem.* **16** 438 (1898)
484. B N Kabanov *Elektrokhimiya Metallov i Adsorbtsiya* (Electrochemistry of Metals and Adsorption) (Moscow: Nauka, 1966)
485. B N Kabanov, I I Astakhov, I G Kiseleva *Electrochim. Acta* **24** 167 (1979)
486. A I Koshelev, E P Grigor'eva, Yu D Kudryavtsev, D P Semchenko *Trudy Novocherkasskogo Politekh. In-ta* **197** 79 (1969)
487. A I Ionkin, V M Karavaev, A I Koshelev, Yu D Kudryavtsev, V R Sal'man, D P Semchenko *Trudy Novocherkasskogo Politekh. In-ta* **217** 768 (1970)
488. X Chen, S Chen, W Huang, J F Zheng, Z L Li *Electrochim. Acta* **54** 7370 (2009)
489. W Huang, L Fu, Y C Yang, S Hu, C Li, Z L Li *Electrochem. Solid State Lett.* **13** K46 (2010)
490. W Huang, S Chen, J F Zheng, Z L Li *Electrochem. Commun.* **11** 469 (2009)
491. J Liu, W Huang, S Chen, S Hu, F Liu, Z L Li *Int. J. Electrochem. Sci.* **4** 1302 (2009)
492. A I Yanson, P Rodriguez, N Garcia-Araez, R V Mom, F D Tichelaar, M T M Koper *Angew. Chem., Int. Ed.* **50** 6346 (2011)
493. P Rodriguez, F D Tichelaar, M T M Koper, A I Yanson *J. Am. Chem. Soc.* **133** 17626 (2011)
494. I Leontyev, A Kuriganova, Yu Kudryavtsev, B Dkhil, N Smirnova *Appl. Catal., A* **431** – **432** 120 (2012)
495. Yu I Yanson, A I Yanson *Low Temp. Phys.* **39** 304 (2013)
496. Y-X Chen, A Lavacchi, S-P Chen, F di Benedetto, M Bevilacqua, C Bianchini, P Fornasiero, M Innocenti, M Marelli, W Oberhauser, S -G Sun, F Vizza *Angew. Chem., Int. Ed.* **51** 8500 (2012)
497. A N Frumkin, O A Petrii *Electrochim. Acta* **20** 347 (1975)
498. M T Reetz, W Helbig *J. Am. Chem. Soc.* **116** 7401 (1994)
499. M R Reetz, W Helbig, S A Quaiser, U Stimming, N Breuer, R Vogel *Science* **267** 367 (1995)
500. M T Reetz, M Winter, R Breinbauer, T Thurn-Albrecht, W Vogel *Chem. – Eur. J.* **7** 1084 (2001)
501. M Tokuda, N Mimura, T Karasawa, H Fujita, H Suginome *Tetrahedron Lett.* **37** 7607 (1993)
502. M T Reetz, W Helbig, S A Quaiser *Chem. Mater.* **7** 2227 (1995)
503. J A Becker, R Schafer, R Festag, W Ruland, J H Wendorff, J Pebler, S A Quaiser, W Helbig, M T Reetz *J. Chem. Phys.* **103** 2520 (1995)
504. M T Reetz, S A Quaiser, C Merk *Chem. Ber.* **129** 741 (1996)
505. M T Reetz, G Lohmer *Chem. Commun.* 1921 (1996)
506. A Pundt, M Suleiman, C Bahtz, M T Reetz, R Kirchheim, N M Jisrawi *Mater. Sci. Eng. B* **108** 19 (2004)
507. M B Mohamed, Z L Wang, M A El-Sayed *J. Phys. Chem. A* **103** 10255 (1999)
508. L Rodriguez-Sanches, M C Blanco, M A Lopez-Quintela *J. Phys. Chem. B* **104** 9683 (2000)
509. M Starowicz, B Stypula, J Banas *Electrochem. Commun.* **8** 227 (2006)
510. R A Khaydarov, R R Khaydarov, O Garupova, Yu Estrin, T Scheper *J. Nanopart. Res.* **11** 1193 (2009)
511. N Vilar-Vidal, M C Blanco, M A Lopez-Quintela, J Rivas, C Serra *J. Phys. Chem. C* **114** 15924 (2010)
512. B J Murray, Q Li, J T Newberg, E J Menke, J C Hemminger, R M Penner *Nano Lett.* **5** 2319 (2005)
513. L D Pachon, M B Thathagar, F Hartl, G Rothenberg *Phys. Chem. Chem. Phys.* **8** 151 (2006)
514. V V Yanilkin, G R Nasybullina,A Yu Ziganshina, I R Nizamiev, M K Kadirov, D E Korsin, A I Konovalov *Mendeleev Commun.* **24** 108 (2014)
515. A Katagiri, M Nakata *J. Electrochem. Soc.* **150** C585 (2003)
516. T Welton *Chem. Rev.* **99** 2071 (1999)
517. R Hagiwara, Y Ito *J. Fluorine Chem.* **105** 221(2000)
518. M C Buzzeo, R G Evans, R G Compton *ChemPhysChem* **5** 1106 (2004)
519. *Electrochemical Aspects of Ionic Liquids* (Ed. H Ohno) (New York: Wiley, 2005)
520. L A Aslanov, M A Zakharov, N L Abramycheva *Ionnye Zhidkosti Sredi Rastvoritelei* (Ionic Liquids among Solvents) (Moscow: Moscow State University, 2005)
521. F Endres, S Zein El Abedin *Phys. Chem. Chem. Phys.* **8** 2101 (2006)
522. A P Abbot, K J McKenzie *Phys. Chem. Chem. Phys.* **8** 4265 (2006)
523. S Zein El Abedin, F Endres *ChemPhysChem* **7** 58 (2006)
524. N V Plechkova, K R Seddon *Chem. Soc. Rev.* **37** 123 (2008)
525. M Armand, F Endres, D R MacFarlane, H Ohno, B Scrosati *Nat. Mater.* **8** 621 (2009)
526. N Borisenko, S Zein El Abedin, F Endres *J. Phys. Chem. B* **110** 6250 (2006)
527. F Endres *ChemPhysChem* **3** 144 (2002)
528. F Endres, M Bukowski, R Hempelmann, H Natter *Angew. Chem., Int. Ed.* **42** 3428 (2003)
529. W Freyland, C A Zell, S Zein El-Abedin, F Endres *Electrochim. Acta* **48**3053 (2003)
530. R Al-Salman, S Zein El Abedin, F Endres *Phys. Chem. Chem. Phys.* **10** 4650 (2008)
531. S Zein El Abedin, E M Moustafa, R Hempelmann, H Natter, F Endres *Electrochem. Commun.* **7** 1111 (2005)
532. S Zein El Abedin, E M Moustafa, R Hempelmann, H Natter, F Endres *ChemPhysChem* **7** 1535 (2006)
533. S Zein El Abedin, H K Farag, E M Moustafa, U Welz-Biermann, F Endres *Phys. Chem. Chem. Phys.* **7** 2333 (2005)
534. R Al-Salman, F Endres *J. Mater. Chem.* **19** 7228 (2009)
535. X Meng, R Al-Salman, J Zhao, N Borissenko, Y Li, F Endres *Angew. Chem., Int. Ed.* **48** 2703 (2009)
536. I Mukhopadhyay, W Freyland *Langmuir* **19** 1951 (2003)
537. I Mukhopadhyay, C L Arravinda, D Borissov, W Freyland *Electrochim. Acta* **50** 1275 (2005)
538. F Endres, S Zein El Abedin, A Y Saad, E M Moustafa, N Borisenko, W E Price, G G Wallace, D R MacFarlane, P J Newman, A Bund *Phys. Chem. Chem. Phys.* **10** 2189 (2008)
539. P He, H Liu, Z Li, Y Liu, X Xu, J Li *Langmuir* **20** 10260 (2004)
540. P Yu, Q Qian, Y Lin, L Mao *J. Phys. Chem. C* **114** 3575 (2010)
541. A P Abbott, F Qiu, H M A Abood, M R Ali, K S Ryder *Phys. Chem., Chem Phys.* **12** 1862 (2010)

542. A Lahiri, M Olschewski, O Hofft, S Zein El Abedin, F Endres *J. Phys. Chem. C* **117** 1722 (2013)
543. F Endres, O Hofft, N Borisenko, L H Gasparotto, A Prowald, R Al-Salman, T Carstens, R Atkin, A Bund, S Zein El Abedin *Phys. Chem. Chem. Phys.* **12** 1724 (2010)
544. Y-Z Su, Y-C Fu, Y-M Wei, J-W Yan, B-W Mao *ChemPhysChem* **11** 2764 (2010)
545. R Hayes, N Borisenko, M K Tam, P C Howlett, F Endres, R Atkin *J. Phys. Chem. C* **115** 6855 (2011)
546. F Endres, N Borisenko, S Zein El Abedin, R Hayes, R Atkin *Faraday Discuss.* **154** 221 (2012)
547. S Baldelli *Acc. Chem. Res.* **41** 421 (2008)
548. M V Fedorov, N Gejrgi, A A Kornyshev *Electrochem. Commun.* **12** 296 (2010)
549. W Zhou, S Inoue, T Iwahashi, K Kanai, K Seki, T Miyamae, D Kim, Y Katayama, Y Ouchi *Electrochem. Commun.* **12** 672 (2010)
550. S A Meiss, M Rohnke, L Kienle, S Zein El Abedin, F Endres, J Janek *ChemPhysChem* **8** 50 (2007)
551. M Brettholle, O Hofft, L Klarhofer, S Mathes, W Maus-Friedrichs, S Zein El Abedin, S Krischok, J Janek, F Endres *Phys. Chem., Chem. Phys.* **12** 1750 (2010)
552. Y-B Xie, C-J Liu *Plasma Proc. Polym.* **5** 239 (2008)
553. M Guainazzi, G Silvestri, G Serravalle *J. Chem. Soc. Chem. Commun.* 200 (1975)
554. Y Cheng, D J Schiffrin *J. Chem. Soc., Faraday Trans.* **92** 3865 (1996)
555. M Brust, M Walker, D Bethell, D J Schiffrin, R Whyman *J. Chem. Soc., Chem. Commun.* 801 (1994)
556. Y Li, O Zaluzhna, B Xu, Y Gao, J M Modest, Y J Tong *J. Am. Chem. Soc.* **133** 2092 (2011)
557. Z Samec *Pure Appl. Chem.* **76** 2147 (2004)
558. C Johans, R Lahtinen, K Kontturi, D J Schiffrin *J. Electroanal. Chem.* **488** 99 (2000)
559. C Johans, K Kontturi, D J Schiffrin *J. Electroanal. Chem.* **526** 29 (2002)
560. C Johans, P Liljeroth, K Konturri *Phys. Chem. Chem. Phys.* **4** 1067 (2002)
561. A Trojanek, J Langmaier, Z Samec *J. Electroanal. Chem.* **599** 160 (2007)
562. B Su, J-P Abid, D J Fermin, H H Girault, H Hoffmannova, P Krtil, Z Samec *J. Am. Chem. Soc.* **126** 915 (2004)
563. C Johans, J Clohessy, S Fantini, K Kontturi, V Cunnane *Electrochem. Commun.* **4** 227 (2002)
564. R A W Dryfe *Phys. Chem. Chem. Phys.* **8** 1869 (2006)
565. M Platt, R A W Dryfe, E P L Roberts *Chem. Commun.* 3037 (2002)
566. R A W Dryfe, A O Simm, B Kralj *J. Am. Chem. Soc.* **125** 13014 (2003)
567. M Platt, R A W Dryfe, E P L Roberts *Electrochim. Acta* **48** 3037 (2003)
568. M Platt, E P L Roberts, R A W Dryfe *Electrochim. Acta* **49** 3937 (2004)
569. M Platt, R A W Dryfe *Phys. Chem. Chem. Phys.* **7** 1807 (2005)
570. M Platt, R A W Dryfe *J. Electroanal. Chem.* **599** 323 (2007)
571. A Martinez, A Colina, R A W Dryfe, V Ruiz *Electrochim. Acta* **54** 5071 (2009)
572. D Izquierdo, A Martinez, A Heras, J Lopez-Palacious, V Ruiz, R A W Dryfe, A Colina *Anal. Chem.* **84** 5723 (2012)
573. M E Flatte, A A Kornyshev, M Urbakh *Faraday Discuss.* **143** 109 (2009)
574. J Guo, T Tokimoto, R Othman, P R Unwin *Electrochem. Commun.* **5** 1005 (2003)
575. G Taylor, H H Girault *J. Electroanal. Chem.* **208** 175 (1986)
576. C E Banks, T J Davies, R G Evans, G Hignett, A J Wain, N S Lawrence, J D Wadhawan, F Marken, R G Compton *Phys. Chem. Chem. Phys.* **5** 4053 (2003)
577. F Scholz, U Schroder, R Gulaboski *Electrochemistry of Immobilized Particles and Droplets* (Berlin: Springer, 2005)
578. I Kaminska, M Jonsson-Niedziolka, A Kaminska, M Pisarek, R Holyst, M Opalo, J Niedziolka-Jonsson *J. Phys. Chem. C* **116** 22476 (2012)
579. W Li, J A Virtanen, R M Penner *Appl. Phys. Lett.* **60** 1181 (1992)
580. W Li, J A Virtanen, R M Penner *J. Phys. Chem.* **96** 6529 (1992)
581. R M Nyffenegger, R M Penner *J. Phys. Chem.* **100** 17041 (1996)
582. R M Nyffenegger, R M Penner *Chem. Rev.* **97** 1195 (1997)
583. D M Kolb, R Ullmann, T Will *Science* **275** 1097 (1997)
584. G E Engelmann, J C Ziegler, D M Kolb *J. Electrochem. Soc.* **145** L33 (1998)
585. D M Kolb, G E Engelman, J C Ziegler *Solid State Ionics* **131** 69 (2000)
586. F P Zamborini, R M Crooks *J. Am. Chem. Soc.* **120** 9700 (1998)
587. Y Li, B W Maynor, J Liu *J. Am. Chem Soc.* **123** 2105 (2001)
588. D M Kolb, G E Engelman J C Ziegler *Angew. Chem., Int. Ed.* **39** 1123 (2000)
589. M G Del Popolo, E P M Leiva, W Schmickler *Angew. Chem., Int. Ed.,* **41** 4674 (2001)
590. M G Del Popolo, E P M Leiva, H Kleine, J Meier, U Stimming, M Mariscal, W Schmickler *Electrochim. Acta* **48** 1287 (2003)
591. C G Sanchez, E P M Leiva, W Schmickler *Electrochem. Commun.* **5** 584 (2003)
592. M G Del Popolo, E P M Leiva, M Mariscal, W Schmikler *Surf. Sci.* **597** 133 (2005)
593. Y Zhang, S Maupai, P Schmuki *Surf. Sci.* **551** L33 (2004)
594. M Nielinger, H Baltruschat *ChemPhysChem* **4** 1022 (2003)
595. W Schindler, P Hugelmann, M Hugelmann, F X Kartner *J. Electroanal. Chem.* **522** 49 (2002)
596. W Schindler, D Hofmann, J Kirschner *J. Appl. Phys.* **87** 7007 (2000)
597. Y M Wei, X S Zhou, J G Wang, J Tang, B W Mao, D M Kolb *Small* **4** 1355 (2008)
598. J G Wang, J Tang, Y C Fu, Y M Wei, Z B Chen, B W Mao *Electrochem. Commun.* **9** 633 (2007)
599. P Berenz, X Xiao, H Baltruschst *J. Phys. Chem. B* **106** 3673 (2002)
600. S G Garcia, D R Salinas, C E Mayer, W J Lorenz, G Staikov *Electrochim. Acta* **48** 1279 (2003)
601. M Hugelman, P Hugelman, W J Lorenz, W Schindler *Surf. Sci.* **597** 156 (2005)
602. Z P Zhdanov, B Kasemo *Surf. Sci. Rep.* **39** 25 (2000)
603. K Seo, E Borguet *Langmuir* **22** 1388 (2006)
604. M Nielinger, P Berenz, X Xiao, H Baltruschst *Surf. Sci.* **597** 1 (2005)
605. Z-X Xie, D M Kolb *J. Electroanal. Chem.* **481** 177 (2000)
606. J-M Noel, Y Yu, M V Mirkin *Langmuir* **29** 1346 (2013)
607. R Tel-Vered, A J Bard *J. Phys. Chem. B* **110** 25279 (2006)
608. H X He, S Boussaad, B Q Xu, C Z Li, N J Tao *J. Electroanal. Chem.* **522** 167 (2002)
609. N J Tao *Nat. Nanotechnol.* **1** 173 (2006)
610. F Chen, J Hihath, Z Huang, X Li, N J Tao *Annu. Rev. Phys. Chem.* **58** 535 (2007)
611. R Subbaraman, N Danilovic, P P Lopes, D Tripkovic, D Strmnick, V R Stamenkovic, N M Markovic *J. Phys. Chem. C* **116** 22231 (2012)
612. C Amatore *ChemPhysChem* **10** 20 (2009)
613. M Gratzel *Acc. Chem. Res.* **42** 1788 (2009)